Russian Chemical Reviews **77** (10) 837 – 873 (2008) © 2008 Russian Academy of Sciences and Turpion Ltd

DOI 10.1070/RC2008v077n10ABEH003789

New nanoforms of carbon and boron nitride

V V Pokropivny (deceased), A L Ivanovskii

Contents

I.	Introduction	837
II.	Classification of nanostructures	838
III.	New carbon nanoforms based on fullerenes, nanotubes and related nanostructures	838
IV.	Nanodiamonds	846
V.	Non-graphite nanostructures	852
VI.	Carbon – carbon nanocomposites	855
VII.	Boron nitride nanostructures	860
VIII.	Conclusion	866

Abstract. Data on new carbon nanostructures including those based on fullerenes, nanotubes as well as monolithic diamond-like nanoparticles, nanofibres, various nanocomposites, *etc*., published in the last decade are generalised. The experimental and theoretical data on their atomic and electronic structures, the nature of chemical bonds and physicochemical properties are discussed. These data are compared with the results obtained in studies of nanoforms of boron nitride, an isoelectronic analogue of carbon. Potential fields of applications of the new nanostructures are considered. The bibliography includes 486 references.

I. Introduction

The carbon atom can form various types of chemical bonds due to hybridisation of s- and p-orbitals. This unique feature distinguishes carbon from other elements. According to D I Mendeleev,[1] 'among volatile carbon compounds, there are well known many containing C_2, ..., C_{10}, ..., C_{20}, ..., C_{30}, ... *etc*., generally, C_n units, where n can be rather large, and none of the elements can compete with carbon in ability to form complex structures'. Four valence electrons in carbon atoms can form the sp^1, sp^2 and sp^3 bond configurations, which predetermine the ability of carbon to form various allotropes, *i.e*., linear, planar and three-dimensional structures with a coordination number of 2, 3 and 4 and the bond angles of 180°, 120° and 109.47°, respectively.

The structures, properties and applications of conventional carbon allotropes have been the subject of numerous monographs and reviews (see, *e.g*., Refs 2 – 15). They include diamond and lonsdalite having sp^3-bond configuration; graphite (hexagonal, rhombohedral and their polytypes) with sp^2-bond configuration and linear polymers with sp^1-bonds. A variety of modern structural, tool, thermally stable, polymeric, *etc*. materials based on carbon allotropes have been designed. Various forms of technical and mineral carbon (coke, natural graphite, anthracite, glassy carbon, carbositall, *etc*.) are known.

Boron nitride, the closest isoelectronic analogue of carbon, also forms numerous polymorphs.[15]

Data on the compounds listed above as well as numerous unusual carbon allotropes and BN polymorphs can be found in periodic literature, monographs and textbooks. The structures of many of them remain unknown so far. Unusual carbon allotropes were discovered in meteorites and sediments;[7] they were synthesised for the first time in the early 1960s. The authors of a review [14] pointed that not only diamond and graphite, but also some other carbon modifications were reported in the literature, namely, up to eight carbyne forms, metallic carbon, C_8, *etc*., whose structures were unknown at that time. An attempt to systematise all carbon modifications known to the late 1980s (before the discovery of fullerenes) was also made.[15] New BN polymorphs have been considered in a review.[16] They are synthesised under severe conditions. Usually, small amounts of these polymorphs are obtained in mixtures with other known phases.

The synthesis of carbon fullerenes (cage carbon clusters C_n containing pentagons C_5 and hexagons C_6) and nanotubes (single- or multi-layer cylinders whose walls are formed of hexagons C_6) [17 – 79] gave an impetus to extensive experimental and theoretical search for and obtaining of new nanoforms of carbon and related boron nitride nanostructures.

V V Pokropivny Institute for Problems of Materials Science of National Academy of Sciences of Ukraine, ul. Krzhyzhanovskogo 3, 03142 Kiev, Ukraine. Fax (38-044) 242 21 31
A L Ivanovskii Institute of Solid State Chemistry, Urals Branch of the Russian Academy of Sciences, ul. Pervomaiskaya 91, 620041 Ekaterinburg, Russian Federation. Fax (7-343) 374 44 95, tel. (7-343) 374 53 31, e-mail: ivanovskii@ihim.uran.ru

Received 14 March 2008
Uspekhi Khimii **77** (10) 899 – 937 (2008); translated by A M Raevskiy

At present, the structures and properties of fullerenes and nanotubes have been well investigated and thoroughly reviewed (see, *e.g.*, Refs 37–59 and 62–70); therefore, they can be treated as traditional (conventional) forms of carbon. In this review we leave these nanostructures out of consideration. At the same time, a great body of information on new non-icosahedral fullerene-like clusters and nanotubes as well as new nanoforms of carbon and BN has been accumulated recently.

In this review we attempt to clasify and systematise the recently obtained data (mainly reported in the last five to ten years) on new nanoforms of carbon including those based on fullerenes and nanotubes, as well as on monolithic diamond-like nanoparticles, nanofibres, various nanocomposites, *etc*.

II. Classification of nanostructures

The discovery of fullerenes and nanotubes, fabrication of quantum dots, nanofibres, nanolayers and various heterostructures gave an impetus to progress in nanomaterials science, which recently has transformed to a more general field called nanotechnology.[77] Nanotechnology deals with nanostructure materials, *e.g.*, those structures and forms of materials whose 'building blocks' have a submicrometre or nanometre size at least in one dimension. Such objects exhibit special size effects.

Various classifications of nanostructure materials are available. One of the first schemes was proposed in the mid-1990s (Ref. 78) by Gleiter who divided all nanostructure materials into polymeric and nonpolymeric ones and classified only nonpolymeric three-dimensional (3D) materials. The classification was based on the shape and chemical composition of crystallites. As applied to nanostructures, it was of course (i) incomplete because zero-dimensional (0D), one- (1D) and two-dimensional (2D) structures were ignored and (ii) combined because the key indications were the shape and chemical composition of crystallites. More recently,[79–81] Gleiter's scheme was extended by including the type of chemical bond in order to classify nanostructures.

When classifying nanostructures (first of all, carbon ones), the type of electronic configuration of the carbon atom is most widely used as the key indication.[44–58,82–84] In this case one can divide all allotropes into three large families, namely, sp^3, sp^2 and sp^1 and choose a total of seven main groups including sp^1, sp^2, sp^3, sp^1+sp^2, sp^1+sp^3, sp^2+sp^3 and $sp^1+sp^2+sp^3$. This classification appears logical and attractive; however, it should be taken into account that unambiguous assignment of certain nanostructures to a particular group is not always possible. For instance, the sp^2+sp^3 group includes a number of nanoforms with different-type structures and properties, namely, covalently polymerised fullerene or nanotube assemblies, diamond-like crystallites and their combinations, *etc*. Despite some drawbacks of this classification, we will use it in the text below.

III. New carbon nanoforms based on fullerenes, nanotubes and related nanostructures

The atomic structures and morphologies of some fullerene-like and nanotubular forms of carbon are shown in Fig. 1. The discovery of these forms has stimulated both the search for new nanoforms based on fullerenes and nanotubes and the studies on structure determination of the known unusual carbon allotropes and BN polymorphs.

1. Amorphous nanocarbon

Amorphous carbon has long been known. A characteristic feature of amorphous carbon is a diffuse halo in the X-ray pattern, indicating a short-range order. Amorphous carbon (a-C) and tetrahedral amorphous carbon (ta-C) including hydrogenated (a-C:H, ta-C:H) phases were isolated.[85] They are prepared by, *e.g.*, vapour phase deposition, detonation of explosives, grinding, high-temperature shock compression of charcoal, *etc*. Long-term grinding of graphite in a mill induces phase transitions of graphite to turbostratic graphite and then to amorphous carbon, which is characterised by a large specific inner surface area (~ 335 m^2 g^{-1} after grinding for 15 h).[86] This fact, as well as the results of a transmission electron microscopy (TEM) study indicate a nanoporous structure of a-C.

Amorphous carbon with a cage structure of sp^2-bonds and a density, ρ, of 2.9 g cm^{-3} (intermediate value between those of graphite and diamond) was prepared by high-temperature shock compression of charcoal.[87,88] At high temperatures, the C_{60} and C_{70} fullerites go to amorphous state.[89]

The short-range order structure in amorphous carbon is still to be clarified. It is known that the structure of this form of carbon is strongly dependent on the reaction duration and on the substrate temperature. One can assume that the nanoparticle size (d) depends on the reaction rate (v_r) and duration (t_r)

$$d \sim v_r t_r .$$

When using detonation-induced or vapour phase depositon, the time t_r is short; this precludes the growth of large particles. The substrate temperature determines the relaxation time, *i.e.*, the characteristic time of transformation of the nonequilibrium configuration to a stable one. This time is also short and insufficient for diffusion processes to occur. Only small fragments and atomic clusters, *e.g.*, C_2 dimers, C_6 hexagons, one-dimensional chains, 3D small fullerenes C_{20}, C_{24}, C_{28}, C_{36}, C_{48}, *etc*. can form under nonequilibrium conditions.

Deposition causes the substrate surface to be simultaneously covered with randomly arranged atoms, molecules, clusters, fullerenes, nanotubes and nanoparticles having various configurations, size, concentration and types of bond hybridisation (sp^1, sp^2, sp^3). Such a mixture can be identified as 'amorphous nanocarbon', because the superposition of the X-ray diffraction patterns from each component of the mixture appears as a single diffuse line.

2. C_8 carbon

A cage structure of the C_8 carbon phase was proposed.[90] The sites in half-filled body-centred cubic (BCC) lattice are occupied by tetrahedra built of carbon atoms forming diamond-like sp^3-bonds. This phase is less dense than diamond and its structure can be treated as hypertetrahedron.

3. Fullerenes and fullerites

As mentioned above, the discovery of C_n fullerenes and their heteroatom analogues gave a strong impetus to the progress of research on unusual nanoforms of carbon and boron nitride. Numerous publications are devoted to studies of the properties of C_{60} and C_{70} fullerenes for which

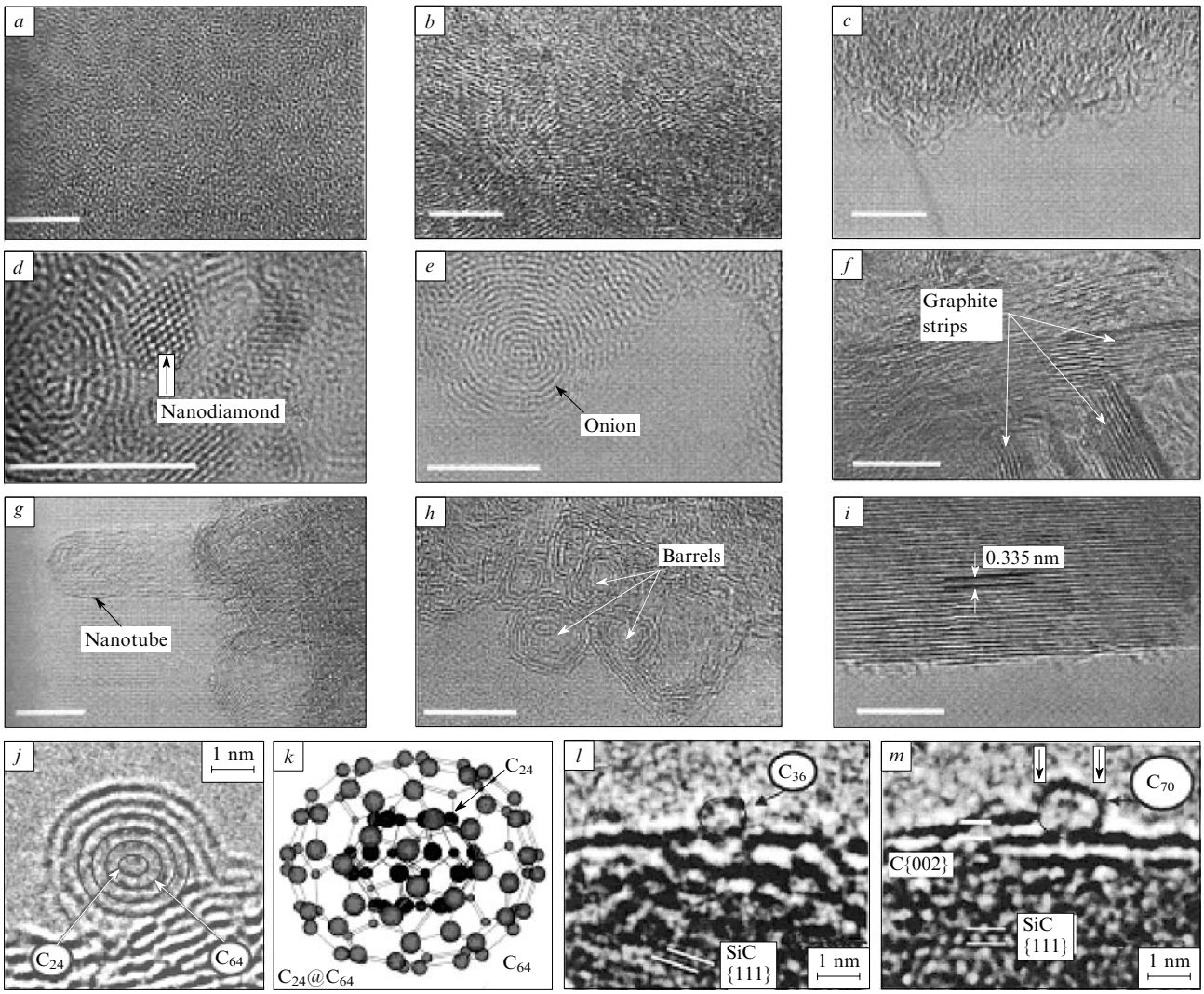


Figure 1. Micrographs of various carbon nanostructures prepared by chlorination of carbides (*a*–*i*)[76] and electron irradiation (*j*–*m*).[19,20] Amorphous carbon consisting of randomly arranged graphite microfragments (*a*); turbostratic carbon consisting of randomly arranged microfragments of graphite sheets (graphenes) (*b*); fullerene-like carbon consisting of fullerene clusters (*c*); nanodiamond consisting of randomly arranged diamond nanocrystals (*d*); an onion (multishell structure consisting of nested polyhedral clusters) (*e*); graphite strips (*f*); a nanotube (*g*); barrels, or imperfect cylindrical nanotubes and barrel-like nanoparticles (*h*); ordered graphite (*i*); onions with $C_{24}@C_{64}$ clusters on SiC surface (*j*, *k*);[25] and the C_{36} and C_{70} clusters on SiC surface (*l*, *m*).[24] Horizontal white segments of straight lines in (*a*)–(*i*) set the scale length: 5 nm in each case.

unique properties were predicted[91] (in particular, the possibility of formation, from C_{60}, of a phase whose hardness is higher than that of diamond).[92] At present, a number of interesting high-strength carbon materials including those based on C_{60} and C_{70} fullerenes have been synthesised.[93–97] A feature of these materials consists in polymerisation of particular fullerenes with the formation of sp^3-bonds (due to pressure treatment at elevated temperatures[93,95–97]); however, no 'superhard fullerite' molecular crystal from C_{60} fullerenes was obtained.

The reason is that, from the standpoint of crystal chemistry, C_{60} is an irregular polyhedron unsuitable for building close-packed molecular crystals. Therefore, the so-called non-icosahedral small fullerenes $C_{n<60}$ (see Fig. 2) seem to be more appropriate.

The discovery of C_n fullerenes gave an impetus to the design of carbon materials by condensation of C_n resulting in various systems, namely, polymeric (quasi-1D), film (layered, 2D) or crystalline (three-dimensional, 3D) ones. Taking account of specific features of atom–atom interactions, the crystalline systems can conditionally be divided into subgroups.

The first subgroup includes 3D molecular fullerites with closed-shell fullerenes as crystal-forming blocks. These fullerenes occupy the crystal lattice sites and interact between one another through weak van der Waals bonds. Typical representatives of this group are 3D fullerites based on C_{60} and fullerides (doped fullerites).[36,45,46]

The second group comprises covalently bonded fullerites with strong covalent interactions between fullerenes. The formation of such crystals is characteristic of open-shell small fullerenes.[47]

The third group includes fullerites in which fullerenes are bonded through both covalent and van der Waals forces.

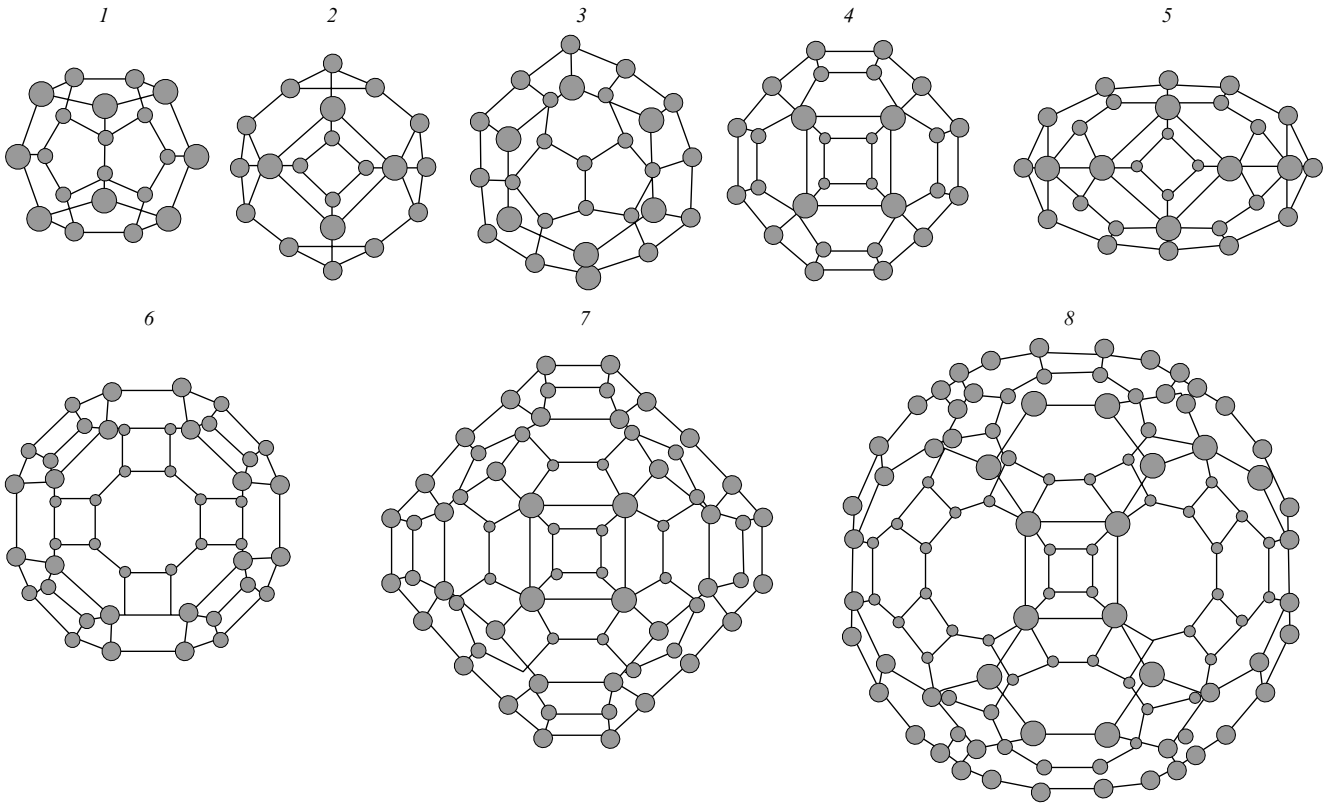


Figure 2. Optimised configurations of crystal-forming polyhedral clusters C_{2n}.
C_{20} (T_h, 12p) (*1*), C_{24} (T_h, 6c + 8h) (*2*), C_{28} (D_{2d}, 12p + 4h) (*3*), C_{32} (T_h, 6c + 12h) (*4*), C_{36} (D_{6h}, 6c + 14h) (*5*), C_{48} (O, 12c + 8h + 6o) (*6*), C_{72} (T_h, 6c + 32h) (*7*) and C_{120} (T_h, 30c + 20h + 12d) (*8*). The symmetry and number of faces are given in parentheses. Notations of faces: c is square, p is pentagonal, h is hexagonal, o is octahedral and d is decagonal.

Fullerenes, as well as carbon polyhedra, clusters and nanotubes can be copolymerised through vertices, edges or faces to form (1D – 3D)-structures with mixed ($sp^1 + sp^2 + sp^3$)-bonds.

The most close-packed crystals can be prepared using copolymerisation of the so-called crystal-forming polyhedra through faces (see Fig. 2). Such polyhedra should only have polygonal faces with even number of edges (4, 6, 8, 10).[98] There is a limited class of crystal-forming polyhedra,[22, 23, 98] (*e.g.*, C_{24}, C_{48}) and related heteroatomic clusters $X_{n12}Y_{n12}$, $n = 1, 2, 3\ldots$, which are characterised by not only point symmetry group, but also a crystal symmetry group. A feature of crystal formation by copolymerisation of such polyhedra through faces is manifestation of strong sp^3-bonds that stabilise the crystals. In this case, all atoms may be involved in sp^3-interactions. Examples are provided by fullerites based on C_{24} with a simple cubic lattice, C_{48} with face-centred cubic (FCC) lattice (FCCF-C_{48}) and some other systems. Among this type of fullerites, there are a few tetrahedral systems (T_d symmetry), *i.e.*, with the diamond or sphalerite lattice. sp^3-Bonds in them are formed between both individual polyhedra and individual atoms.[22, 23, 99, 100]

Fullerene crystals have porous structures with molecular-size pores. Taking account of this fact offers prospects for search for novel materials: artificial zeolites.

4. Orthorhombic and tetragonal fullerites OF-C_{20} and TF-C_{20}

A dodecahedral cluster C_{20} (Refs 101, 102) is the smallest fullerene whose atomic cage consists of 12 pentagons C_5 (Fig. 2). High reactivity of C_{20} fullerenes[47] should favour[103] spontaneous polymerisation of these systems to form various disordered or (1D – 3D)-structures including both sp^2- and sp^3-atoms (*i.e.*, the atoms forming sp^2- and sp^3-type chemical bonds). Such hypothetical structures include fullerites[103] with orthorhombic and tetragonal lattices, OF-C_{20} and TF-C_{20}, respectively.

According to theoretical estimates,[104, 105] electron – phonon interactions in the phases based on C_{20} fullerenes are much stronger than in the C_{60}-based phases, which suggests manifestation of superconducting properties in the former case.[104, 106] This is the reason for interest in search for the C_{20} condenced phases. Calculations[103, 106, 107] showed that 1D-structures where the proportion of sp^3-atoms can be as high as about 80% and the crystal of simple cubic fullerite SCF-C_{20} have high densities of states near the Fermi level; this favours the onset of superconductivity. However, these structures are metastable with respect to OF-C_{20} and TF-C_{20}. For instance, the energy cohesive of SCF-C_{20} is $\sim$8.6 eV (*cf.* 14.9 and 14.0 eV for OF-C_{20} and TF-C_{20}, respectively). The last two phases are semiconductors with a forbidden gap (FG) of $\sim$1.4 – 1.8 eV.[103]

5. Cubic graphite SCF-C_{24}

The existence of the so-called cubic (cubic crystal system) graphite (CG) was experimentally proved by many researchers.[108 – 114]

The first CG sample was synthesised[114] from graphite at low temperatures (77 – 296 K) and a pressure higher than 150 kbar. The structural parameters of CG are as follows: lattice constant $a = 0.5545$ nm, density $\rho = 2.80$ g cm^{-3}, and the number of atoms in the unit cell $Z = 24$. The

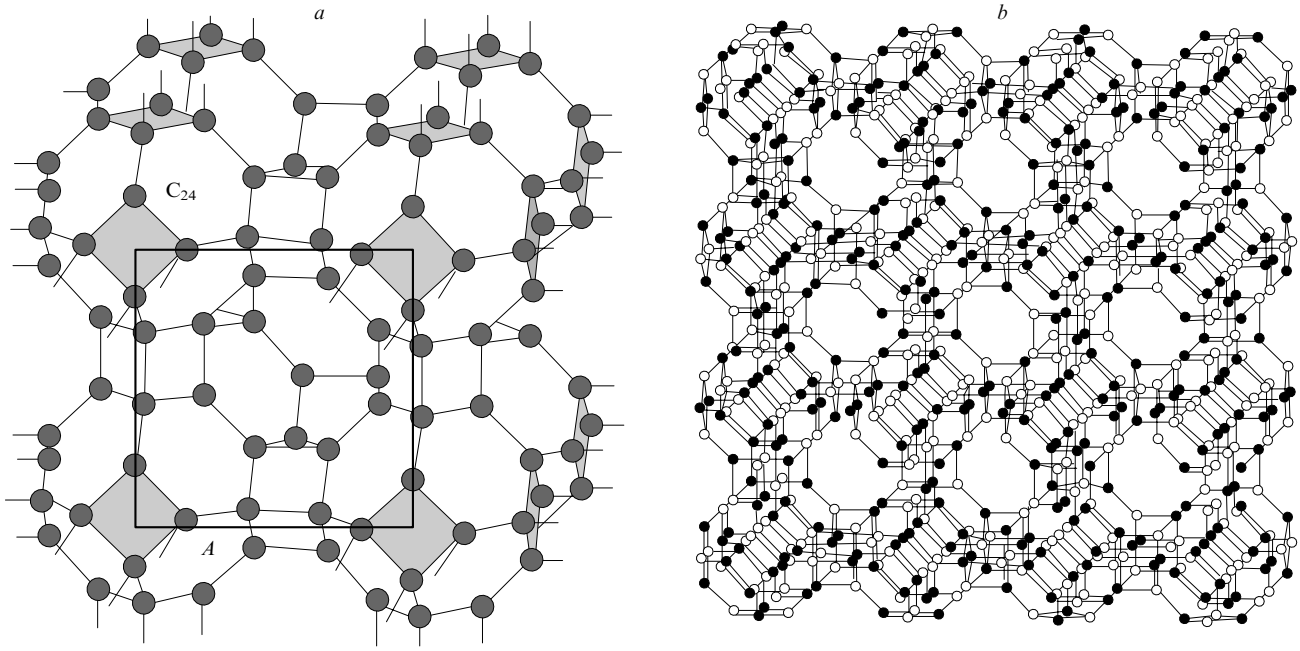


Figure 3. The unit cell of SCF-C_{24} (*a*)[113] and the 4×4 lattice of SCF-$B_{12}N_{12}$ (*b*).[22,23] *A* is the lattice constant.

synthesis of CG in the course of preparation of ultradisperse diamond powders from methane and other hydrocarbons was reported.[110] A carbon phase (cubic crystal system) with average values $a = 0.56$ nm and $\rho = 2.78$ g cm^{-3} was synthesised.[112] These opaque crystals of various shape are characterised by a hardness of 1–5 GPa.

A structure determination study of CG was reported.[113] Analysis of possible cubic unit cells containing 24 carbon atoms[35,115–117] showed that C_{24} fullerene is the best candidate[117,118] for the formation of the CG structure (see Fig. 2). The C_{24} molecule is the smallest one, which obeys the isolated square rule (a stability rule similar to the isolated pentagon rule for C_{60} fullerene). This rule follows from the principle of conservation of valence (it equals to four for all carbon atoms in molecule). Parameters of the molecule are as follows: T_h symmetry, energy of atomisation per two atoms $E_a = 11.875$ kcal mol^{-1}; the bond lengths are $l_{6,6} = 0.1386$ nm and $l_{6,4} = 0.1503$ nm; the average radius of the molecule $R = (5/2)^{1/2} l_{C-C}$, where l_{C-C} is the C–C bond length; and the radii from the centre of the molecule to the centres of the square and hexagonal faces are respectively $R_4 = (2)^{1/2} l_{C-C}$ and $R_6 = (3/2)^{1/2} l_{C-C}$.[118]

Fullerene C_{24} is the smallest polyhedron in which the number of faces (6 squares and 8 hexagons) is sufficient to form a simple cubic lattice with covalently bonded C_{24} molecules through the bonds between atoms of adjacent square faces (Fig. 3). This structure is called a simple cubic fullerite (SCF-C_{24} 0; here all carbon atoms are bonded by sp^3-bonds as in diamond. The calculated[113] parameters of SCF-C_{24} are as follows: space group O_h^1, lattice constant $a = 0.5545$ nm, density $\rho = 2.808$ g cm^{-3}; this is in agreement with experimental data. According to calculations,[119,120] SCF-C_{24} is a stable phase and the dependence of its total energy on the C–C bond length is similar to that known for diamond. The elastic constants SCF-C_{24}, the bulk modulus and the equilibrium lattice constant were calculated using the molecular dynamics method. The results obtained are as follows: the equilibrium lattice constant $a_0 = 0.60\,546$ nm, the bond lengths $l_{6,6} = 1.5032$ nm and $l_{6,4} = 1.5032$ nm, the bulk elastic modulus $B = 196.1$ GPa and the elastic coefficients $C_{11} = 337.6$ and $C_{12} = 139.5$ and $C_{44} = 29.8$ GPa. Thus, the conditions for mechanical stability of SCF-C_{24}: $B > 0$, $C_{11} - C_{12} > 0$ and $C_{44} > 0$ are met. The bond lengths differ from the bond length in diamond by at most 5.8% and can therefore be treated as diamond-like sp^3-bonds. Simple cubic fullerene C_{24} is a semiconductor with a forbidden gap of ~ 1.6 eV. Similarly to zeolites, the SCF-C_{24} structure includes a two-dimensional lattice of cylindrical nanopores 0.41 nm in diameter. This type of structures can be used as molecular sieves.

6. Molecular hyperdiamond fullerites MHDF-C_{28} and MHDF-C_{40}

Small fullerenes C_n ($n = 28, 40$) belong to the most interesting representatives of open-shell cage clusters $C_{n<60}$. For instance, a stable C_{28} isomer with T_d symmetry is built of four hexagons C_6 and four groups of pentagons C_5; its shell includes three groups of nonequivalent atoms C(1)–C(3) (Fig. 4*a*). This fullerene is a radical having four unpaired electrons localised on C(1)-type atoms occupying the vertices shared by pentagons. As a result, C_{28} is unstable and highly reactive.[47,84,121–128] The C_{40} fullerene is similar in electronic properties to the C_{28} fullerene; the most stable isomer of C_{40} fullerene also has T_d symmetry and four unpaired electrons localised on C(1)-type atoms.

Thus, both fullerenes, C_{28} and C_{40}, are highly reactive. Such structures can be stabilised by saturating noncompensated bonds as a result of their interactions between one another upon condensation to crystalline state.[47,84,96,126] Formally, C_n fullerenes are similar to carbon atom in structure of their electron shells. Therefore, in the condensed state they can form lattices similar to those of crystalline carbon allotropes (diamond and lonsdalite with sp^3-bonds). The theoretically designed C_{28} phases[96,127] are

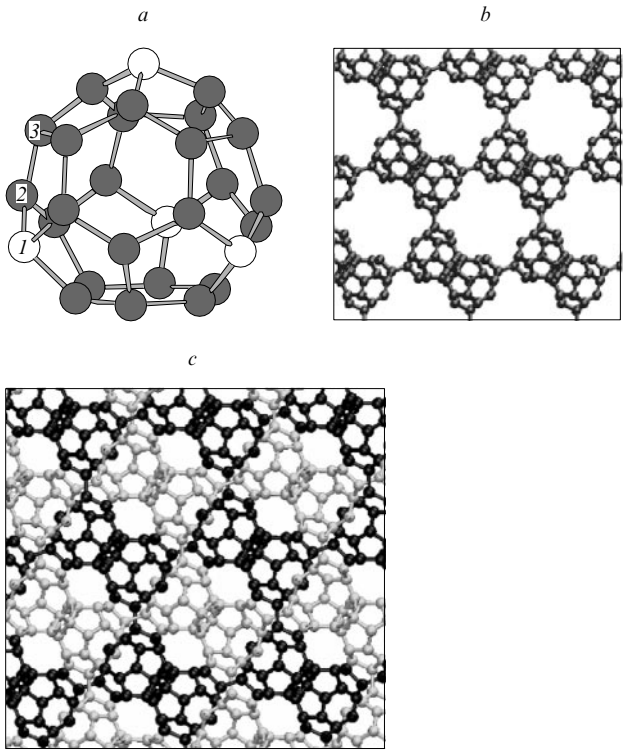


Figure 4. Atomic structure of C_{28} fullerene (*a*) and fragments of the crystal lattices of hyperdiamond (*b*) and molecular hyperdiamond fullerite (*c*) based on C_{28} fullerene.[128]
Shown are three nonequivalent types of atoms, C(1), C(2) and C(3) for C_{28} fullerene (*a*) and fullerenes incorporated into structural voids of the initial hyperdiamond lattice for MHDF (*c*).

sometimes called a hyperdiamond (HD) (see Fig. 4*b*) and hyperlonsdalite (HL).

The most attractive features of HD-C_{28} consist in its low density (ρ = 1.10 g cm^{-3}, this is one third of the density of diamond) and presence of large structural voids whose radii ($\sim$0.46 nm) are larger than those of C_{28} fullerenes ($\sim$0.268 nm) that form the HD lattice. This suggests the possibility of 'autointercalation' of HD-C_{28}, *i.e.*, filling of structural voids by additional C_{28} fullerenes.

Recently,[128] a model for a new 3D-phase, molecular hyperdiamond fullerite based on HD-C_{28} (MHDF-C_{28}), was proposed. Here, voids are filled with the same C_{28} fullerenes (see Fig. 4). When filling these voids in the initial HD-C_{28} lattice, the intercalated fullerenes are arranged in such a manner that form their own diamond-like lattice; therefore, the structure of MHDF-C_{28} can be described as two 'nested' lattices of C_{28} hyperdiamond (see Fig. 4*c*). Simlar hypothetical diamond-like phases, namely, a hyperdiamond, hyperlonsdalite and self-intercalated hyperdiamond, were designed based on C_{40} fullerene.[129] Modelling of the phases based on C_{28} and C_{40} allowed their structural parameters (*a*, *c*), densities, elastic moduli and energies of formation to be determined and the electronic structures to be studied.[128–131]

It was found[128, 129] that the lattice parameter *a* remains almost unchanged on filling of voids in the HD lattice by additional fullerenes (it differs by at most 5×10^{-3} nm for the optimised structures of HD and MHDF). The energy of formation of MHDF is 13.6 kJ mol^{-1} higher than that of HD (calculated with respect to C_{28} fullerene). This indicates the onset of interactions between diamond-like sublattices in MHDF.

The shell-to-shell distance between neighbouring C_{28} fullerenes belonging to different diamond-like sublattices in MHDF is 0.304 nm. This is almost equal to the size of the van der Waals gap (characteristic distance between graphene sheets in graphite or the wall-to-wall spacing between neighbouring nanotubes in coaxial multilayer carbon nanotubes, or between neighbouring fullerene shells in onions corresponding to the onset of van der Waals interactions between these carbon structural motifs). Thus, MHDF exhibits a combined type of interaction, that is, strong covalent bonds between neighbouring C_{28} fullerenes in each diamond-like sublattice and the van der Waals interactions between neighbouring fullerenes from different sublattices. This is atypical of fullerites.

Self-intercalation of HD causes significant changes in its physical properties (Table 1). In particular, the density of MHDF becomes twice as high as that of HD. The elastic modulus of MHDF increases particularly abruptly (by a factor of about 2.7) and reaches a value of 122.83 GPa. Among the known C_n fullerites (see review[131]), only BCC-C_{20} (B = 201.9 GPa, calculated value) and SCF-C_{24} (B = 310 GPa) have greater bulk compression moduli compared to hypothetical MHDF.[119, 120] The HD-C_{28} and MHDF-C_{28} phases are insulators with a forbidden gap of $\sim$1.80 and 1.31 eV, respectively.

Table 1. Energies of formation (E_{form} /kJ mol^{-1}), lattice constants (a and c /nm), density (ρ /g cm^{-3}), elastic modulus (B /GPa) and forbidden gap (E_g /eV) for hyperdiamonds, hyperlonsdalites and self-intercalated hyperdiamonds based on C_{28} and C_{40}.[128, 129]

Crystal	E_{form}	a	c	ρ	B	E_g
HD-C_{28}	602.8	1.5952	–	1.10	45.54	1.80
HL-C_{28}	598.7	1.1286	1.8429	1.10	45.90	1.76
MHDF-C_{28}	616.4	1.6004	–	2.18	122.83	1.31
HD-C_{40}	427.04	1.8924	–	0.94	29.22	1.01
HL-C_{40}	422.83	1.3386	2.1860	0.78	30.25	1.01
MHDF-C_{40}	427.59	1.8922	–	1.88	60.31	0.94

Analogous calculations[129] of C_{40} diamond-like phases revealed the following order with respect to the energy of formation:

MHDF-C_{40} > HD-C_{40} > HL-C_{40}.

The energy-of-formation difference between MHDF-C_{40} and HD-C_{40} is much smaller than between the analogous phases based on C_{28}. This can be explained by weakening of additional (van der Waals) interactions between the carbon shells of neighbouring fullerenes in MHDF-C_{40}. Similarly to MHDF-C_{28}, self-intercalation of HD-C_{40} leads to a noticeable increase (by a factor of 2.1) in the elastic modulus, however, the elastic modulus of MHDF-C_{40} is almost half that of MHDF-C_{28}.

Analysis of the energetic stability of the hypothetical phases HD-C_{28} and MHDF-C_{28} compared to other possible crystalline phases based on other C_n fullerenes ($n \neq 28$) is an important task immediately related to estimation of the possibility of their synthesis. Selected properties of HD were compared with those of crystalline phases BCC-C_{20} and FCC-C_{60}.[130] It was established that the stability and properties of such phases are determined by two factors, namely, the type of bond hybridisation in fullerenes and the type of

the fullerene–fullerene interaction during their condensation in crystal. For instance, the bond configurations of carbon atoms in the BCC-phases of C_{20} fullerene (most unstable fullerene in the molecular state) are similar to sp^3. Among the fullerites considered above, BCC-C_{20} is characterised by the maximum density and elastic modulus. The properties of this crystal (including the binding energy) depend on the interactions between C_{20} fullerenes. The reverse is the situation with FCC-C_{60}, namely, free C_{60} fullerenes are characterised by maximum stability, and weak $C_{60}-C_{60}$ bonds make a small contribution to the energy of FCC-C_{60}.

From this point of view hypothetical phases based on C_{28}, C_{34} and C_{36} (Refs 132–134) can be treated as intermediate ones, because their total energies will be determined by competition between the intra- and inter-fullerene carbon–carbon bonds. However, the stabilities of these molecules are significantly different depending on the type of packing to, *e.g.*, graphite-like or clathrate structures. In particular, high stability of hexagonal clathrate is due to formation of sp^3-bonds between all atoms.[133]

7. Lattices built of different C_n clusters

Synthesis under nonequilibrium conditions can result in simultaneous formation of C_n clusters with different n values, suitable for the design of various structures. For instance, C_n clusters deposited on a substrate surface can form either disordered (amorphous) films or various close-packed lattices.[135,136] An example is provided by hypothetical clathrate structures based on C_{20}, C_{24} and C_{46} clusters.[31] The characteristic features of such lattices are as follows: a large number of atoms in the unit cell, large lattice parameters and large molecular voids. For example, the unit cell of a face-centred close-packed (FCCP) lattice built of the C_{120} and C_{48} molecules contains a total of 168 carbon atoms. These lattices are similar to those of zeolites and other minerals that are also built of atomic polyhedra.

8. Schwarzites

Embedding pentagons C_5 and heptagons C_7 into a flat graphene sheet is followed by the formation of local convex regions with positive and negative curvature, respectively. Therefore, the topologies of fullerene or nanotube structures can be varied by introducing carbon pentagons and heptagons into them. Corresponding nanoforms of carbon (Fig. 5) were called schwarzites.

An example of a negative-curvature carbon nanostructure is provided by the simple cubic schwarzite P192 (density 1.16 g cm^{-3}) having 192 carbon atoms in the unit cell.[138] Yet another type of schwarzite structures is presented by schwarzite D168,[139] which has a simple cubic lattice (ρ = 1.2–1.3 g cm^{-3}) and the unit cell comprised of schwarzones containing 56 hexagons and 24 isolated heptagons. Schwarzite P216 also has a simple cubic lattice (ρ = 1.02 g cm^{-3}) and the unit cell built of schwarzones containing 80 hexagons and 24 isolated heptagons.[140]

9. Toroids

A class of giant C_n ring molecules (toroids) that can be obtained by, *e.g.*, joining nanotubes at ends was proposed.[141,142] To date, such structures have been synthesised [143] and detailed studies of their electronic, magnetic and mechanical properties were also reported.[144–151] A mathematical theory of toroidal structures has been developed.[152,153]

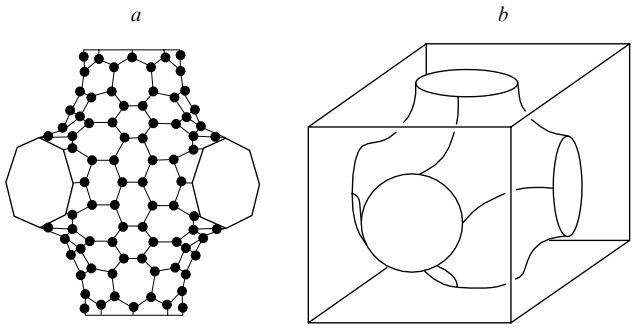


Figure 5. Structures of schwarzone, a negative-curvature fullerene (*a*)[137] and schwarzite, a crystal built of schwarzones (*b*).

10. Tubular nanostructures

In addition to 2D and 3D carbon nanostructures based on C_n fullerenes, new 2D- and 3D-materials based on carbon nanotubes have been synthesised (or hypothesised). Similarly to fullerene crystals, tubular associates can be divided into two groups. One group includes molecular associates (nanotube bundles, bunches, ropes or tubular crystals) in which neighbouring tubes are held together by weak van der Waals interactions. The other group comprises associates of covalently bonded nanotubes in which neighbouring tubes are linked through strong covalent C–C bonds. Similarly to isolated nanotubes the first group of associates retains the sp^2-type of bonding. The second group of nanostructures belongs to carbon nanoforms with mixed (sp^2+sp^3) type of chemical bonds.

Hypothetical tubular structures, *e.g.*, covalent lattices built of conjugated fragments of nanotubes can be considered a particular family of new 2D- and 3D-nanostructures.

a. Nanotube bundles. Nanotubular crystals

Depending on the method of synthesis of carbon nanotubes, reaction products can contain both isolated nanotubes and various nanotube associates.[63,68] Some nanotube bundles can form rings [154] or entangle with one another; this results in a dense film called 'nanopaper', which exhibits very interesting properties.[155–157]

In some cases, close-packed associates of aligned nanotubes were obtained.[158–160] In turn, certain nanotube bundles can form associates,[161] namely, a specific kind of self-associates called bundle arrays (Fig. 6).

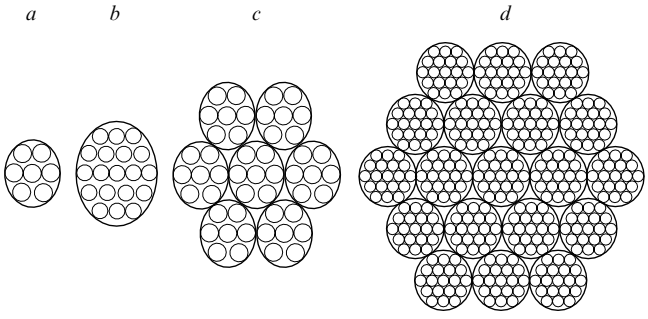


Figure 6. Cross-sections of individual carbon nanotube bundles (*a*, *b*) and their possible self-associates (*c*, *d*).[161]
Chirality indices of carbon nanotubes: (7,0) (*a*) and (19,0) (*b*).

Taking account of the aforesaid, the possibility for molecular crystals (periodically ordered nanotube assemblies) to exist was suggested. These 3D-materials were called 'nanotubular crystals' (NTCs). They can be grown from, *e.g.*, fullerene 'nuclei' forming an ordered structure on the substrate surface.

Nanotubular crystals are still a subject of theoretical research.[50, 84, 162] Usually, simulation of these structures involves consideration of various packing types of identical nanotubes resulting in the formation of, *e.g.*, hexagonal or tetragonal unit cells. The results of calculations are used for prediction of the relative stability and electronic properties of the simulated phases, on the nature of atom–atom interactions, *etc*. Nanotubular crystals are treated as possible matrices for various intercalation processes.

Association of nanotubes into bundles is accompanied by maifestation of an interesting effect, namely, polygonisation of nanotube cross sections (faceting of walls), *i.e.*, the morphology of nanotubes changes from ideal cylindrical to prismatic one.[163–166] The effect is due to energy gain upon the formation of quasi-planar areas between the walls of neighbouring tubes; as a consequence, the interaction between tubes in the bundle becomes stronger. A similar effect can also be attained under hydrostatic pressure.[167, 168]

To date, the mechanical,[165–175] electronic and energetic,[176–181] superconducting[182, 183] and thermal[184] properties of nanotube bundles have been studied quite thoroughly. Researchers also have paid attention to the description of molecular adsorption on the external surface of nanotube bundles,[185] intercalation of molecules between nanotubes[186] and to consideration of more complex composite materials based on nanotube bundles.[187]

Nanotubular associates mentioned above are treated as noncovalent (molecular) systems in which nanotubes interact with one another through weak van der Waals forces. Both the associates and their constituents (individual nanotubes) are essentially anisotropic systems.

Models for isotropic molecular crystals formed by packing individual carbon nanotubes into a structure shown in Fig. 7 have been proposed.[188] Preliminary calculations revealed a negative difference between the energies of formation of nanotubular crystals and those of isolated nanotubes. This means that compaction of nanotubes to form the lattices suggested is energetically favourable.

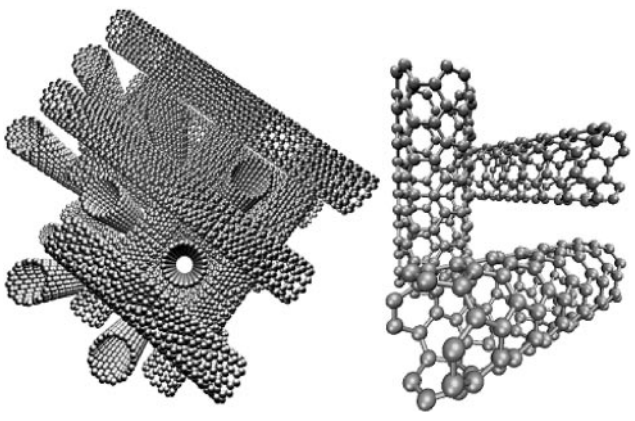


Figure 7. Fragment of cubic isotropic molecular crystal formed by packing nanotubes (*a*) and its unit cell (*b*).[188]

According to calculations,[188] the bulk elastic modulus of such crystals can be very high (up to 550–650 GPa). In addition, a crystal obtained by compacting individual nanotubes retains their conductivity type (metal or semiconductor).

It was assumed[188] that nanotubular crystals can be obtained by stacking horizontally aligned layers comprised of individual nanotubes on an ordered system of vertically aligned identical nanotubes arranged at a specified distance from one another. Such systems are available at present.[189] Clearly, the technique allows one to obtain molecular crystals including non-cubic (*e.g.*, hexagonal) ones or crystals built of multilayer nanotubes, nanotube bundles or based on different-composition nanotubes, *e.g.*, BN, $B_xC_yN_z$, *etc*.

b. Covalently bonded associates of nanotubes. Nanofoam

A special group of nanotubular 2D- and 3D-materials [carbon nanoforms with mixed (sp^2+sp^3)-bonds] includes covalently bonded nanotube associates. The onset of covalent sp^3-interactions between neighbouring tubes[190] is governed by some factors (external pressure, temperature, nanotube size, presence of structural vacancies in nanotube walls) which have been studied in considerable detail for pairs of contacting nanotubes.[191–193] Note that covalently bonded nanotube and fullerene assemblies also belong to the (sp^2+sp^3)-nanostructures under study.

The energy of covalent carbon–carbon sp^2-bonds in nanotube wall ($\sim$0.2 eV per atom) is higher than that of the interaction between neighbouring tubes ($\sim$15 meV per atom).[163, 194, 195] It is assumed that, similarly to the interaction between neighbouring walls in multilayer nanotubes,[196] the formation of additional covalent sp^3-bonds between walls of neighbouring tubes in a bundle affects not only the electronic properties, but also the cohesive and mechanical characteristics, just as the formation of interlayer sp^3-bonds in graphite (under, *e.g.*, neutron irradiation)[197] causes its shear modulus to increase.[198]

Simulation[199, 200] of formation of covalent sp^3-bonds in a nanotube bundle upon compression and heating showed that small-diameter nanotubes most readily undergo polymerisation (these systems can be the most probable candidates for the design of superhard tubular 2D- and 3D-materials). There exists a critical external pressure,[199] such that at higher pressures large-diameter nanotubes are transformed to scroll-like nanostructures while small-diameter nanotube scrolls undergo graphitisation. Such assemblies are characterised by various types of nanotube distortion and configurations of intertubular C–C-bonds (Fig. 8).

A number of regular 3D-structures built of covalently bonded nanotubes was proposed.[190, 193, 201, 202] Electronic structure calculations showed that the forbidden gaps of these materials depend on the type of polymerisation of individual nanotubes, namely, they increase as the number of intertubular sp^3-bonds increases. Noteworthy is the structure of a 'nanotubular clathrate' based on (6,6)-tubes,[202] here all sp^3-atoms have a coordinaton number of 4. Preliminary calculations[201] showed that regular crystals built of covalently bonded nanotubes are less stable than graphite or isolated nanotubes.

Yet another kind of covalently bonded (sp^2+sp^3)-nanoforms is provided by model nanofoams[203–206] representing specific nanotextured carbon materials.[207–211] Nanofoam models (note that the actual structure of these materials can

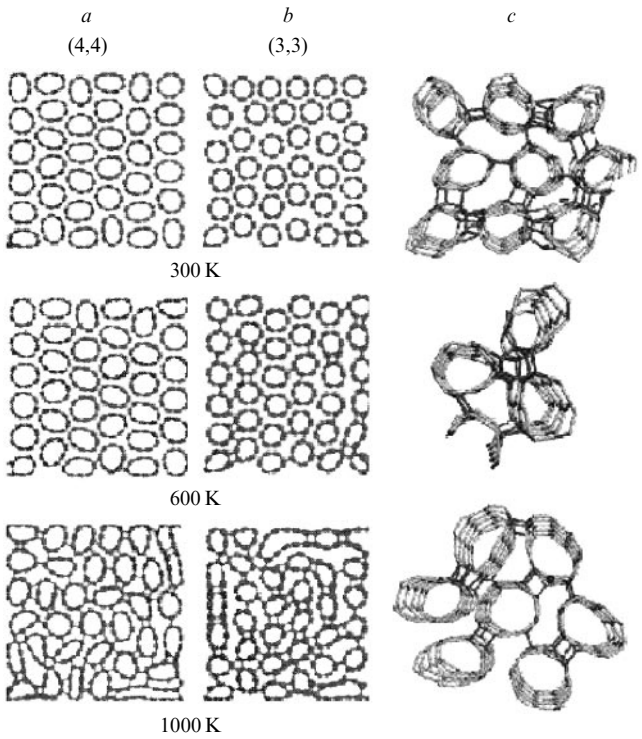


Figure 8. Polymerisation patterns of assemblies of (3,3)- and (4,4)-carbon nanotubes on heating (*a*, *b*) and selected types of intertubular covalent bonds (*c*).[199]

be much more complex[206]) represent[203] porous structures (Fig. 9) comprised of graphite-like nanoplatelets with sp^2-bonds linked by C(sp^3) atoms. Such systems are stable. Similarly to nanotubes, nanofoams can exhibit metal-like or semiconductor properties depending on their structure (armchair or zigzag); their elastic moduli can vary from 5 to 300 GPa[203] depending on the ratio of graphite-to-diamond-like segments.

c. Nanotube lattices. Supertubes

The ability of nanotubes to form Γ-, T-, Y- and X-shaped junctions[48–51,212–214] was used[215] to simulate various regular 2D (graphite-like) and 3D (diamond-like) covalent lattices. The electronic and mechanical properties of nanoforms having these lattices were predicted.[215] These properties depend first of all on the lattice symmetry. Note that all carbon atoms in the lattices have a coordination number of 3 and an sp^2-like bond configuration. This fundamentally distinguishes the systems in question from the covalently bonded ($sp^2 + sp^3$) tubular 2D- and 3D-nanosystems mentioned in the preceding subsection.

An interesting example of structures built of nanotube fragments with Y-junctions is provided by the so-called supertubes (Fig. 10).[216–218] Schematically, the formation of supertubes can be illlustrated by replacing each C–C bond in a conventional nanotube by a nanotube fragment, or by rolling a cylinder from a graphite-like nanotube lattice. Atomic models of some supertubes were used for studying their electronic and mechanical characteristics.[193–195] Hypothetical supertubes are classified as tubular nanostructures with sp^2-bonds.

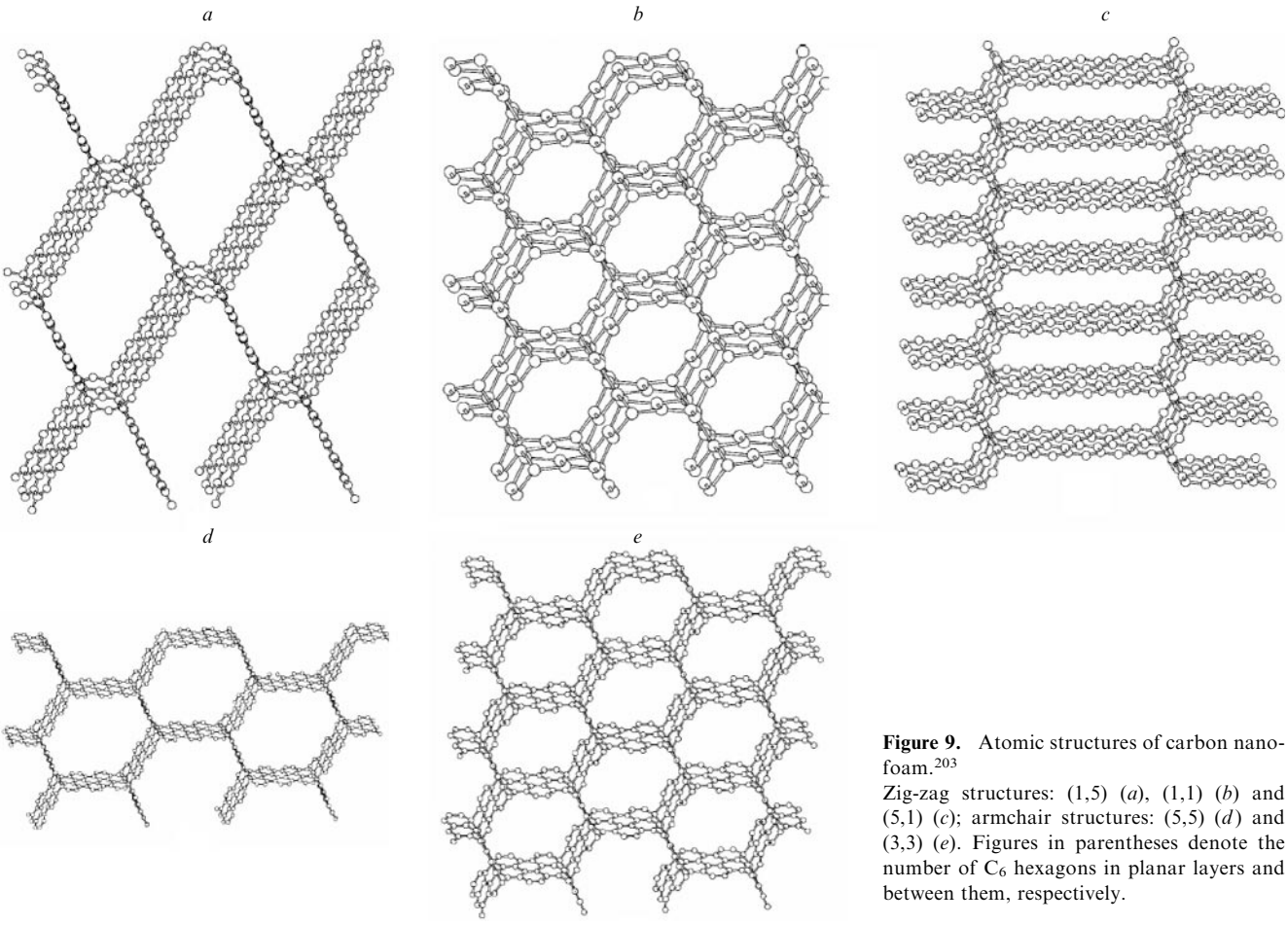


Figure 9. Atomic structures of carbon nanofoam.[203]
Zig-zag structures: (1,5) (*a*), (1,1) (*b*) and (5,1) (*c*); armchair structures: (5,5) (*d*) and (3,3) (*e*). Figures in parentheses denote the number of C_6 hexagons in planar layers and between them, respectively.

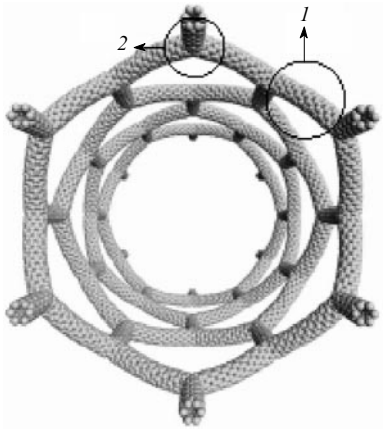


Figure 10. Fragment of supertube structure .[216] Conventional nanotube (*1*) and Y-junction (*2*).

11. Hexagonal carbynes and chaoite

The synthesis and structure of carbynes have been debatable in the scientific literature since the discovery† of these systems up to the moment. It is assumed that carbyne is built of long weakly interacting linear chains including about 10^3 carbon atoms with alternating $-C\equiv C-C\equiv C-$ (α-carbyne) or double $=C=C=C=$ (β-carbyne) sp^1-bonds.[6] However, according to one of the authors of the discovery, '... unfortunately, no rigorous and structurally unambiguous proofs of the existence of carbynes are available as yet'.[6] The structure of carbyne was, in particular, represented by linear chains copolymerised through one atom, which form a 'quasi-nanotube' similar to a square-shaped well.[219] Yet another carbyne structure [220, 221] was represented by an ordered array of aligned, folded carbon chains which form a tetragonal 2D-lattice with the parameters $a = 0.460$ nm and $b = 0.746$ nm. A variety of carbynes with other structures were designed using the graph theory; however, no mutual consistence between the structure, parameters and density was obtained for them. Sometimes carbynes are confused in the literature with chaoite discovered [222] in gneiss samples from the Ries crater (Germany). Chaoite has a hexagonal lattice with the lattice constants $a = 0.8948$ nm and $c = 1.4078$ nm,[2, 91] whereas the carbyne lattice constants are $a = 0.892$ nm and $c = 1.536$ nm.[2, 223] Turbostratic carbyne (new cubic superhard carbon allotrope) [224] has the lattice constant $a = 1.46970$ nm;[225] unfortunately, no unit-cell type was reported.

Hexagonal carbynes can be constructed only from hexagonal clusters or fullerene molecules (C_{36} and C_{72}) rather than cubic (C_{24}, C_{48}) or icosahedral (C_{60}) ones. Hexagonal polycrystalline powders and films tentatively composed of a mixture of C_{36} and C_{60} molecules were synthesised in arc discharge.[226] The proposed structure of these substances contains complexes $C_{60}/7C_{36}$ (C_{60} fullerene is surrounded by seven C_{36} molecules; intermolecular distance is 0.668 nm). These complexes are only suitable for forming molecular rather than close-packed crystals. Note that the C_{36} fullerenes are metastable because the steric angles (120°, 60°, 60°, 60°) deviate from the equilibrium value of 109.47°.

Theoretical analysis showed that linking C_{36} molecules through faces causes their 'opening' and transformation to rings built of strips with the unit cell of (6,0)-nanotube. From this it follows that hexagonal carbynes have the same unit cell as the (6,0)-nanotube. This assumption is confirmed by chemical inertness of carbynes towards oxidants, which indicates diamond-like sp^3-bonds between nanotubes rather than sp^1-bonds between linear chains.

A variety of hexagonal nanotube crystals of different diameter, length, chirality, packing type and intertubular bonds can be simulated. For instance, molecular crystals comprised of aligned, high pressure-copolymerised nanotubes forming a 2D honeycomb hexagonal structure were reported.[226] A 2D structure built of long aligned (6,0)-nanotubes covalently bonded through adjacent faces was proposed.[227, 228] This type of nanotube crystals seems not to be improbable, but this is clearly not crystalline 3D-carbynes.

IV. Nanodiamonds

A large group of carbon nanoforms known as nanodiamonds comprises various nanostructures containing carbon atoms with a coordination number of 4 typical of crystalline diamond and sp^3-like bonds. Nanodiamonds include quasi-0D and quasi-1D structures, which in turn can be monolithic [so-called diamond-like nanocrystallites (DLNC) and diamond-like nanofibres (DLNF) [56, 84, 229–237]] or hollow. Nanodiamonds were first obtained in 1960 by detonation of explosives in a closed volume; therefore, they are also called ultradisperse detonation diamonds.[229–231]

1. 0D-Nanodiamonds

0D-Nanodiamonds of mineral, artificial and interstellar origin are best studied. The smallest (about 1 nm) diamond-like hydrocarbon clusters were isolated from oil. These 'diamond molecules', known as diamondoids, represent cage structures comprised of a few tens of carbon atoms and having terminal hydrogen atoms and a mixed ($sp^1 + sp^3$) type of bonds. Diamondoids, in particular $C_{26}H_{32}$ and $C_{35}H_{36}$, show a variety of shapes including rods, disks, pyramids, helicoids, *etc*. They are divided into higher (particle size up to 1–2 nm) and lower ones (particle size less than 1 nm) (Fig. 11). Diamondoids can form molecular crystals belonging to orthorhombic, triclinic or monoclinic systems. They have not been synthesised so far and mechanisms of their formation are still unclear.

Natural diamond-like nanocarbon in the form of sp^3-clusters (particle size less than 10 nm) is known. These clusters can forn disordered aggregates of size to a few micrometres, which represent the so-called mineral amorphous diamond-like carbon.[232]

Meteoritic 0D-nanodiamonds are constituents of interstellar dust; they attract the attention of researchers as cosmochemistry objects that allow one to study specific features of nuclear and physicochemical processes beyond the Solar system.[233, 234] Next we will consider the structure and properties of the key groups of diamond-like nanostructures.

† USSR Discovery Certificate No 107 (19.03.1973) for the discovery 'of the existence of new crystalline form of carbon called carbyne, which is characterised, in contrast to diamond and graphite, by a chain (linear) structure of carbon macromolecules' was given to researchers from the Institute of Organoelement Compounds, USSR Academy of Sciences A M Sladkov, V I Kasatochkin, V V Korshak and Yu P Kudryavtsev.

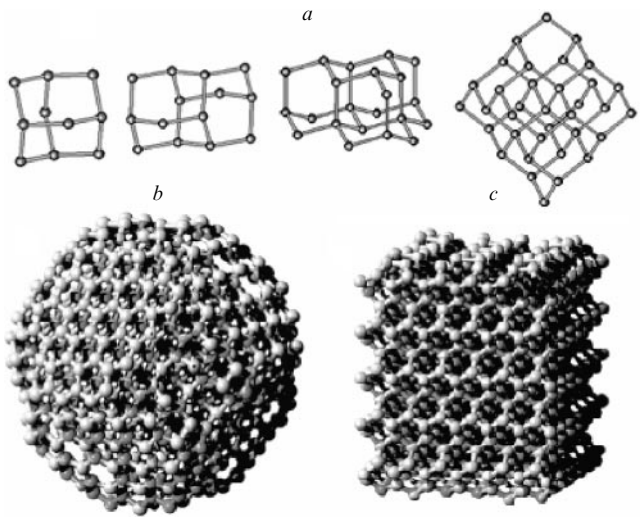


Figure 11. Nanodiamonds.
Four lower diamondoids (*a*)[238] and main morphological types of diamond nanocrystallites: spherical grains (*b*) and polyhedral particles (*c*).[239]

2. Diamond-like nanocrystals

There are two main types of DLNCs with respect to their morphology, non-spherical (fullerene-like) and polyhedral ones. The latter type comprises diamond-like particles (grains) faceted in various (octahedral, cubooctahedral or pentagonal) manner.

Attempts to elucidate subtle details of the atomic structure of DLNCs, to establish how their stability depends on the morphology, grain size and other factors (*e.g.*, hydrogenation or heat treatment of the surface) were carried out using quantum chemistry and molecular dynamics methods. The mechanisms and conditions for nanodiamonds $\leftrightarrow$ fullerenes phase transformations were analysed and the effect of various impurities on the stability and electronic properties of DLNCs was also studied.[238, 239] A series of studies aimed at establishing correlations between changes in the atomic structure and stability of DLNCs and the particle size, crystallite morphology and thermal conditions was carried out.

The particle size belongs to the key parameters determining the morphology and phase stability of the 0D-nanoforms of carbon. The dependence of the morphology of carbon nanoparticles on their size (number of atoms or mean diameter, d) was studied in the framework of thermodynamic models.[240–244] According to the results obtained, preferred formation of sp^3-DLNCs will occur for particles containing from $\sim$1100 to $\sim$25 000 atoms. Beyond this interval, the sp^2-nanoforms of carbon including fullerenes (onions) and nanographites are more stable. This is in agreement with the results of calculations[245–247] in which the energies of the sp^3- (nanodiamonds) and sp^2-nanoforms of carbon (onions and nanographites) were estimated and compared and the 'scale' for their phase stability was proposed. According to the results obtained, the formation of sp^3-diamond-like grains can be expected at particle sizes in the interval $1.9 < d < 5.2$ nm. Particles of paricular diameters ($1.7 < d < 2.2$ nm) can have intermediate ($sp^2 + sp^3$) structures built of diamond-like cores surrounded by fullerene shells.

The relative stability of DLNCs is governed by not only the particle size, but also their morphology. A comparison of the energy estimates of non-spherical or polyhedral (octahedral, cubooctahedra or cubic grains) diamond-like nanoparticles revealed[243] significant structural rearrangements due to changes in the type of atomic coordination (electronic configuration) from fourfold (sp^3-type) to threefold (sp^2-type) in all polyhedral particles. Structural rearrangements are most pronounced for the carbon atoms in the outer layer of grains, which makes it possible to consider 'graphitisation' of the outer shells of diamond grains.

When synthesising diamond-like nanoparticles, hydrogen is often present in the atmosphere within reactors.[48, 49, 51, 55, 56, 84, 248, 249] The passivating action of hydrogen atoms on 'pendant' bonds formed by the outer atoms of DLNCs is an important factor of stability control of their morphological forms.[56, 84, 243, 250–254] Analysis of the structures and energy states of hydrogenated DLNCs showed that the formation of hydrogen shells precludes the nanodiamonds $\rightarrow$ onions transformations characteristic of 'pure' DLNC (see reviews[56, 84, 243]).

External factors including temperature, pressure, irradiation, *etc.* are of great importance in performing and controlling sp^3-nanodiamonds $\leftrightarrow$ sp^2-onions interconversions.[255–262] For instance, heat treatment can lead to graphitisation of DLNCs and formation of onions. The reverse process, *i.e.*, degradation of the cage structure of onion shells and their transformation to DLNCs can be conducted under irradiation.

The conditions and mechanisms of nanodiamonds $\rightarrow$ onions transformations were predicted.[263–268] For instance, in a molecular dynamics study[265] 'heating' of DLNCs (particle size from 1.2 to 1.4 nm) to 3000 K was followed by passing additional energy pulses to the system, which simulated its radiation treatment. In the first step, sp^3-DLNC transformed to a hybrid structure comprised of a fullerene sp^2-shell with a diamond-like sp^3-core inside. The final structure represented an sp^2-onion. In other words, the thermal- and radiation-induced transformation DLNC $\rightarrow$ onion begins with rearrangement of the 'surface' of nanodiamond and then propagates into its 'interior'. Radiation-induced defects cause cleavage of sp^3-bonds, thus favouring a decrease in the barrier to thermal activation of this phase transformation.

In addition to the factors mentioned above, the stability of DLNCs is also affected by their size, the sign of charge (anionic or cationic form),[269] external pressure,[270] chemical composition, impurities (in particular, the effect of boron and nitrogen impurities on the stability of DLNCs was studied[239, 271–273]).

Electronic spectra calculations of diamond-like nanoparticles revealed a rather complex spectrum of 'pure' DLNCs, which can be represented by a superposition of electronic states of nonequivalent sp^3- and sp^2-atoms in the diamond-like core and fullerene-like shell, respectively (Fig. 12). In the electronic spectrum of DLNCs the filled valence band A and the conduction band C are composed of the 2p-orbitals of the sp^3-atoms, whereas the near-Fermi states (band B) are formed by the 2p-orbitals of the 'surface' sp^2-atoms. The spectra can have both the semiconductor (forbidden gap > 0) and metal-like (zero forbidden gap) type, however, no regular dependence of the forbidden gap of crystallites on the particle size and morphology was revealed. The electronic spectrum of nanodiamond grains passivated by hydrogen has a semiconductor type.[274] As the

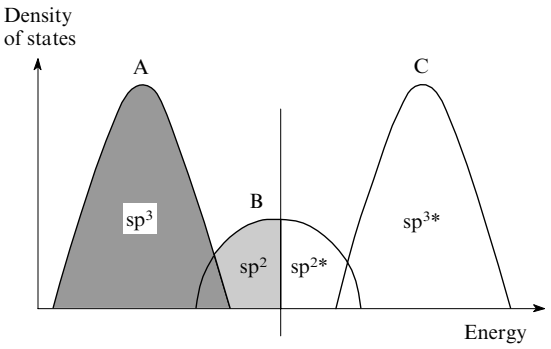


Figure 12. Electronic spectrum of diamond-like nanocrystallites (schematic).
Shown are the energy regions of localisation of the filled and free (asterisked) 2p-orbitals of structurally nonequivalent carbon atoms forming diamond-like sp^3-core and sp^2-grain shells. The vertical line corresponds to the Fermi level.

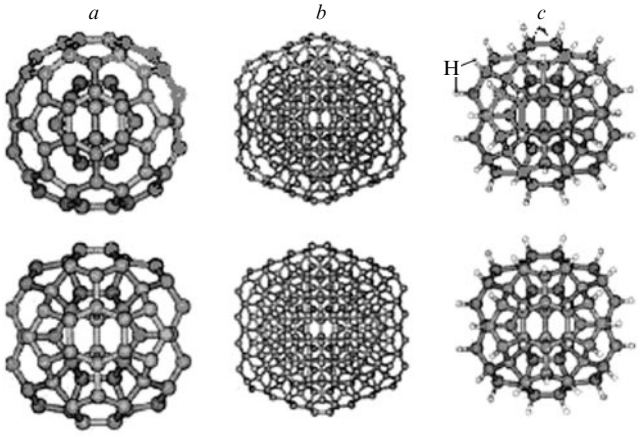


Figure 13. Structures of icosahedral diamond-like nanoparticles before relaxation (lower row) and after geometry optimisation (upper row).[277] C_{100} (*a*), C_{600} (*b*) and $C_{100}H_{60}$ (*c*).

crystallite size increases, the forbidden gap noticeably decreases and approaches the forbidden gap of crystalline diamond ($\sim$5.5 eV) for the particles containing more than 1500 atoms (average grain size $\sim$2.5 nm).

Artificial nanodiamonds have found application in many inductries, such as power engineering and electronics, as well as in biology, pharmaceutics and medicine. In particular, it was proposed to use them as antifriction or abrasive materials, as precursors in growing diamond films and for obtaining of polycrystalline diamonds and reinforcing coatings.

3. Icosahedral nanodiamonds

Structural models for novel carbon nanoforms have been developed.[275–277] They were constructed by joining icosahedral particles in which all carbon atoms have the sp^3 tetrahedral coordination. These spherical particles called icosahedral nanodiamonds (INDs) form a homologous series C_n (n = 100, 280, 600, 1100, 1820 ...). The stability of INDs was compared with that of cage sp^2-structures based on a small fullerene C_{20} (I_h -onions having the same number of atoms as the INDs) in terms of energy characteristics.[277]

Considering small particles (d < 3.3 nm), it was found that cage particles (I_h-onions) are energetically more favourable. As d increases, the relative stability of INDs increases and icosahedral nanodiamond particles become the most stable particles at d > 3.3 nm. Qualitatively, this fact can be explained by the decrease in the proportion of surface atoms with pendant bonds, which leads to enhanced stability of sp^3-nanocrystallites. At a particle size of about 3.3 nm, the total energies of icosahedral sp^2- and sp^3-nanoforms become comparable; at the same time both types of nanoparticles are metastable towards crystalline carbon allotropes. The relative stability of icosahedral sp^2- and sp^3-nanoforms was also estimated[277] with allowance for structure relaxation (possibility of $sp^2 \leftrightarrow sp^3$ interconcersion). A stable form of C_{100} particles is a $C_{20}@C_{80}$ two-shell onion (Fig. 13). As the number of particles increases, INDs do not completely transform to onions and the resulting clusters have intermediate structures.

Saturation of bonds of the surface atoms with hydrogen precludes[277] 'separation' of diamond-like particles C_nH_m into fullerene-like fragments. It is assumed[255] that by varying the degree of hydrogenation of icosahedral nanodiamonds one can control their stability, morphology and parameters of electronic spectrum. This may be quite important when using INDs as components of galvanic coatings, polymeric composites or emitter materials.

4. Diamond-like nanofibres

A large group of sp^3-nanoforms of carbon includes extended monolithic diamond-like nanofibres.[84, 235–237, 278] They are synthesised under laboratory conditions by chemical vapour deposition on nuclei (nanodiamonds) in the presence of catalysts, by plasma treatment (various regimes) of polycrystalline diamond films, from graphite-like nanotubes and using other techniques. Depending on the synthetic procedure and regime, one can obtain either individual DLNFs or their ordered assemblies; the fibres can have various morphologies and their diameters vary from tens of nanometres to a few tens of micrometres. Diamond-like nanofibres attract the attention of researchers first of all as alternative (compared to nanotubes) extended nanostructures with unusual mechanical and thermal properties.

In addition to 0D- and 1D-nanodiamonds (nanocrystallites and nanofibres, respectively) there are two groups of carbon nanomaterials containing carbon atoms with a coordination number of four and the sp^3-type of bonds. These are the so-called diamond-like nanotubes whose walls are built of $C(sp^3)$ atoms and a family of carbon–carbon composites including nanodiamond constituents.

Unlike conventional nanotubes whose walls are made of graphene sheets,[48, 49, 51] the walls of the synthesised diamond-like nanotubes consist of diamond nanograins.[277]

The morphology, atomic structure and stability of DLNFs have been studied.[235–237, 279–281] The stability factors and electronic structure of thin nanofibres (with cross-sections S in the range $5 < S < 280$ Å^2) were analysed as functions of their morphologies and size.[281] Three groups of DLNF (I–III), 'cut' from a diamond crystal normal to the (001), (111) and (110) planes, (Fig. 14), were considered. It was established that Group I DLNFs, for which structural relaxation mainly affects positions of the outer carbon atoms having the maximum number of pendant bonds, are characterised by the smallest structural distortions compared to the initial ideal diamond-like structure. The situation with Group II DLNFs is fundamentally different.

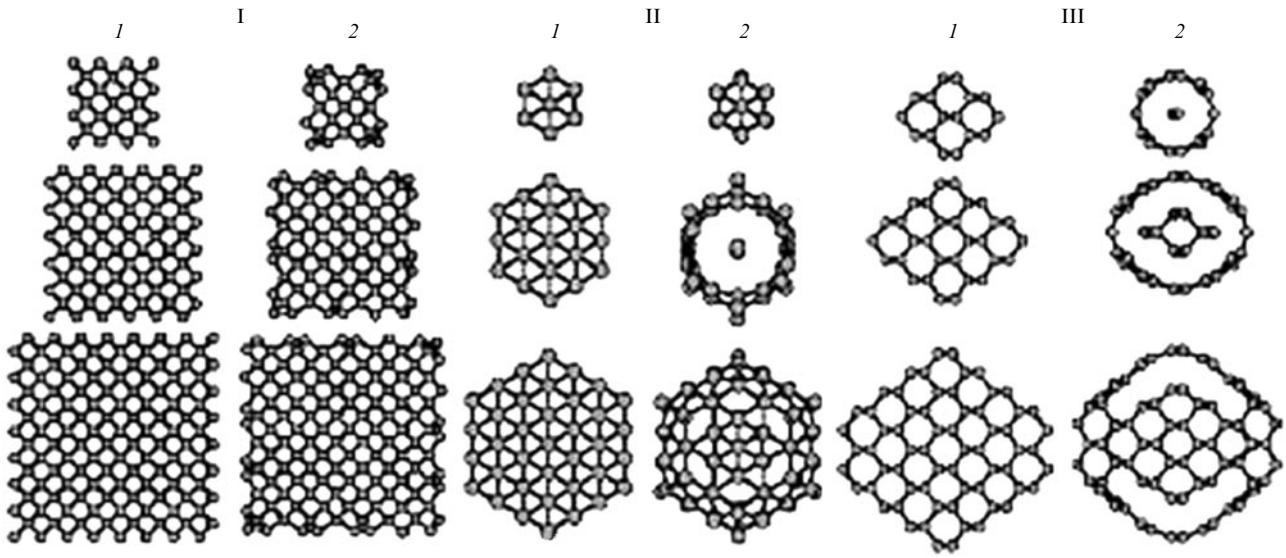


Figure 14. Initial (*1*) and optimised (*2*) atomic structures of cross-sections of diamond-like nanofibres.[281]
I – III denote structural types (see text).

Here, hollow (tubular) nanostructures containing axially aligned chain motifs of carbon atoms are formed within thin ($S < 25$ Å^2) nanofibres. The walls of the distorted nanotubes are built of both various carbon polygons and linear atomic chains. Stabilisation of the diamond-like structure of Group II DLNFs is achieved at $S > 40-50$ Å^2. Particularly interesting is the type of structural relaxation in Group III DLNFs (see also Refs 213 – 215). The thinnest nanofibres considered (up to $S \sim 110-120$ Å^2) exhibit separation in such a fashion that the outer layers undergo 'graphitisation' with the formation of nanotube walls (or fragments of walls) containing encapsulated thinner diamond-like nanofibres (see Fig. 14). These hybrid ($sp^3 + sp^2$)-nanostructures combine the atomic types of 1D-nanostructures, namely, hollow graphite-like sp^2-tubes and monolithic sp^3-fibres, and can be considered as 1D-analogues of the hybrid 0D-nanostructures (diamond-like cores encapsulated in fullerene shells) mentioned above.

The stabilities of all types of DLNFs noticeably increase as their cross-section areas increase.[235 – 237, 279 – 282] At the same time the stabilisation mechanisms are fundamentally different. For thin DLNFs the number of surface atoms having a coordination number of less than four is larger than or comparable with the number of sp^3-atoms 'in the bulk' of the fibre. Structure stabilisation of these systems is due to partial graphitisation and formation of hybrid ($sp^3 + sp^2$)-nanoforms. Contrary to this, more massive DLNFs having a larger number of inner C(sp^3) atoms retain their initial diamond-like structure, whereas structural relaxation mainly affects atoms in the outer layer.[280]

All diamond-like fibres contain not only the main C(sp^3) and C(sp^2) atoms, but also a proportion of carbon atoms with other bond configurations. In addition, different DLNFs contain different sets of nonequivalent types of C – C bonds. The electronic spectra of these nanostructures represent superpositions of the states of individual nonequivalent atoms (atomic groups) and correspond to semiconductor or metal-like type depending on the fibre size and morphology.[260]

Studies aimed at estimating the stabilities of DLNFs compared to those of other carbon nanoforms (first of all, commensurate nanotubes) are available.[235 – 237, 279] It was found that DLNFs will be more stable than nanotubes in a limited interval of cross-section diameters (from 2.7 to 3.7 – 3.9 nm).[236] It should be emphasised that these estimates are averaged. Both the upper and lower bounds of this interval can differ significantly for DLNFs with different morphologies and crystallographic orientations.

Hydrogenation is one of the most important factors affecting the stability of DLNFs. Coverage of the DLNF surface with hydrogen atoms can be done separately or immediately during the synthesis provided that hydrogen is present in the reaction zone.[235, 237] Generally, hydrogenation of DLNFs leads to considerable decrease in relaxation distortions of the atomic 'shell' of nanofibres; this is quite understandable taking into account the role of hydrogen atoms that close the broken bonds of the carbon atoms in the outer layer of the nanofibre.

A study on regularities of changes in DLNF stability as function of their morphology, size, and degree of hydrogenation (H : C atomic ratio) has been reported.[235] The heats of formation of hydrogenated nanofibres were estimated using the relation

$$\mathrm{d}H(\mathrm{DLNF}) = N_\mathrm{C}\mathrm{d}H^\circ(\mathrm{C}) + N_\mathrm{H}\mathrm{d}H^\circ(\mathrm{H}) - E_\mathrm{at},$$

where N_C and N_H are the numbers of carbon and hydrogen atoms in the fibre, $\mathrm{d}H^\circ$(C) and $\mathrm{d}H^\circ$(H) are the enthalpies of formation of corresponding free atoms from graphite and H_2 and E_at is the calculated atomisation energy of DLNF. It was established that the heat of formation of a fibre is proportional to the reciprocal radius of DLNF and that an increase in the $N_\mathrm{H}/N_\mathrm{C}$ ratio can lead to fundamentally different changes in dH values of groups of DLNFs of different morphology. Namely, either stabilisation of fibres (if the fibre size decreases) or their destabilisation [if dH(DLNF) increases] can occur. Some thin hydrogenated fibres were more stable than a carbon nanotube with a comparable $N_\mathrm{H}/N_\mathrm{C}$ ratio.

Additional information on the character of bonds in DLNFs is provided by the results of simulation of their mechanical stability (compared to that of nanotubes), which

was calculated with inclusion of forces required for destruction of these structures.[283] Small-diameter nanotubes are more stable than corresponding nanofibres; however, the reverse occurs as the diameter increases. This effect is simple to explain taking account of the energies of carbon–carbon bonds, namely, sp^3-sp^3-bonds in diamond are weaker than sp^2-sp^2-bonds in graphite. Therefore, nanotubes are more stable than DLNFs provided comparable numbers of interatomic bonds. As the diameter increases, the number of bonds in monolithic fibres increases much faster than in nanotubes; this is the reason for higher stability of DLNFs. At $d > 1.3-3.0$ nm, DLNFs become more stable than commensurate single-wall nanotubes.[283] Yet another interesting result of simulation of mechanical characteristics of DLNFs is that the 'core' is more stable towards external loads than the 'shell'. A similar effect was also obtained for multilayer nanotubes whose degradation under the action of external stress begins with breakdown of outer graphene cylinders.

The dependence of thermally induced distortions of the atomic structure of DLNFs on the surface area of their cross-sections, morphology and crystallographic orientation was studied.[263, 264, 282, 284, 285] These factors can give rise to manifestation of various atomic mechanisms of thermally induced structure deformations in DLNFs. The most characteristic is thermally induced amorphisation of the outer layer of DLNFs. At relatively low temperatures, the fibre represents a diamond-like rod covered with amorphous carbon shell. Raisng the temperature causes the shell to thicken and, at a particular critical temperature, the DLNF undergoes transformation to an amorphous fibre. Unusual mechanisms of thermal deformations were revealed.[282, 285] For instance, thin DLNF are transformed to quasi-1D structures composed of fragments of carbyne chains,[285] or heat treatment of thicker fibres causes them to separate into graphite-like cylinders,[282] which can unroll into strips on further heating. These structural rearrangements can be treated as thermally induced phase transformations $sp^3 \rightarrow sp^1$ and $sp^3 \rightarrow sp^2$, respectively.[286]

5. Diamond-like nanotubes

Unusual extended hollow nanostructures called diamond-like nanotubes (DLNTs) were fabricated.[287] Their walls have a diamond-like single-crystalline atomic structure. DLNT samples were grown by plasma-assisted chemical vapour deposition on polycrystalline diamond substrates in the presence of CH_4-H_2 mixture in the chamber. It was assumed [287] that the formation of DLNTs is due to coalescence of diamond-like nanocrystallites.

Models for the atomic structure of these nanotubes are available.[282, 286] Factors affecting their stability, electronic structure and thermal stability have been studied. It was established [282] that the atomic structure of DLNTs noticeably changes with an increase in the size of the inner cavity, namely, 'graphitisation' occurs (Fig. 15). As a result, the structure of the nanotube walls changes as follows: the diamond-like layer is covered from both sides with graphite-like layers. The nanotube wall stability decreases as their thickness decreases (in some cases, separation of thin films was observed). Therefore, the following qualitative conclusion was made:[282, 286] there is a critical size (thickness) of DLNT walls, which is comparable with the size of internal cavities; in this case the walls are still monolithic. In addition, DLNTs are energetically less stable than DLNFs at comparable cross-section surface areas. This can be understood with ease taking into account the fact that DLNTs contain a larger number of surface atoms. The thermal stability of DLNTs is also much lower than that of DLNFs:[264, 282] at 300 K, diamond-like nanotubes lose their

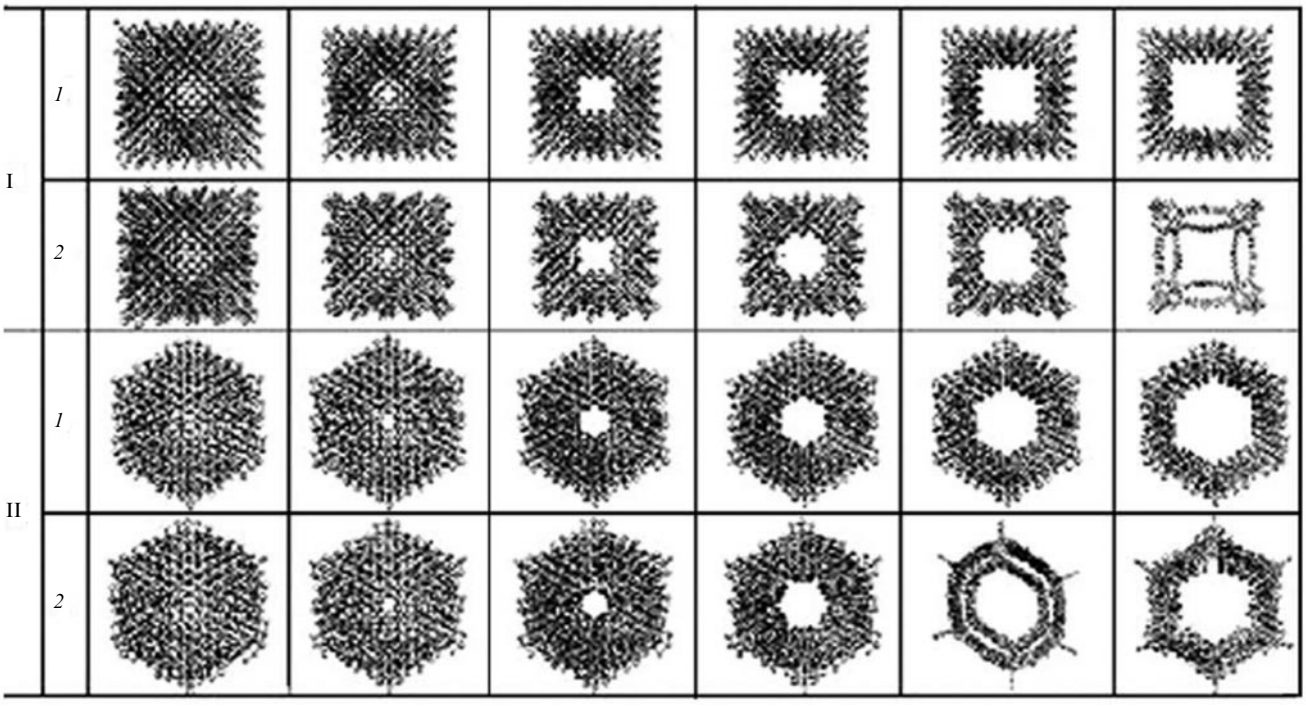


Figure 15. Atomic structures of cross-sections before (*1*) and after (*2*) structural optimisation of DLNTs with internal voids of different size.[282] I and II denote structural types (see text).

initial (at 0 K) shape; the walls of this system include various entanglements and clusters from carbyne chains.

6. Nanodiamonds as constituents of carbon–carbon composites

Nanodiamond crystallites and DLNF considered above can be constituents of various composite materials. A number of nanocomposites have been synthesised. They became the subject of theoretical analysis. In particular, considerable attention was paid to composite (or hybrid) nanostructures including DLNCs and graphite-like nanotubes. The aim of these studies is to design novel carbon–carbon composites with unusual properties due to combination of the characteristics of sp^3-DLNCs and sp^2-nanotubes.

Recently, carbon–carbon composites containing nanodiamonds have attracted the attention of researchers. In terms of dimension these objects can be considered as carbon (0D + 1D)-hybrids, *i.e.*, thay can include sp^3-diamond crystallites and sp^2-nanotubes as constituents. As an example, Fig. 16 presents the so-called nano-mushrooms. These systems are considered as possible prototypes of field emitters and nanodiodes.

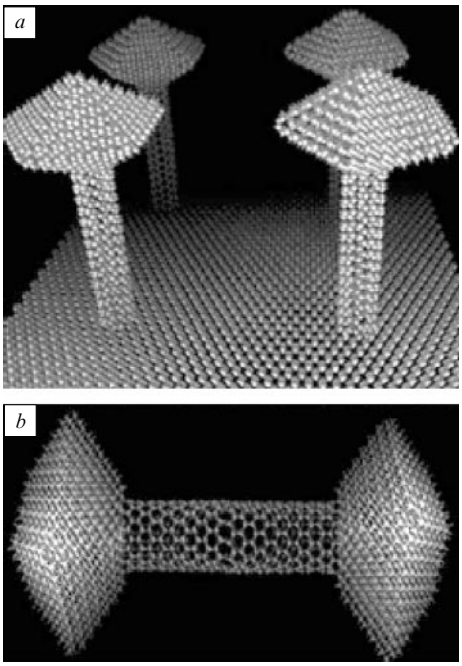


Figure 16. Atomic models of (0D + 1D) carbon composites (nanotube + nanodiamond grains) — prototypes of field emitters (*a*) and nanodiods (*b*).[288]

Yet another family of (0D + 1D)-nanostructures comprises composites made of bundles of single-wall graphite-like sp^2-nanotubes decorated by sp^3-nanodiamond particles from the outside.[289] In this case nanotubes are densely coated with well-faceted diamond-like crystallites of average size $\sim 20-100$ nm. It is assumed[289] that the formation of sp^3-crystallites on the surface of sp^2-nanotubes is due to nucleation occurring in the presence of reactive hydrogen atoms.[290–292] Under particular conditions, hydrogen can[293] 'create' defects in nanotube walls, which favours nucleation of sp^3-grains. It is assumed that these composites can be of interest as materials for production of cold cathodes, cathode ray tubes, light emitters or for micromechanics. The atomic structure and electronic properties of these composites have not ben studied in detail so far.

Yet another type of (0D + 1D)-nanostructures designed[238] in nanopeapod fashion (see also Section VI) represents a 1D-chain of nanodiamond sp^3-clusters confined within a carbon sp^2-nanotube. The crystallites considered included the smallest diamondoid (C_{10}), $C_{10}H_{16}$ (hydrogen-terminated C_{10}) as well as diamondoids with two, three or four diamond-like shells. The results obtained[238] suggest the possibility of polymerisation of clusters inside the nanotube and formation of new quasi-linear diamond-like polymers under particular conditions. In this case the nanotube cavity acts as nanoreactor.

Of course, the number of carbon–carbon nanocomposites containing diamond-like nanostructures is not limited to those considered above. For instance, one cas assume the existence of various (0D + 1D)-hybrids whose structures are composed of monolithic sp^3-DLNFs and sp^2-fullerenes, (1D + 1D)-hybrids (sp^3-diamond nanofibres + graphite-like sp^2-nanotubes) or (0D + 0D)-hybrids (sp^3-diamond crystallites + graphite-like sp^2-fullerenes), and some other structures.[162]

7. Concerning stability of nanostructures

Evaluation of the relative stability of various novel nanoforms of carbon is topical (for some estimates, see above). For instance, model calculations predicted that reduction of nanoparticle size is followed by transformation of 0D-graphite to 0D-nanodiamond (particle size about 5 nm) and subsequent stratification with formation of 0D-onions and fullerenes. Depending on their size, 1D-nanofibres can undergo transformation to nanotubes.

Size-dependent structural transformations of carbon nanoforms can be explained taking into account the fact that the key factors responsible for particle stability on the nanostructural level include the particle size (d), morphology and surface energy (γ) related by the Laplace equation

$$P = \frac{\gamma}{d}.$$

In the case of a liquid the parameter P can be treated as capillary pressure, which 'tends' to reduce the surface area and the total surface energy of the liquid. By analogy, the phase transition of nanographite to nanodiamond with a decrease in the particle size to $d^* \approx 5-10$ nm can be interpreted as equalisation of the total energies of both phases. In this case the surface tension is stronger than the bulk forces, which causes nanographite to shrink and transform to nanodiamond.

To explain the second transition (stratification and graphitisation of nanodiamond into onion), one should take into account the fact that the energy of sp^2-bonds in a graphite layer is higher than that of sp^3-bonds in diamond under normal conditions. The system tends to decrease the total energy of chemical bonds by increasing the surface area, which for graphite is larger than for diamond. Therefore, transformation of nanodiamond to an onion and an increase in the surface area with the decrease in the particle size to the critical value ($d^* \approx 2$ nm) can be explained by an increase in the bnding energy of the onion owing to the change in the surface itself and the surface energy (in nanodiamond, the surface atoms are bonded to the bulk atoms by three covalent sp^3-bonds; *cf.* three covalent intralayer sp^2-bonds in onion).

V. Non-graphite nanostructures

In addition to planar hexagonal graphitic sheet (graphene) there exist [294, 295] a variety of other networks built of conjugates including squares C_4, hexagons C_6, octagons C_8, decagons C_{10}, *etc.* having equal edges. These are, *e.g.*, the (4,6), (4,6,8), (6,10) networks, *etc.* Among them, one can select subsets of networks with atomic coordination numbers of 2 and 3 and a subset of cage structures with atomic coordination number of 4; they can serve models for sp^1-, sp^2- and sp^3-bonds in carbon 1D-chains, 2D-planes and 3D-crystals, respectively. If the angles between particular bonds differ only slightly from the equilibrium value (120°), these networks and cages can be obtained as metastable modifications of carbon. Now we will consider non-graphite layered nanoforms of carbon and models for nanostructures designed using atomic motifs of these phases, the so-called non-graphene fullerenes and nanotubes, which include pentaheptites, graphynes, haeckelites, *etc.*

Similarly to graphite, layered systems are built of planar atomic networks. In each network, atoms are bonded by strong covalent bonds. Neighbouring networks interact through weak (van der Waals type) bonds. A salient feature distinguishing these 2D-systems from graphene is that their atomic networks include various combinations of carbon rings $C_{n \neq 6}$.

Note that the presence of $C_{n \neq 6}$ rings in carbon nanostructures is well known. In particuar, pentagons C_5 are essential constituents of fullerene cage: for instance, C_{60} fullerene is comprised of hexagons and 12 pentagons. Fullerene-like structures with negative Gaussian curvature (schwarzites, see above) contain periodically embedded heptagons C_7 or octagons C_8. In addition, the introduction of pentagons, heptagons or other C_n rings as topological defects into walls (shells) of carbon nanotubes (fullerenes) is an efficient method of modification of their structures and properties and a promising method of search for new nanostructured forms of carbon.[36–43, 47–51, 56–58, 70–75]

1. Pentaheptites

The possibility for 2D non-graphite carbon nanostructures to exist can be substantiated using simple structural arguments. It is known that introduction of pentagons C_5 or heptagons C_7 into graphene sheet leads to its distortion. However, planar character of the network is retained if equal numbers of C_5 and C_7 are available.[296, 297] This can be achieved by, *e.g.*, the formation of a Stone–Wales defect,[298] which appears in the graphene sheet upon rotation of a C–C bond by 90°, namely, in this case four neighbouring hexagons are transformed to two pentagon–heptagon pairs (Fig. 17)

$$4\,C_6 \longrightarrow 2\,C_5 + 2\,C_7 .$$

A non-graphite 2D carbon allotrope formed by planar atomic networks containing $[C_5]_2$ 'clusters' surrounded by six heptagons was proposed.[296] This structure is built of pentagons and heptagons only, thus being called pentaheptite (PH). The energy of the pentaheptite network is higher, by about 0.3 eV per atom, than that of the graphite network; this is a metastable allotrope prone to transformation to graphite.[296] Pentaheptite has a metal-like electronic spectrum, the density of states at the Fermi level is rather high (about 0.1 eV^{-1} $atom^{-1}$). Taking account of the covalent type of atom–atom bonds, this allotrope can be treated as covalent metal. It is assumed [296] that PH can be obtained by pressure treatment of graphite or under the action of other physical (or chemical) factors capable of initiating the necessary rotation of bonds. In addition to highly symmetrical structure of pure PH network comprised of pentagons and heptagons only, researchers have studied the possibility of extending the pentaheptite family by embedding higher polygons into the network.[299] Note that some kinds of pentaheptite atomic motifs are known for a number of inorganic compounds; *e.g.*, boron atomic networks in the structure of ternary borides $YCrB_4$ and $ThMoB_4$ have the pentaheptite type (see Fig. 17).

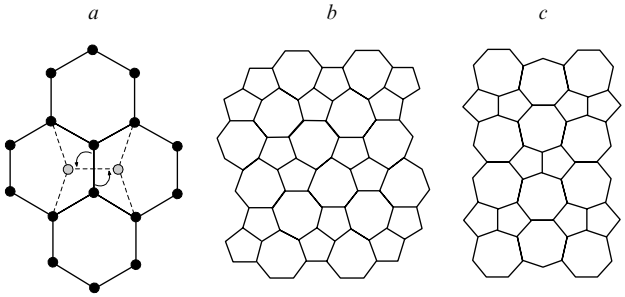


Figure 17. Scheme of formation of heptagon + pentagon pairs in graphene sheet: Stone–Wales defect (*a*),[296] boron pentaheptite sheets in structures of ternary borides $YCrB_4$ (*b*) and $ThMoB_4$ (*c*).[300]

2. Haeckelites. Graphynes

A family of layered forms of carbon containing various ordered combinations of polygons was proposed.[301] These structures were called [301] haeckelites.‡

All haeckelites were divided [301] into three groups: (i) rectangular haeckelites ($R_{5,7}$), which contain only various combinations of pentagon/heptagon pairs; (ii) hexagonal haeckelites ($H_{5,6,7}$) whose networks are comprised of repeating clusters built of three heptagons surrounded by alternating pentagons and hexagons; and (iii) bent haeckelites ($O_{5,6,7}$) containing C_5 and C_7, coordinated by hexagons (Fig. 18). Pentaheptites represent a group (first group) of the haeckelite family. All haeckelite networks contain equal numbers of the C_5 and C_7 rings, but the total number of both types of rings differs from one haeckelite to another. The first and second groups of haeckelites have planar networks, whereas the third group has folded networks. Haeckelites are less stable than graphite, but more stable than C_{60} fullerenes. According to calculations,[301] all haeckelites exhibit metal-like conducting properties.

Yet another group of hypothetical 2D-nanostructures includes planar polycylic modifications of carbon. Among them, graphynes are best known.[302–304] Graphynes and related graphdiynes [305] can be considered as hybrid polymeric systems combining structural elements of graphite and carbyne (Fig. 19). For instance, the structure of the α-graphyne network is such that carbon atoms in the neighbouring vertices of each hexagon are linked by an 'additional' C_2 unit and the total number of atoms in each hexagon equals 18 $\{C_6 + 6\,C_2\}$. The β-, γ-graphyne (graphdiyne) networks also include C_6 hexagons, but their vertices

‡ The haeckelites are named in honour of German zoologist E Haeckel who reported images of radiolaria (simplest protistic organisms) whose structures are similar to those of the layered forms of carbon in question.

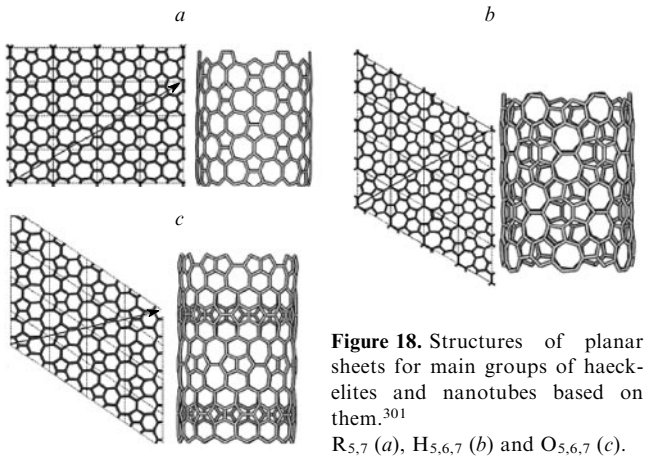


Figure 18. Structures of planar sheets for main groups of haeckelites and nanotubes based on them.[301]
$R_{5,7}$ (*a*), $H_{5,6,7}$ (*b*) and $O_{5,6,7}$ (*c*).

are linked through C_2 units (or their multiples, linear chains nC_2, see Ref. 305). In these structures the ...=C=C=C=... bonds typical of graphene sheet are partially replaced by polyyne bonds ...−C≡C−... and carbon atoms have the coordination numbers 2 or 3 and the sp^1 or sp^2 electronic configurations.

It is assumed [302] that graphynes will be thermally stable and similar to graphite in mechanical properties. β-Graphyne is a semiconductor [302] with a forbidden gap of about 1.2 eV. Quasi-1D planar strips 'cut' from graphyne nets also exhibit semiconductor properties.[306] These systems have attracted the attention of researchers who did search for novel materials, namely, π-bonded polymers and oligomers showing nonlinear optical properties. Analysis [307] of linear molecular systems including fragments of some complex polymers, in which four benzene rings are linked by cumulene units, showed that their energy spectrum exhibits a very broad (∼3–5 eV) gap between the highest occupied and lowest unoccupied molecular orbitals (HOMO and LUMO, respectively), which became narrower with elongation of the $(=C=C=)_n$ atomic chain. The major contributions to the HOMO and LUMO come from the π-states of the atoms of cumulene chain; atomic oscillations depending on the length and interatomic distances provide an interesting example of the onset of quasi-1D charge-density wave. For more detailed analysis of the electronic states of various carbyne chains see, for *e.g.*, Refs 308–313.

The structural and energy properties of graphynes and graphdiynes have been studied.[303, 304] As the length of the carbyne units connecting hexagons increases, the graphyne networks become less stable, whereas the width of the forbidden gap varies insignificantly [281] and remains in the interval ∼0.5–0.6 eV. Possible polymorphs of crystalline β-graphyne [303] differ from one another in alternation pattern of planar networks along the *c* axis, that is, *AAA* (α) and three types of the *ABAB* packing type (β_1, β_2 and β_3). All of them have been analysed. Depending on the packing type, β-graphyne crystals exhibit fundamentally different electrophysical properties. Namely, the α and β_3 polymorphs are zero-gap semimetals characterised by low density of states at the Fermi level, whereas the most stable forms, β_1 and β_2, are semiconductors with considerably different witdths of the forbidden gap (0.19 and 0.50 eV, respectively). These features are due to differences between the 'inter-plane' interactions of $C2p_\pi$-orbitals. The interlayer distances in the graphyne polymorphs are ∼4%–9% longer than in graphite.

To date, certain types of the graphyne structural motifs were identified in a number of supramolecular systems.[314, 315] For instance, graphyne-like networks are parts of crystalline 2,4,6-triethynyl-1,3,5-triazine;[314] hexagonal networks form triazine rings with C(sp)−H···N bonding pattern.

3. Polycyclic 2D-forms of carbon

A number of hypothetical 2D-forms of carbon representing strained-ring polycyclic networks (Fig. 20) was proposed.[316] Information on these systems is scarce. Quantum chemical calculations of a planar polymeric motif comprised of alternating benzene and cyclobutadiene rings have been reported.[316] The system is a wide-gap semiconductor with a forbidden gap width of about 2 eV.

Non-graphite 2D-nanostructures are difficult to synthesise because the formation of various strained rings within

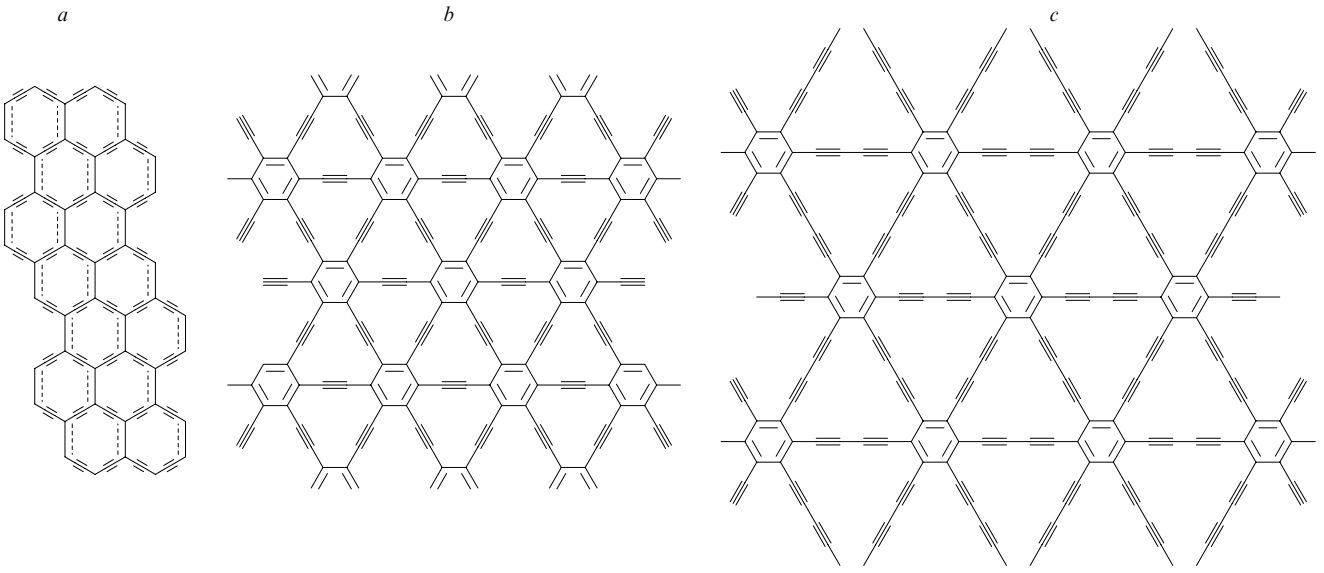


Figure 19. Structures of α- (*a*), β- (*b*) and γ-graphynes (*c*).[302–304]

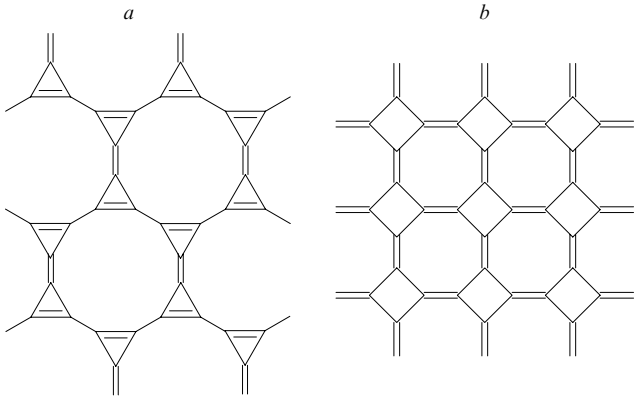


Figure 20. Examples of planar polycyclic carbon sheets with strained three- (*a*) and four-membered (*b*) rings.[316]

planar carbon networks requires large energy expenditure and the final systems become metastable. At the same time, observation of $C_{n\neq 6}$ rings, as topological defects, in conventional graphite-like nanotubes is not infrequent.[48–51] Some types of $C_{n\neq 6}$ rings are essential structural units in fullerenes, 'caps' of graphite-like nanotubes and nanocones. Topological defects are present in giant spherical fullerenes or in negative-curvature fragments of multi-wall nanotubes, X-, Y-, L-shaped nanotubes, *etc*. Moreover, microscopic studies[317,318] showed that up to 10% of nanotubes synthesised by high-energy methods (laser ablation, pyrolysis, electric arc technique, *etc*.)[55] have 'inetr-tubular' intergrowth regions containing topological defects capable of changing the curvature and chirality type of tubulenes. It is natural to assume that the structural motifs of the networks of non-graphite 2D carbon allotropes (see above) can realise in low-dimensional (0D, 1D) forms of carbon, thus predetermining unusual properties of the latter systems compared to the properties of classical graphite-like nanotubes and fullerenes.[319]

4. Pentaheptite and haeckelite nanotubes

A series of nanotubes designed based on pentaheptite and haeckelite networks has been studied.[301] All nanotubes have metal-like electronic spectra irrespective of the tube diameter and chirality. Probably, hexagonal ($H_{5,6,7}$) and haeckelite nanotubes characterised by intense peak of the density of states at the Fermi level possess superconducting properties.

One of the most important features of nanotubes is that they can have extremal mechanical characteristics. Young's modulus (Y) of conventional graphite tubes is known to be as high as $\sim$1.2 TPa.[49–57] Estimate showed[301] that haeckelite tubes are characterised by somewhat lower Y values ($\sim$0.9–1.1 TPa) that are, however, higher than those of, *e.g*., BN nanotubes ($\sim$0.8 TPa) or SiC nanorods ($\sim$0.6 TPa). At very small diameters (less than 0.4 nm), the energy states of the haeckelite and graphite nanotubes are similar; an increase in nanotube diameter causes the total energy difference (δE) to increase to 0.20–0.35 eV per atom, which is comparable with the δE value of planar haeckelite and graphene sheets ($\sim$0.32 eV per atom.[320] The deformation energies of Haeckelite nanotubes (calculated relative to the energies of planar networks from which the tubes were 'rolled') are lower than those of conventional graphite nanotubes.This is considered[320] as an argument in favour of possible fabrication of these systems. A possible synthetic route involves electron irradiation of graphite nanotubes resulting in the appearance of defects (five- or seven-membered rings) in nanotube walls.[321,322] Other methods include reconstruction of graphite nanotube walls upon treatment with strong acids, annealing of nanotubes in inert atmosphere or other processes appropriate for activation of rearrangement of some valence bonds.

Atomic models for non-graphite nanotubes and related nanostructures (toroids, helical nanotubes, 1D-structures of the 'pearl necklace' type) built of so-called azulene units (C_5+C_7 pairs where pentagons share an edge) and hexagons[303] have been proposed.[320,323–325] When rolling corresponding atomic strips, the bond shared by two neighbouring pentagons acts as a mechanical stress concentrator. These bonds were called 'stressors'; they initiate changes in the local curvature of nanotubes leading to appearance of local convex or concave regions in nanotube wall. If stressors are arranged periodically, surface-modulated nanotubes are formed. They exhibit[324] semiconductor properties with a forbidden gap of about 0.6 eV provided that the tube diameter lies in the range 0.223–1.119 nm.

In addition to nanotubes, pentaheptite fullerene structures C_{28}, C_{44} and C_{92} (point symmetry groups is D_{7d}, D_{3h} and C_{3v}, respectively) and a series of icosahedral fullerenes C_n (n = 20, 60, 80, 140) have been proposed.[299]

5. Graphyne nanotubes and fullerenes

A family of graphyne-based nanotubes (g-NTs) has been proposed.[326,327] Depending on the diameter and geometry, theory predicts for them a vast variety of changes in electronic properties compared to conventional graphite nanotubes. α-, β- and γ-Graphyne sheets used as precursors were 'rolled' to obtain infinite cylinders belonging to achiral armchair (n,n), zig-zag (n,0) and chiral (n,m) g-NTs.

The closest analogues of graphite nanotubes are α-graphyne-based nanotubes whose walls are formed by regular hexagons $\{C_6+6C_2\}$. They also show similar electronic properties. For instance, irrespective of NT diameter, all armchair α-g-NTs exhibit metallic properties, whereas zig-zag α-g-NTs exhibit the properties of semimetals (if their indices n are multiples of three). All other zig-zag nanotubes are semiconductors, their forbidden gaps decrease as the tube diameter increases. Specific structural features of the β-graphyne network determines a more complex dependence of the forbidden gap width on the nanotube geometry and diameters. Namely, the zig-zag β-g-NTs exhibit metal-like properties only at particular n values while all armchair β-g-NTs show the properties of semiconductors. Theory predicts semiconductor properties for γ-g-NTs (forbidden gap width $\sim$0.4–0.5 eV); the pattern of their atomic configurations affects the symmetry type of the bottom of the conduction band. Therefore, one can expect that the armchair and zig-zag γ-g-NT exhibit significantly different optical and conducting properties, which, in particular, depend on the effective masses of electrons oscillating upon variation of nanotube diameter. Estimation of the energy effects acompanying the roliing of graphyne networks showed[326] that the formation of tubular forms based on γ-graphyne is most probable. The width of the forbidden gap in semiconductor g-NTs was studied as function of tension–compression uniaxial deformations and regularities of its variation have been predicted.[327]

Models for single- and multi-wall nanotubes and fullerene-like molecules based on β-graphyne have been pro-

posed.[328, 329] Their relative stabilities were estimated by the molecular dynamics method. The formation of multi-wall β-g-NTs was found to be less probable than that of single-wall β-g-NTs.

A new class of cage structures based on modified graphite (hexagons in the planar network are partially replaced by pentagons) was predicted.[329] In this case the role of 'building blocks' is played by graphanes representing planar layers in which short chains of carbon atoms are linked by five-membered rings. These blocks comprise both sp^2- and sp^3-bonds and allow one to design various cage structures (graphanofullerenes) and graphane nanotubes.

According to calculations,[330] fullerene-like α-graphyne molecules (g-C_{80}, g-C_{240}) are less stable than graphite-like isomers due to narrower HOMO–LUMO energy gaps. Graphyne structural fragments were identified in a number of complex polymer systems.[331–339]

A variety of cage structures representing 3D-entanglements of distorted graphite rings have been proposed.[340] These systems can form in intermediate stages of formation of the diamond lattice from graphite.

Clearly, graphyne-like nanotubes and fullerene-like molecules can by and large be treated as metastable modifications of conventional graphite-like nanostructures. These objects are most interesting because of much greater versatility of their structures and electronic properties compared to the properties of graphite-like analogues. In addition, these nanostructures have lower densities and highly porous walls (shells). Taking into account these properties, the nanostructures in question can probably be used as matrices in various intercalation processes, in particular, as hydrogen storage systems. Note that the key problem in using fullerenes and nanotubes for hydrogen storage is to carry out dehydrogenation (high temperature is required for hydrogen release); at the same time, highly porous walls (shells) can favour dehydrogenation. Finally, non-graphite carbon nanostructures have become parent structures in simulation of their heteroatomic analogues just as conventional graphite-like nanotubes are considered as prototypes in search for nanotubular forms of other inorganic substances and compounds. Some examples will be considered below.

Summing up, even more complex hybrid systems combining structural elements of the two families of non-graphite 2D-structures (haeckelites and graphynes) considered above can also be proposed with ease.[319] For instance, by forming bond rotation defects (rotation of some $-C-C\equiv C-C-$ bonds by 90°) in the α-graphyne network one can obtain planar networks comprised of pentagons $\{C_5+5C_2\}$, hexagons $\{C_6+6C_2\}$ and heptagons $\{C_7+7C_2\}$, *i.e.*, a combination of 'graphyne + haeckelite' structural motifs with a mixed (sp^1+sp^2)-bonding type. These networks can be employed in further simulation of new 1D- and 0D-nanostructures with $sp^1+sp^2+sp^3$ bond configurations.

VI. Carbon–carbon nanocomposites

In this Section we will cosider carbon–carbon nanocomposites (NCs) containing carbon nanostructures (or their elements) of different dimension, coordination number and bond type. Such materials are sometimes called 'symbiotic', or 'hybrid', ones. Some examples of NCs containing diamond crystallites and nanotubes were considered above (see Section IV).

Methods of formation of NCs are similar to those used for functionalisation of nanostructures (fullerenes or nanotubes). Targeted control of properties can be attained,[38–41, 46–51, 62–70, 84, 162] first, by doping (partial replacement of nanotube or fullerene atoms by other atoms); second, by exohedral funcionalisation (adsorption on surface), *i.e.*, by attaching extra atoms or molecules to the outer nanotube (fullerene) walls; and third, by endohedral funcionalisation, *i.e.*, introduction of atoms or molecules into the nanotube (fullerene) cavity or into the space between neighbouring tubes in nanotube bundles. The last-mentioned technique was practically implemented[341] by researchers who discovered a specific group of composite nanostructures, the so-called nanopeapods.

1. Nanopeapods

Recently, a group of NCs representing a combination of two types of different-dimension (0D + 1D) nanostructures has become famous. These systems are often called nanopeapods. They are comprised of quasi-1D nanostructures (nanotubes) containing quasi-0D nanoclusters (fullerenes) in the cavity. Two main families of nanopeapods synthesised to date are based on carbon nanotubes containing fullerenes or endohedral metallofullerenes in cavities.[342–345] Carbon peapods C_n@C-NTs, *i.e.*, ordered 1D-assemblies of C_n fullerenes ($n = 28–82$) encapsulated into carbon nanotubes (Fig. 21), are the best known representatives of these hybrid (0D + 1D)-systems.

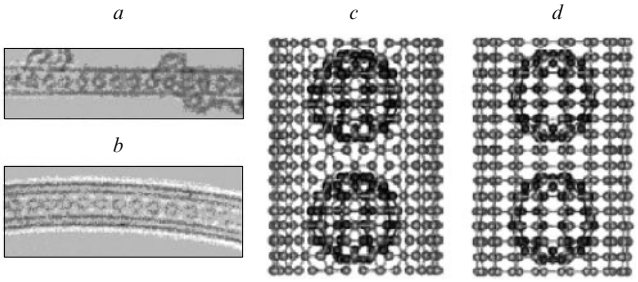


Figure 21. Micrographs (*a*, *b*)[346] and atomic structure models (*c*, *d*) for peapods.[347]
Peapods: C_{60} confined within single-wall nanotubes (*a*); C_{60} confined within two-layer nanotubes (*b*); C_{60}@(10,10)C-NT (*c*) and C_{60}@(9,9)C-NT (*d*).

Filling of single-wall nanotube cavities was first observed[341] in a high-resolution TEM (HRTEM) study of a material prepared by pulsed laser vaporisation of a graphite target containing impurities (metal catalysts) followed by annealing at 1100 °C and treatment with acid. These results were confirmed experimentally.[346, 348, 349] Clear HRTEM images of (C_{60}, C_{70})@C-NT hybrid structures show[346, 348] that the available nanotube fragments contain not only single-wall nanotubes containing regular fullerenes chains, but also molecular clusters (dimers, trimers, *etc.*) and ~2-nm long extended nanocapsules 'capped' at both ends. Possible mechanisms of formation of these structures include (i) fullerene diffusion through the open ends of nanotubes or through wall defects and (ii) rolling of graphene sheet on the inner nanotube wall to give a fullerene in the reaction of joint formation of nanotube and fullerenes.

At present, a variety of peapods containing various fullerenes (from C_{36} to C_{90}) and some endofullerenes have been synthesised, certain properties of these systems have been studied, the growth scenarios were proposed and electronic characteristics were simulated.[342–345, 350, 351] Methods of synthesis of peapods include pulsed laser vaporisation of a graphite target (see above) and a vapour-phase technique,[352, 353] which uses nanotubes and fullerenes as 'reactants'. A low-temperature (~ 70 °C) method of synthesis of peapods involves nanotube filling with fullerenes in solution.[354]

Peapods are stable to ~ 800 °C; at higher temperatures, fullerenes coalesce with the formation of extended nanocapsules and tubular cylindrical fragments.[355] At ~ 1200 °C, individual C_{60} fullerenes almost completely disappear and the peapods transformed to two-layer nanotubes. Polymerisation of C_{60} inside a nanotube can be induced by introducing dopants, *e.g.*, potassium atoms.[356] These linear polymers can be obtained only inside nanotube cavities which in this case act as nanoreactors.

An ideal structural model for C_{60}@C-NT peapods represents a single-wall carbon nanotube containing a regular linear chain of encapsulated fullerenes placed on the nanotube axis (see Fig. 21 *c*,*d*). The distances between fullerenes in peapods are longer than in free polymer chains but shorter than in molecular crystals formed by corresponding fullerenes. For instance, in C_{60}@C-NT the distance between centres of molecules (*a* is the 'lattice constant' of quasi-1D crystal) is ~ 0.97 nm and the distance between fullerenes and nanotubes is ~ 0.35 nm.§

Peapods containing non-spherical isomers of higher fullerenes (C_{70}, C_{80}) form[357, 358] two types of structures with $a_{1,2} = 1.00$ and 1.10 nm differing in mutual orientation of fullerenes (Fig. 22). It was proposed[358] to consider them as individual phases. A study of C_{80}@C-NT revealed[357] a mixed (anisotropic) orientation of molecules. It is assumed that mutual arrangement of non-spherical fullerenes (*i.e.*, the lattice constants of corresponding 1D-crystals) can be controlled by varying the diameters of carbon nanotubes.

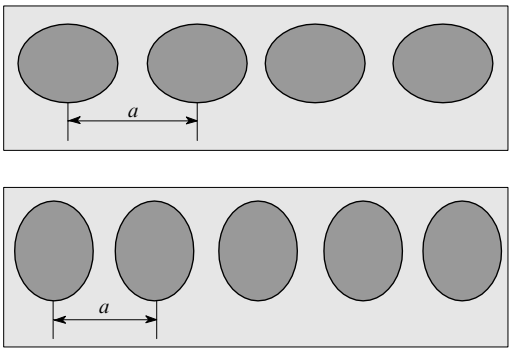


Figure 22. Quasi-1D 'phases' of non-spherical C_{70} fullerenes in C_{70}@C-HT peapods with different mutual orientation of fullerenes.[357] The 'lattice parameter' *a* of these 'phases' depends on fullerene orientation.

§ This is the so-called van der Waals gap of the third type. The van der Waals gap of the first and second types are the distance between walls of neighbouring coaxial cylinders in multilayer nanotubes and the distance between external walls of neighbouring tubes in compact bundles, respectively.

From the standpoint of fullerene encapsulation the smallest size is 1.37 (C_{60}), 1.45 (C_{76}, C_{78}) and 1.54 nm (C_{84}).[359]

Specific features of atom–atom interactions and selected properties of peapods were studied using quantum chemistry methods.[342–345, 350, 351] According to calculations,[360] the minimum diameter of a carbon nanotube for encapsulation of C_{60} is 1.29 nm, the optimal being 1.36 nm. Analysis[361] showed that peapods containing fullerenes placed on the nanotube axis are most stable. This is explained by repulsive van der Waals interactions. Covalent interactions between C_{60} and nanotubes almost do not occur. The structural properties and energy characteristics of C_{60}@C-NT peapods have been simulated.[347, 362–367] For instance, C_{60}@(10,10)C-NT (nanotube diameter 1.357 nm) showed almost no changes in the geometry of the peapod-forming nanotube and fullerenes. As the nanotube diameter decreases, deformation (ellipsoidal distortions) of both nanotubes and fullerenes occurs. The calculated peapod formation energies (ΔE) are -0.51, 0.27 and 15.19 eV for the chirality indices equal to 10, 9 and 8, respectively.[362] In other words, insertion of C_{60} into a (10,10)C-NT will be exothermic, whereas for smaller-diameter nanotubes (starting with ~ 1.28 nm) it will be endothermic ($\Delta E > 0$). The energy effects of encapsulation of non-spherical C_{70} fullerenes depend not only on the nanotube diameter, but also on their relative orientation.[366] For thin nanotubes, the on-the-tube-axis orientation is preferable; as the nanotube diameter increases, C_{70} fullerenes are arranged in such a fashion that their long axes become perpendicular to the nanotube axis (see Fig. 22).

Calculations[178, 368] of the potential energies of the interaction between C_{60} and carbon nanotubes revealed an interval of nanotube diameters suitable for the formation of hybrid structures with regular arrangement of encapsulated fullerenes (linear chains). For the C_{60}@(10,10)C-NT system, the $E(C_{60}-NT)$ curve has only one symmetrical minimum on the nanotube axis. In the case of C_{60}@(15,15)C-NT (diameter 2.04 nm), energy minima are located near nanotube walls and the local maximum is on the axis. For larger-diameter tubes ($d > 1.46$ nm),[178] linear periodicity in the fullerene distribution along the axis is violated. An additional disordering factor is abrupt weakening of fullerene–nanotube interactions. For instance, the C_{60}–nanotube binding energy has an extremal value at a nanotube diameter of 1.356 nm and decreases as the nanotube diameter decreases and asymptotically approaches the binding energy of C_{60} with flat graphene sheet.

Peapods exhibit a variety of interesting physical and chemical properties.[342, 350, 351] These compounds seem to be promising for application in micro- and nanoelectronics, they attract increasing attention as model systems for studying quasi-1D diffusion, structural and phase transformations and chemical reactions.

2. Bunker phases

If the inner diameters of nanotubes are much larger than the fullerene diameter and the fullerene concentration is high, fullerene–fullerene interaction becomes possible; this leads to ordering with the formation of quasi-crystalline phases inside the nanotubes. Such structures are called 'bunker' phases. A solution[369] to a mathematical problem of arrangement of ideal spheres in a cylinder (bunker) showed that, depending on the diameter of the cylinder, one can obtain a number of ordered phases with different packing motifs. A similar task aimed at minimising the packing

energy of C_{60} molecules in carbon nanotubes with $1.25 < d < 2.70$ nm was solved by the Monte Carlo method.[370] Ten chiral and achiral configurations governed by the nanotube diameter were revealed. It was shown that generally the molecular packing motifs are determined by the nanotube size, concentration of encapsulated fullerenes and by the energies of the fullerene–fullerene and fullerene–nanotube wall interactions.

A number of bunker phases have been synthesised to date. Analysis of peapods[346] based on two-layer carbon nanotubes (TLNT) with inner diameters lying in the interval 1.1–2.6 nm showed that four packing types of C_{60} molecules are possible. At $d < 1.5$ nm, fullerenes form linear chains, as in the peapods based on single-wall nanotubes. As the nanotube diameter increases, linear chains are transformed to zig-zag ones. At $d > 2$ nm, a number of chiral structures appear; their lattice constants are related to the nanotube diameter. Yet another packing type is achiral two-molecular motif. Experiments[346] revealed a clear correlation between the formation of ordered fullerene 'phases' in the nanotube and the degree of its filling with molecules (N). At $N < 90\%$, there is no ordering and fullerenes form an 'amorphous phase', just like it was predicted.[370] Therefore, the structure of the quasi-1D 'phase' can be varied with ease using bunker nanotubes with appropriate diameters and particular number of encapsulated fullerenes. The types of molecular ordering in cylinders and the structural factors are controlled by the fullerene–fullerene and fullerene–nanotube wall (van der Waals) interactions.

A series of bunker phases was observed[371] in C_{60}@BN-NT peapods. At small diameters of BN-nanotubes ($d = 2$ nm), the C_{60} fullerene packing motif is similar to a linear chain. As the nanotube diameter increases to 2.8 nm, the C_{60} molecules in the chain form triangles rotated by 60° relative to one another. Further increase in the nanotube diameter causes more complex packing types of C_{60} molecules to appear, *e.g.*, a mixed configuration combining two screw packings at $d = 3.3$ nm. The last-mentioned structure is one of many possible incommensurate structures[348, 349] with two (or more) C_{60} motifs of different axial periodicity (Fig. 23). Crystallographically, these structures are intermediate between known structures with double periodicity (systems with charge-density waves) and orientationally ordered systems without long-range translational order (quasi-crystals). The types of fullerene packing in bunker crystals are completely different from the packing types of fullerenes confined within thin films or fullerites.

One can also expect the formation of bunker crystals in more complex systems upon, *e.g.*, ordering of ensembles of fullerene dimers or endofullerenes within the nanotube.[342–345]

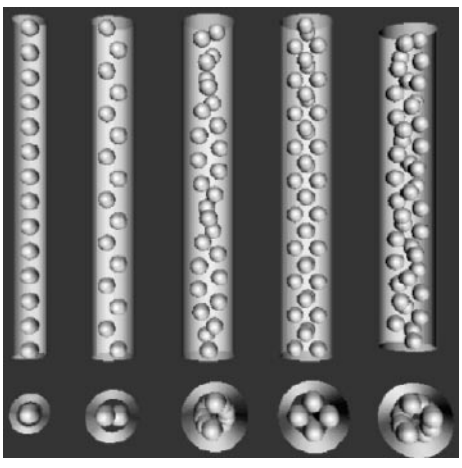


Figure 23. Models for possible types of fullerene packing in nanotubes — bunker phases.[371]

3. Nanobuds

New composite (0D + 1D)-carbon nanostructures called 'nanobuds' have been synthesised recently.[372] These structures represent single-wall nanotubes (i) covered with C_{42} and C_{60} fullerenes from the outside or (ii) grown in reactions of co-synthesis of nanotubes and fullerenes (Fig. 24).

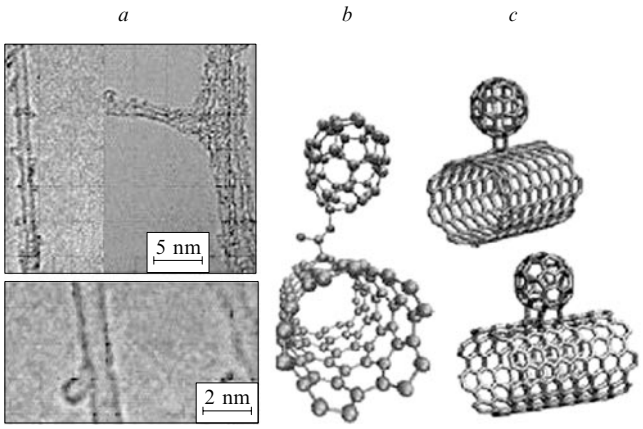


Figure 24. Micrographs of nanobuds (carbon nanotubes with attached fullerenes) (*a*) and atomic models for nanobuds (*b*, *c*).[372]

Depending on the synthesis conditions, the density of fullerenes on the nanotube walls can be higher than 1 fullerene nm^{-1} (Ref. 372). Fullerenes are tightly bound to nanotubes; they do not dissolve in organic solvents and can not be displaced under the action of the probe tip of a scanning tunnelling microscope, electron beam of a transmission microscope or on heating to 700 °C. It is assumed that the stability of nanobuds is due to formation of additional covalent sp^3-bonds between fullerenes and the nanotube. From the standpoint of materials science an attractive feature of nanobuds consists[372] in the presence of numerous curved 'surfaces' of (0D + 1D)-structures, which favours autoemission and an increase in emission current (compared to 'smooth' nanotubes). High nonuniformity of the distribution of electron states along nanotube axes can also be useful for their applications in nanoelectronics as memory devices, decoders and quantum dots. Compared to nanotubes, nanobuds have a much more developed outer surface and can therefore serve efficient adsorbents and catalysts.

4. Nanobeads

The term 'nanobeads' (or 'pearl necklace') is used in the literature to denote a number of different-type quasi-1D nanostructures morphologically similar to threaded beads. For instance, this term was used[320] to describe quasi-tubular nanostructures obtained by rolling particular types of haeckelite strips. The largest group of linear structures with nanobead morphology is based on carbon fullerenes, in

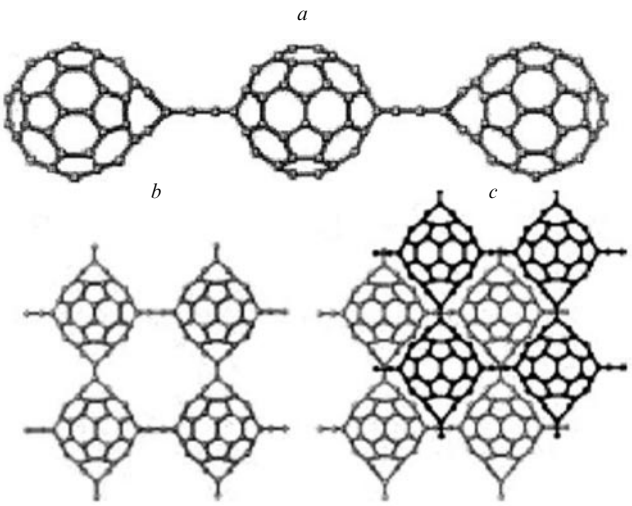


Figure 25. Fragments of periodic quasi-1D structure (nanobeads) built of C_{60} fullerenes linked by carbon chains (*a*) and hypothetical 2D (*b*) and 3D (*c*) structures based on nanobeads.[374]
Fragments of: planar sheet (*b*) and crystal (*c*).

particular, small fullerenes $C_{n<60}$ (Ref. 47). Polymerisation of these reactive fullerenes in chain is, as a rule, due to the interaction between certain atoms, which form various rings between fullerenes. Stable-shell higher fullerenes can be joined [373–375] to form linear chains using 'additional' fragments of carbyne chains.

Linear structures (nanobeads) are often used as parent compounds in search for new film (2D) or crystalline (3D) carbon structures. Examples of hypothetical films and crystals based on nanobeads [374] are shown in Fig. 25. Two- and three-dimensional structures built of nanobeads differ from fullerites in that fullerene constituents are bonded by covalent bonds rather than through weak van der Waals forces. These bonds are formed due to participation of ordinary, double, ternary, *etc*. chains of carbon atoms connecting vertices, edges and faces of neighbouring fullerenes. Owing to fivefold icosahedral symmetry, close packing and connection of fullerenes at all faces is impossible; therefore, they are connected through vertices, edges and some faces. A great variety of combinations of these bonds is possible and each of them will represent an alternative reaction channel leading to formation of a crystal from nanobeads. At moderate temperatures and pressures, various types of covalent bonds between fullerenes are possible; X-ray diffraction patterns of such a phase will be similar to those of amorphous phase.

5. Nanotube/platelet composites

One of the key problems in research on *exo*-functionalised nanotubes is to design carbon nanomaterials suitable for being used as efficient accumulators of hydrogen and other lightweight gases.[376, 377] Since hydrogen condenses on the nanotube surface (or within its cavity),[377] a clearly seen method of increasing the hydrogen adsorption capacity of carbon materials is to design novel tubular structures with a larger surface area. This method was implemented in practice.[378] Deposition of graphite nanoplatelets on nanotube walls (Fig. 26) led to an increase in the nanotube surface area from ~ 90 m^2 g^{-1} to 131 m^2 g^{-1} in the graphite nanotube/platelets composite material. These carbon materials can also be used for the synthesis of catalysts or fabrication of electrodes for fuel cells.[378]

Atomic models of such composites (nanotube + fragment of graphene sheet) are available.[379] The effects of the type of carbon nanotubes (chiral or achiral), graphene fragments and possible types of adsorption of these planar structures on the outer nanotube walls (see Fig. 26) on the stabilities and electronic properties of the composites were studied. It was established that owing to strong covalent C–C bonds, the composites retain their aggregate structure (do not separate to initial 'building blocks', *i.e*., graphene and nanotube fragments). After structural relaxation the structure of tubes remains almost unchanged, whereas the structures of attached graphene platelets differ significantly from their initial models, namely, some C–C bonds in hexagons are cleaved and corresponding atoms form fragments of carbyne-like atomic chains.

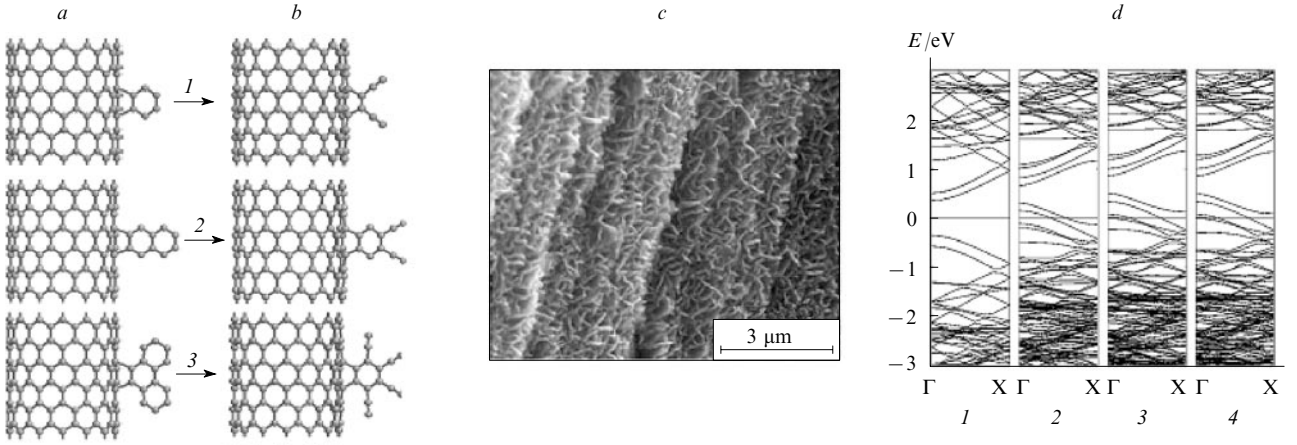


Figure 26. Atomic models [379] for initial (*a*) and optimised (*b*) structures of (14,0)-NT with covalently bonded graphite platelets (types *1–4*); a micrograph [378] of a carbon nanotube covered with graphite nanoplatelets (*c*), and energy band structures [379] of isolated and modified (14,0)-carbon nanotube (*d*).
Initial nanotube (*1*) and modified nanotube (*2–4*). The Fermi level is 0.0 eV.

Thus, nanotube/platelet composites contain three types of carbon atoms, that is, four-, three- and two-coordinate ones. Most atoms (in C_6 hexagons responsible for the formation of nanotube walls and platelets) have a coordination number of 3 and sp^2-bonds. Four-coordinate sp^3-atoms are the atoms of nanotube walls participating in the covalent bonds with fragments of graphene platelets. Finally, the sp^1-atoms in carbyne-like chains are two-coordinate. In terms of electronic configuration, nanotube/platelet composites can be treated as new carbon nanoforms with mixed $(sp^1 + sp^2 + sp^3)$-type of bonding. In this respect they are similar to the nanobeads considered above.

According to calculations,[379] joining various graphene fragments and nanotubes should be followed by the formation of some preferred configurations (forms), which indicates that formation of periodically decorated nanostructures is energetically favourable. The type of platelet ordering on the nanotube surface depends on the size and geometry of the graphene platelets and on the chirality of the carbon nanotube. Therefore, variation of these factors for the initial nanostructures (platelets and nanotubes) can be an efficient method of nanotube decoration and targeted 'tuning' of the properties of such composites. Finally, band structure calculations (see Fig. 26 *d*) showed that all composites under study have partially filled bands near the Fermi level; therefore, their electronic spectra are of metal-like type.

6. Nanoflowers

There exist systems which can be considered related to nanotube/platelet composites discussed above. These are the so-called 'nanoflowers',[380] *i.e.*, spheres 200 to 600 nm in diameter composed of many graphite-like flakes (thickness less than 5 nm each) that are 'linked' in some way. Nanoflowers have hollow cores. It is assumed[380] that these structures can (i) find application as materials for catalysts and (ii) be interesting for the design of electric and magnetic nanodevices. More detailed information on the atomic structure and character of interatomic interactions in these materials is unavailable as yet.

7. Nanodisks and nano-batons

Unusual composite materials are formed upon incorporating additional carbon clusters into cage nanostructures. Inner 'linking' in these structures can be due to participation of atoms of the fullerene or nanotube walls.[381] Hypothetical cage structures built of carbon atoms forming 3 and 4 covalent bonds with neighbouring atoms were respectively called[381] carbon nanodisks (NDs) — analogues of fullerenes — and carbon nano-batons (NBs) — analogues of carbon nanotubes. Unlike conventional nanotubes and fullerenes, these structures contain not only $C(sp^2)$ atoms with a coordination number of 3, but also $C(sp^3)$ atoms with a coordination number of 4 (Fig. 27).

A homologous series of simplest nanodisks containing two $C(sp^3)$ atoms to form an sp^3-bond and thus to 'link' two half-disks was proposed.[381] This series includes NDs containing the number of atoms given by the following expression:

$$C_i = 44 + 48\,i + 12\,i^2,$$

where $i = 0, 1, 2, \ldots$. One can assume[84, 360] the existence of more complex nanodisk structures containing more than two $C(sp^3)$ atoms. Such structures can also have a disk-like shape, but they contain a larger number of 'links' (provided the same number of atoms, see Fig. 27). Calculations point to stability of NDs.[381] The total number of sp^3-atoms in ND structures can vary from 4 to N_{max}

$$N_{max} = 6\,i^2 + 18\,i + 14,$$

where $i = 0, 1, 2, \ldots$.

Nano-batons[381] can be obtained from nanodisks just like carbon nanotubes are made of fullerenes, *i.e.*, by 'cutting' nanodisks into two pieces and inserting fragments with two $C(sp^3)$ atoms between the half-disks. Similarly to carbon nanotubes, nano-batons can differ in orientation of carbon–carbon bonds relative to the axis.

The total (E_{tot}) and specific (E_{sp}) energies were estimated for the optimised structures of NDs and NBs.[381] It was established that for nanodisks the E_{sp} value monotonically decreases as the number of atoms increases; in other words, the formation of large NDs is energetically favourable. The formation of NBs is less favourable compared to NDs and the energies E_{sp} of zig-zag NBs are lower than those of armchair NBs. It is assumed[84, 381] that these structures can be obtained from fullerenes and short nanotubes in the case of formation of strong covalent bonds between neighbouring fullerene or nanotube walls. Probably, these bonds can form upon high-pressure treatment of fullerenes and nanotubes when the oppositely lying walls of

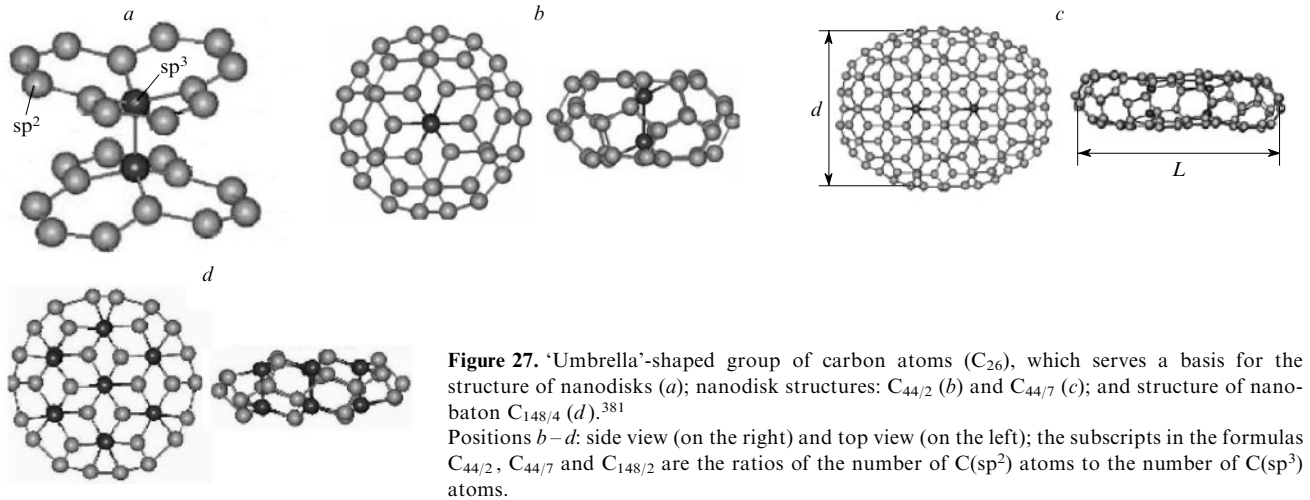


Figure 27. 'Umbrella'-shaped group of carbon atoms (C_{26}), which serves a basis for the structure of nanodisks (*a*); nanodisk structures: $C_{44/2}$ (*b*) and $C_{44/7}$ (*c*); and structure of nano-baton $C_{148/4}$ (*d*).[381]
Positions *b*–*d*: side view (on the right) and top view (on the left); the subscripts in the formulas $C_{44/2}$, $C_{44/7}$ and $C_{148/2}$ are the ratios of the number of $C(sp^2)$ atoms to the number of $C(sp^3)$ atoms.

deformed structures can approach one another to form covalent bonds between them.

VII. Boron nitride nanostructures

1. Clusters, onions, nanotubes and horns

There exist a number of crystalline boron nitride polymorphs. These are sphalerite-type c-BN (analogue of cubic sp^3-diamond), würtzite-type w-BN (analogue of sp^3-lonsdalite), graphite-like h-BN (analogue of sp^2-graphite) and its hexagonal (2H, 4H, 6H), cubic (3C) and rhombohedral (3R, 15R, 21R) polytypes, turbostratic t-BN, *etc*.[15, 63, 382] Short affter the discovery of carbon fullerenes, onions, nanotubes and other nanostructures, their BN-analogues were synthesised or corresponding atomic models were reported.[383–411] The atomic structure, properties and possible fields of application of BN-nanostructures have been studied quite thoroughly.[50, 162, 383–387] Here we will consider new boron nitride nanoforms based on the BN-nanostructures mentioned above.

2. Fulborenes, a family of fullerene analogues

An atlas of carbon fullerenes includes thousands of fullerenes.[412] The question arises of which boron nitride polyhedra are analogues of C_n fullerenes. Carbon fullerenes with homopolar C–C bonds are comprised of hexagons and pentagons; their structures contain no squares with strained bonds that are much weaker due to deviation of the bond angles from the equilibrium values. In BN-fullerenes, the $B^- - B^-$ and $N^+ - N^+$ bonds are much weaker than $B^- - N^+$ heteropolar bonds; therefore, ring formation from squares, octagons and decagons is more favourable than from pentagons. Thus, stable BN-analogues of carbon fullerenes should not contain pentagons.

As mentioned above, icosahedral carbon fullerenes can bond to one another through vertices, edges and (in some cases) faces; in this case the formation of close-packed covalent diamond-like crystals is impossible. Contrary to this, crystal-forming B_nN_n polyhedra can form close-packed crystals. According to a general approach,[98] crystal-forming X_nY_n polyhedra used to form close-packed crystals should be convex polygons and meet the following conditions:

(*1*) Euler's rule

$$f + v = l + 2,$$

where f, v, l are the numbers of faces, edges and vertices, respectively;

(*2*) faces should be square, hexagonal, octagonal, decagonal, *etc*. (generally, contain only even number of edges, *i.e*., 4, 6, 8, 10, *etc*.); in contrast to C_n fullerenes, these polygons should not contain pentagons;

(*3*) the isolated ring (square, octagon, decagon, *etc*.) rule analogous to the isolated pentagon rule for fullerenes;

(*4*) contain only alternating X–Y covalent bonds that are more stable than the X–X and Y–Y bonds;

(*5*) the number of isolated faces should be consistent with the crystal system. If it is equal to 4, 6, 8, one deals with tetrahedral, cubic and hexagonal symmetry, respectively. Joining clusters through these faces using the same bonds as those between the atoms located at polygon vertices allows one to obtain close-packed crystals with sphalerite, simple cubic (SC), body-centred, face-centred cubic or hexagonal close-packed lattice (Table 2).

Crystal formation by copolymerisation through faces causes formation of strong diamond-like sp^3-bonds, which stabilise cluster crystals; if all isolated faces in a crystal are copolymerised, all bonds in the crystal are diamond-like ones. The conditions *3* and *4* are stability criteria for clusters and the conditions *2* and *5* are the criteria for crystal-forming ability.

As an example, we will calculate the smallest crystal-forming (4,6)-clusters comprised of squares and hexagons. If the number of squares (hexagons) is equal to c (h), the total number of faces is

$$f = c + h,$$

and the total number of edges is

$$l = \frac{4c + 6h}{2},$$

because each square and hexagon has 4 and 6 edges, respectively, one of them being shared between two faces. Taking into account the fact that each vertex is shared by three faces, the total number of vertices is

$$v = \frac{4c + 6h}{3}.$$

Table 2. Parameters of the smallest crystal-forming (4,6)-clusters.

c	h	$f = c + h$	$l = (4c + 6h)/2$	$v = (4c + 6h)/3$	Cluster	Lattice
6	4	10	24	16	C_{16}, X_8Y_8	sphalerite
	6	12	30	20	C_{20}, $X_{10}Y_{10}$	SC
	8	14	36	24	C_{24}, $X_{12}Y^*_{12}$	SC, BCC
	12	18	48	32	C_{32}, $X_{16}Y^*_{16}$	SC, FCC/FCCP
	14	20	54	36	C_{36}, $X_{18}Y^*_{18}$	SC
12	4	16	36	24	C_{24}, $X_{12}Y_{12}$	FCC/FCCP, sphalerite
	6	18	42	28	C_{28}, $X_{14}Y_{14}$	SC, FCC/FCCP
	8	20	48	32	C_{32}, $X_{16}Y_{16}$	FCC/FCCP,BCC
	12	24	60	40	C_{40}, $X_{20}Y_{20}$	FCC/FCCP
18	4	22	48	32	C_{32}, $X_{16}Y_{16}$	sphalerite
	6	24	54	36	C_{36}, $X_{18}Y_{18}$	SC
	8	26	60	40	C_{40}, $X_{20}Y_{20}$	BCC
	12	30	72	48	C_{48}, $X_{24}Y_{24}$	FCC/FCCP

Substituting these expression into Euler's relation, one gets the following equation:

$$c + h + \left(\frac{4c + 6h}{3}\right) = \left(\frac{4c + 6h}{2}\right) + 2,$$

which has the solution $c = 6$. It follows that the number of square faces in (4,6)-clusters should be equal to or multiple of six, $c = 6\,i$ ($i = 1, 2, 3, \ldots$), while the number of hexagons can be arbitrary. By sequentially searching for i and specifying h in accordance with the crystal system, one can obtain a complete set of all possible crystal-forming clusters.

Similar relations can also be derived for other basic non-hexagonal networks. For instance, the $B_{24}N_{24}$ cluster (Fig. 28) is built of (4,6,8)-rings and the $B_{60}N_{60}$ cluster is built of (4,8,10)-rings. Clearly, there exist isomers containing same-composition clusters of different structure, *e.g.*, three $B_{16}N_{16}$ isomers.

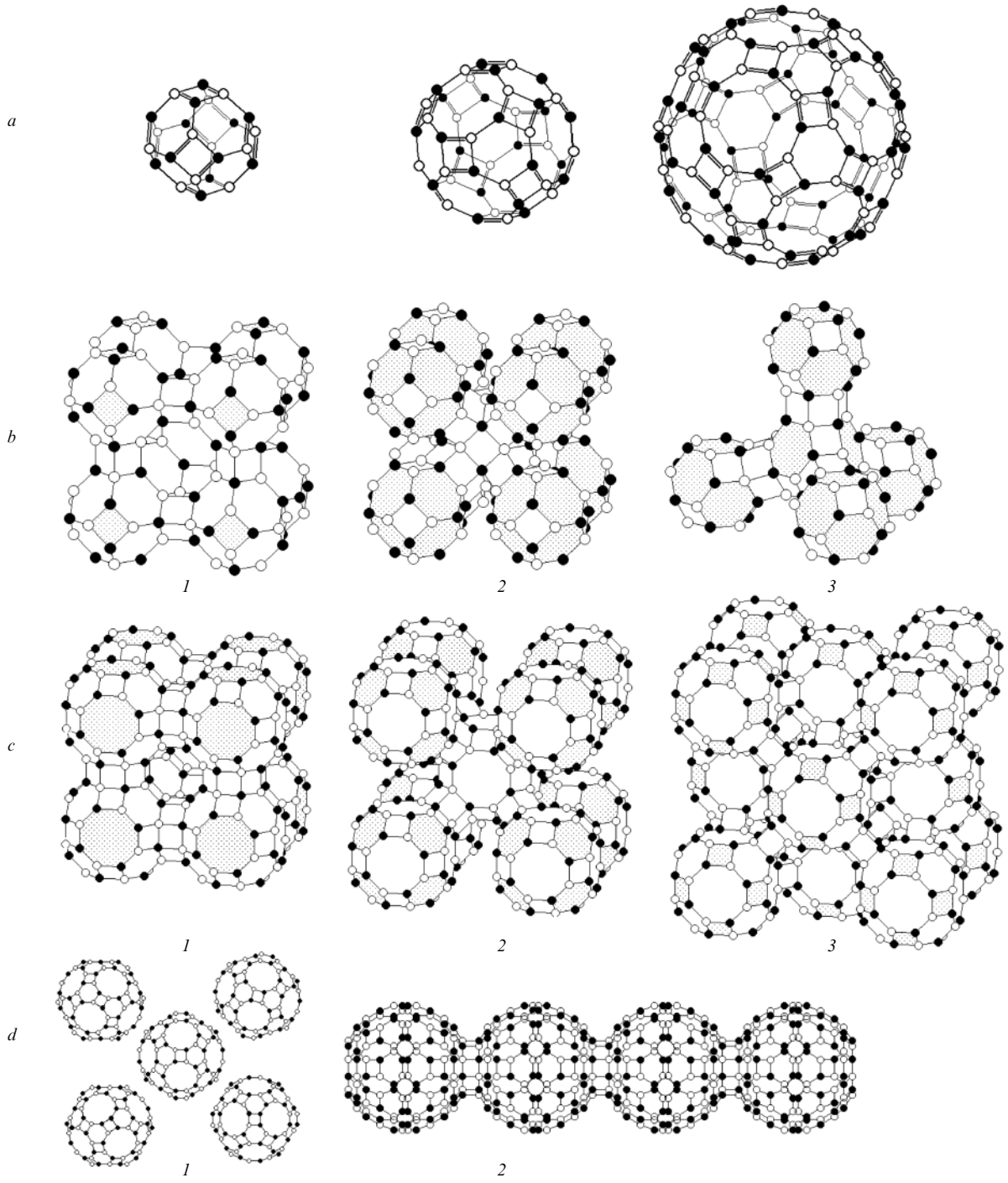


Figure 28. Structures of fulborenes (*a*) and crystals based on them, fulborenites (*b*, *c*).[22,23]
Fulborene molecules (*a*); the unit cells of fulborenites built of $B_{12}N_{12}$ fulborenes with the SC- (*1*) and BCC- (*2*) lattices and the coordination tetrahedron of the würtzite and sphalerite lattices (*3*) (*b*); the unit cells of fulborenites built of $B_{24}N_{24}$ fulborenes with the SC- (*1*), BCC- (*2*) and FCC- (*3*) lattices (*c*); and the unit cell of molecular FCC-crystal (*1*) and a polymer chain (*2*) formed by $B_{60}N_{60}$ fulborenes (*d*).

Based on the conditions *1–5*, which specify the total number and structure of crystal-forming clusters, and using the Schlegel diagrams, one can simulate the structure of these clusters and determine coordinates of all atoms. Next, one can determine the symmetry groups and crystal lattice types for these clusters.

For example, fullerene-like boron nitride clusters $B_{12}N_{12}$, $B_{24}N_{24}$, $B_{60}N_{60}$ called fulborenes were considered as crystal-forming clusters.[22,23] They were synthesised by laser ablation of hexagonal BN and detected by time-of-flight mass spectroscopy and high-resolution electron microscopy.[24,25,413] Note that a large group of BN-clusters is available at present, in particular, $B_{28}N_{28}$ (Ref. 414), $B_{36}N_{36}$ (Ref. 415), *etc*.

3. Fulborenites, crystals built of $B_{12}N_{12}$ and $B_{24}N_{24}$ fulborenes

Boron nitride has not only conventional polymorphs (see above), but also a number of unusual ones.[16] Some of them have been synthesised; their densities are intermediate between those of h-BN (2.28 g cm^{-3}) and c-BN (3.5 g cm^{-3}).[416–420]

For instance, the E-phase (explosive) was obtained as tiny crystals (size 0.1–0.5 mm, density 2.51–2.60 g cm^{-3}) by exploding hexogen ($\sim$100 g) over hexagonal BN.[416] The E-Phase was also synthesised[421–423] by deposition of h-BN powders on a cold Si-substrate; vapour phase crystallisation of, *e.g.*, BH_3+NH_3 obtained from a $B_2O_3+N_2+H_2$ mixture; crystallisation of the BN-phase obtained by laser or electron irradiation of h-BN under normal pressure. The IR spectrum of B_9N_9 cluster was calculated; taking account of coincidence of the theoretical frequencies of three vibrational modes (960, 1247 and 1459 cm^{-1}) with experimental data, it was concluded that the E-phase is built of B_9N_9 molecular clusters with sp^2- and sp^3-bonds.[422] A new boron nitride polymorph[424] is also similar to the E-phase.

An approach to structure determination of such polymorphs has been reported.[22,23] BN-crystals with SC-, FCC-, BCC- and diamond lattices were built of the fulborenes mentioned above. Note that obtaining an equilibrium and stable structure upon joining crystal-forming $X_{2n}Y_{2n}$ heteromolecules requires rigorous alternation of X–Y heteroatomic bonds, which is not always possible. For instance, Fig. 29 presents the matching of $X_{24}Y_{24}$ polyhedra through edges and faces in the formation of BCC-lattice and tetrahedra in the sphalerite and diamond structures. In all cases, an ideal matching of faces to form only hybridised X–Y bonds is impossible, because weaker X–X and Y–Y bonds are formed unavoidably.

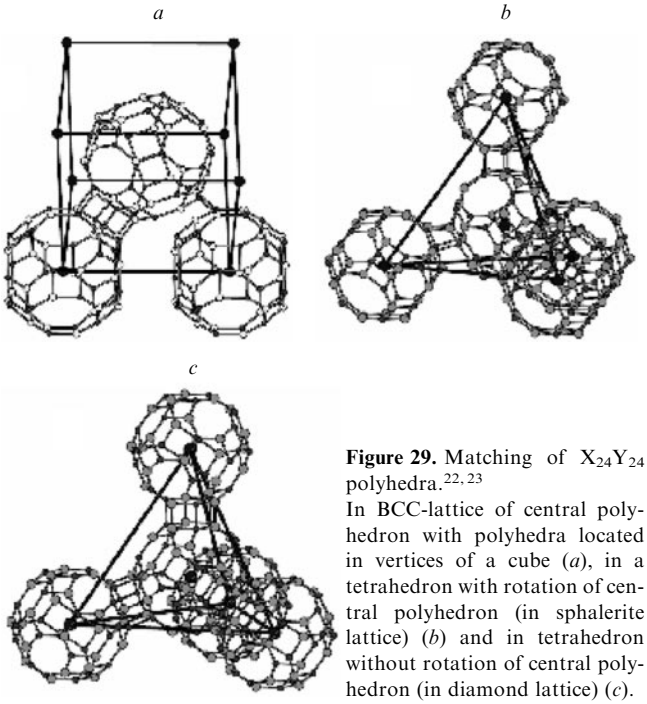


Figure 29. Matching of $X_{24}Y_{24}$ polyhedra.[22,23]
In BCC-lattice of central polyhedron with polyhedra located in vertices of a cube (*a*), in a tetrahedron with rotation of central polyhedron (in sphalerite lattice) (*b*) and in tetrahedron without rotation of central polyhedron (in diamond lattice) (*c*).

a. Hyperdiamond fulborenite HDF-$B_{12}N_{12}$

The unit cell of hyperdiamond fulborenite HDF-$B_{12}N_{12}$ is shown in Fig. 30.[99] This is a sphalerite lattice whose sites are occupied by $B_{12}N_{12}$ fulborenes. Hyperdiamond fulborenite $B_{12}N_{12}$ has a porous structure belonging to faujasite structural type (natural zeolite). The lattice parameter and density of HDF-$B_{12}N_{12}$ calculated[402,403] using a value of 0.145 nm for the B–N bond length are $a = 1.152$ nm and $\rho = 2.59$ g cm^{-3}, being in good agreement with experimental data for the E-phase ($a = 1.114$ nm, $\rho = 2.5–2.6$ g cm^{-3}).[83,423] This suggests that the E-phase is actually HDF-$B_{12}N_{12}$. The fulborenite in question is a semiconductor with a forbidden gap of 3.5 eV.

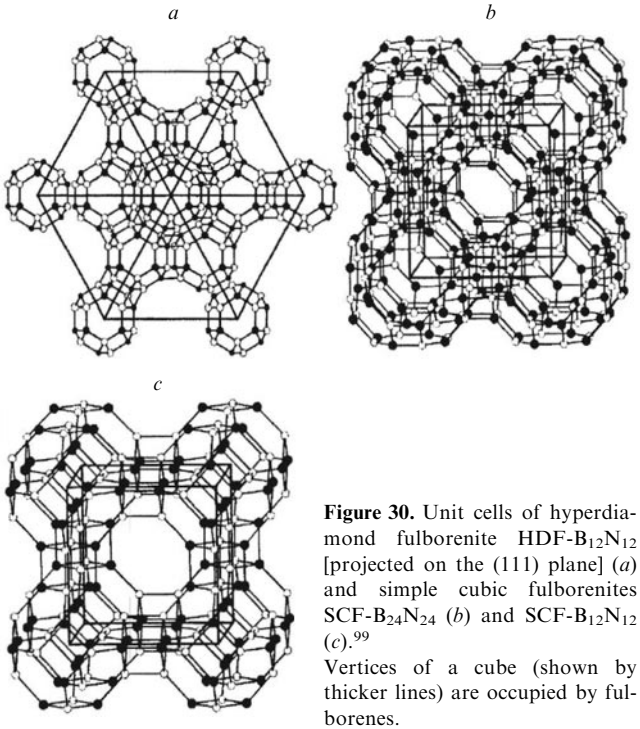


Figure 30. Unit cells of hyperdiamond fulborenite HDF-$B_{12}N_{12}$ [projected on the (111) plane] (*a*) and simple cubic fulborenites SCF-$B_{24}N_{24}$ (*b*) and SCF-$B_{12}N_{12}$ (*c*).[99]
Vertices of a cube (shown by thicker lines) are occupied by fulborenes.

The calculated[424,425] bulk modulus of HDF-$B_{12}N_{12}$ ($B = 658$ GPa) is higher than those of diamond ($B = 443$ GPa) and c-BN ($B = 369–400$ GPa), which can be responsible for the increased hardness of this crystal.[426] The elastic moduli depend on the strength of atom–atom bonds and structure. The energy of B–N sp^3-bonds in HDF-$B_{12}N_{12}$ is no higher than that in c-BN ($\sim$4.00 eV) owing to distortions of tetrahedra and deviation of bond angles (90°, 120°) from the equilibrium value (109.47°). Therefore, an increase in the bulk modulus of HDF-$B_{12}N_{12}$ is due to strengthening of the cage. Compared

to the sphalerite-type BN, HDF-$B_{12}N_{12}$ has a distorted, but stronger cage. This can be explained as follows. Compression causes structural distortion but not 'softening', as in diamond; rather, it is followed by structural recovery and transition to a more equilibrium state. The internal strain energy is compensated by external load.

b. Simple cubic fulborenite SCF-$B_{24}N_{24}$

According to calculations,[424] simple cubic fulborenite SCF-$B_{24}N_{24}$ has the following parameters: equilibrium SC-lattice constant $a = 0.7346$ nm, B—N bond length 0.1521 nm, number of atoms in unit cell $Z = 48$, $\rho = 2.495$ g cm^{-3}, $B = 367$ GPa and a forbidden gap of 3.76 eV. The equilibrium B—N bond length is somewhat smaller than in cubic boron nitride (0.1565 nm),[424] being close to the lengths of the bonds between *n*-membered rings in isolated molecule ($l_{8-6} = 0.1425$, $l_{8-4} = 0.1503$, $l_{6-4} = 0.1529$ nm).[413] Besides, SCF-$B_{24}N_{24}$ is characterised by electron density transfer from boron to nitrogen atom; in addition, the B—N bond covalency is higher than its ionicity.

Fulborenite SCF-$B_{24}N_{24}$ is a heteropolar semiconductor whose bulk modulus is comparable with that of cubic boron nitride. At the same time it is a new BN-zeolite with a channel diameter of 0.46 nm. This fulborenite seems to be a new promising semiconductor, ligthweight superhard structural material, molecular sieve and catalyst.

c. Simple cubic fulborenite SCF-$B_{12}N_{12}$

The calculated characteristics of simple cubic fulborenite SCF-$B_{12}N_{12}$ are shown in Table 3. This is a semimetal with a forbidden gap of 0.1 eV. It should be noted that the crystal lattice of SCF-$B_{12}N_{12}$ is not too stable, because it contains the B—B and N—N bonds not present in fulborene $B_{12}N_{12}$ and all known boron compounds with nitrogen. These bonds between two neighbouring fulborenes can be excluded by rotating one of them by 90° about common twofold symmetry axis passing through the centres of the square faces. Consecutive exclusion of B—B and N—N bonds leads to formation of a face-centred NaCl-type lattice in which sodium an chlorine atoms correspond to the initial and rotated $B_{12}N_{12}$ fulborene molecule, respectively.

Table 3. Calculated parameters of fulborenites: bond lengths (l_{B-N}/nm), lattice constants (a/nm), number of atoms in the unit cell (Z), density (ρ/g cm^{-3}), forbidden gap ($\sim E_g$/eV) and bulk modulus (B/GPa).[99]

Fulborenite	l_{B-N}	a	Z	ρ	$\sim E_g$	B
HDF-$B_{12}N_{12}$	0.1405	1.1191	192	2.823	3.05	658
SCF-$B_{24}N_{24}$	0.1521	0.7346	48	2.495	3.76	367
SCF-$B_{12}N_{12}$	0.1537	0.5886	24	2.425	0.1	340

4. BN-nanotube associates

Recently, some advances have been made in the synthesis[427–432] of both random (straw-type or cotton wool-type) and ordered associates of BN-nanotubes in the form of bundles, forest or wheat field. By analogy with carbon nanotube bundles, BN-nanotube bundles were grown on a substrate[406] preliminary coated with catalysts (iron nanoparticles). Nanotubes grow on these particles and then merge to form bundles; therefore, the pattern of nanoparticles on the substrate prescribes the structure of the growing nanotubes.

Ordered associates are fabricated[430–432] by template-assisted vapour phase deposition (or by sol–gel technique) of BN-nanotubes in channels of mesoporous matrices, which include various SiO_2- or Al_2O_3-based membranes prepared by electrochemical etching of plates a few micrometres to a few millimetres thick. They contain hexagonal lattices of cylindrical pores whose diameter (~ 10 nm) depends on the duration of the process (etching).

5. Haeckelite- and graphyne-like boron nitride nanostructures

Among boron nitride nanostructures, graphite-like BN sp^2-nanotubes (h-BN-NT) whose walls are formed by B_3N_3 rings have been best studied.[50, 63, 162, 382–387] In addition, BN-tubes with modified wall structure have been proposed. Namely, B_3N_3 hexagons are replaced by a combination of tetragons (B_2N_2) and octagons (B_4N_4) or by B—N-pentagons or/and heptagons.[433]

It is known that carbon nanostructures are often treated as prototypes in search for their heteroatomic analogues.[50, 63, 162, 382–387] Factors affecting the stability, structure and electronic-energy properties of new BN-nanotubes and fullerenes based on structural motifs of non-graphite forms of carbon, namely, haeckelites and graphynes (see Section V) have been studied.[434–438]

The structures of planar networks of 2D-forms of boron nitride, that is, hexagonal h-BN and hypothetical graphyne-like g-BN (isostructural analogue of α-graphyne), are built of B_3N_3 and $\{B_3N_3(BN)_6\}$ rings, respectively. They are shown in Fig. 31. Estimates[434] of the dependence of the total energies of zig-zag and armchair nanotubes on their diameters showed that nanotubes become less stable as their diameters decrease. The energies of achiral (armchair or zig-zag) tubes are close, *i.e.*, one can expect that the synthesis of g-BN-NT will afford comparable amounts of the armchair and zig-zag nanotubes unlike most inorganic nanotubes,[48–51, 162, 363, 439–441] which are characterised by preferred stability of a particular configuration type.

All g-BN-nanotubes are wide-gap semiconductors (width of forbidden gap is $\sim 5.7–5.9$ eV);[435] with B—N-

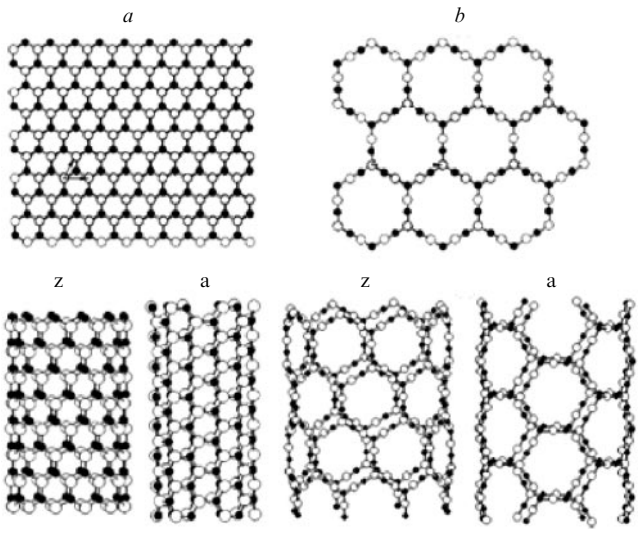


Figure 31. Fragments of planar sheets: h-BN (*a*) and g-BN (*b*) and structural models for corresponding zig-zag (z) and armchair (a) nanotubes.[435]

interactions being the main type of covalent bonds. These nanotubes are characterised by longitudinal and transverse anisotropy of B–N-bonds; the populations of two-centre B–N-bonds in $B_3N_3(BN)_6$ rings are significantly different. This effect, as well as the electron density polarisation along the B → N direction may result in atomic displacements in the nanotube wall and in a radial (or more complex) atomic relaxation, *i.e.*, one can expect[434–436] transformation of 'ideal single-wall' g-BN nanotubes to 'multi-wall' ones, comprised of coaxial 'atomic cylinders' made of various (nonequivalent) boron and nitrogen ions. g-BN nanotubes contain B(sp^1) and N(sp^2) atoms with the coordination numbers 2 and 3, respectively. Similarly to the carbon prototypes (see Section V), they can be classified as mixed ($sp^1 + sp^2$)-type boron nitride nanopolymorphs.

One of the most attractive features of g-BN-NT is their highly porous structure.[434–436] These systems can be considered as promising matrices for the design of a family of novel intercalated nanomaterials with various properties. Magnetisation studies of g-BN-NT with defect walls or impurities (as in the case of 'classical' h-BN-tubes) may appear to be quite interesting.[442,443] Models for graphyne-like cage (fullerene-like) BN particles were also proposed[444] and their stabilities analysed in comparison with those of the carbon analogues.[445]

Haeckelite-like BN-nanotubes are comprised of 4-, 6- and 8-membered boron–nitrogen rings.[437,438] Simulation of their structural and electronic-energy properties showed that they are wide-gap semiconductors (forbidden gap width ~ 3.3–4.1 eV). These systems are less stable than classical h-BN tubes (by 0.3 eV per atom).[437,438] The possibility of using haeckelite-like BN-nanotubes as materials for opto-electronic devices has been discussed.[438]

6. Monolithic BN-nanofibres

Information on monolithic BN-nanofibres is rather scarce. The case in point is that the known BN-fibres with h-BN (in the form of a 'rope' of nested cones rolled from graphite-like h-BN networks),[446–448] t-BN[449] and c-BN[450] structures are, as a rule, fabricated in a mixture with other BN-nanostructures (nanotubes, nanoplatelets, nanocrystallites, fullerenes, *etc.*). Isolation of fibres in a pure state is a complicated task.[449] The structural, thermal and electronic-energy properties of cubic BN-nanofibres were simulated.[451] A complete or partial rearrangement of the cubic to hexagonal structure of BN-nanofibre depending on the size, morphology and thermal treatment was revealed (Fig. 32). Energetically stable c-BN nanofibres are two-phase systems: the nanofibre 'shell' has a hexagonal (sp^2), whereas the 'core' has a cubic (sp^3) structure. Therefore, one deals with the formation of hybrid ($sp^2 + sp^3$) BN-nanofibres combining two structural types, h-BN and c-BN. Experimental evidences for simultaneous presence of sp^2- and sp^3-bonds in BN-nanofibres have been reported.[452] For BN-fibres, the structural rearrangements mentioned above will depend on the nanofibre size (diameter), face type (nonpolar or polar face) and the number of noncompensated (broken) bonds at the atoms located on faces.

Simulation of $sp^2 \leftrightarrow sp^3$ structural transformations including those induced by heat treatment[451] in BN-nanofibres revealed noticeable variation of B–N interatomic distances. This correlates with the change in the coordination number of atoms, which equals 3 for the hexagonal (sp^2) and 4 for the cubic (sp^3) structure. For instance, for the most thin fibres the average coordination number is appreciably smaller than three owing to the presence of numerous 'surface' atoms with broken bonds. The average coordination numbers of the thickest fibres are greater than three due to the presence of sp^3-atoms with a coordination number of four in the cubic 'core' of the nanofibre. As the fibre size increases, the average B–N distances increase from 0.143 nm to 0.155 nm, obeying a known trend in the following order: BN molecule (coordination number 1, $l_{B-N} = 0.128$ nm) → linear chain ...–B–N–B–N–... (coordination number 2, $l_{B-N} = 0.130$ nm) → crystals: h-BN (coordination number 3, $l_{B-N} = 0.145$ nm) → c-BN (coordination number 4, $l_{B-N} = 0.157$ nm).[452,453] Boron–nitrogen nanofibres can possess both semiconductor (forbidden gap is narrower than in c-BN) and metal-like properties.[454]

7. Nanocomposites

In this subsection we will consider main types of composite materials containing boron–nitrogen nanostructures and first of all BN-nanotubes.

a. Nanopeapods

In addition to 'carbon only' peapods (see above), a family of related heteroatomic (0D + 1D)-nanomaterials is known. Here, the role of shells is played by boron–nitrogen nanotubes and the intercalant molecules include C_n fullerenes,[362,371,455–458] $M_m@C_n$ endofullerenes[459] and other cage systems (metallocarbohedrenes M_8C_{12})[460–463] or boron–nitrogen molecules B_nN_n.[391,464,465]

An interesting feature of nanopeapods is the ability of the fullerene ensemble confined within the nanotube to undergo a spontaneous, thermally induced or radiation-induced polymerisation. For instance, a study of C_{60}@BN-NT nanopeapods (regular C_{60} chains within BN nanotubes) suggested[340] coalescence of C_{60} fullerenes with the formation of two-layer nanotubes (carbon NTs inside boron nitride NTs). The system is thought[362] to be a prototype nanowire, that is, a conducting carbon nanotube is sheathed with boron nitride 'insulation shell' (BN-nanotube) possessing the properties of a wide-gap semiconductor (forbidden gap width ~ 5 eV). Exposure of C_n@BN-NT peapods to a high-energy electron beam led to formation of a carbon nanotube inside the BN-NT.[371]

Simulation of $B_{12}N_{12}$@BN-NT nanopeapods based on boron nitride nanotubes with inner cavities filled with 1D-chains of small boron–nitrogen fullerenes $B_{12}N_{12}$ was reported.[465] These structures have attracted the attention of researchers as 'structural units' of new a boron nitride polymorph, E-phase, or hyperdiamond fulborenite (see above). The electronic-energy properties of the boron–nitrogen peapods under study depend on the mutual (symmetrical or asymmetrical) arrangement of neighbouring $B_{12}N_{12}$ molecules, *i.e.*, when the closest atoms in the neighbouring molecules are of the same (B–B or N–N) or different (B–N) nature. Thermally induced deformation of these nanopeapods is of considerable interest:[465] at 300 K, fullerenes in the chain become noticeably distorted due to formation of additional B–N bonds between $B_{12}N_{12}$ particles. Therefore, one can suggest that under standard conditions $B_{12}N_{12}$ fullerenes in structural voids of BN-nanotubes are prone to undergo spontaneous polymerisation with the formation of quasi-1D structures of the 'pearl necklace' type. Further heating to 1000 K causes a complete degadation of individual $B_{12}N_{12}$ particles and formation of a system of monatomic 'threads'

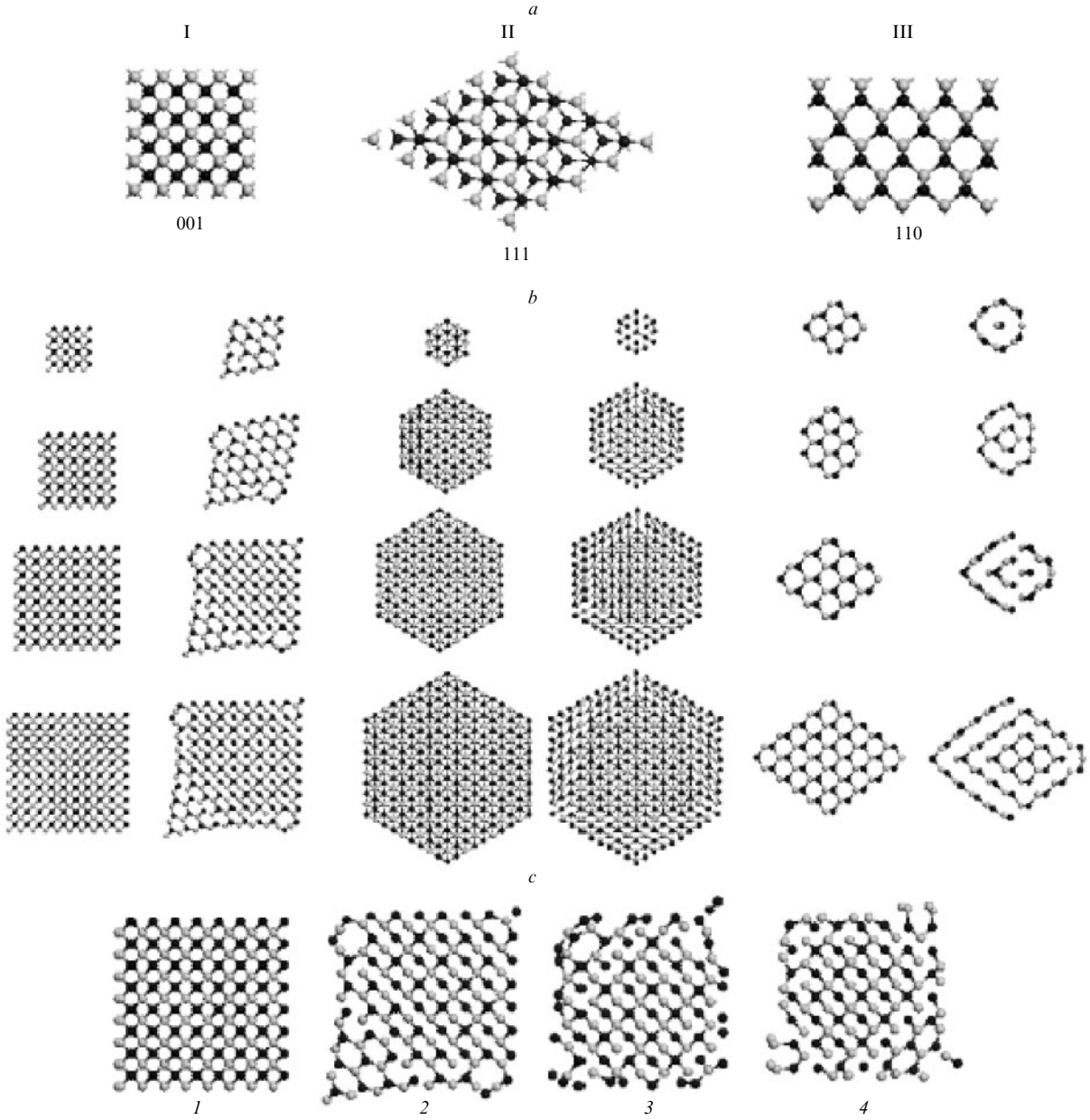


Figure 32. Initial atomic structures of cubic BN crystal (*a*), cross-sections of initial and optimised nanofibres (*b*) and initial and optimised type I nanofibres (*c*).[451]
(*a*) I, II, III denote nanofibre types; 001, 111, 110 denote the directions of 'cutting' boron nitride nanofibres; (*b*) from left to right shown are types I, II and III; (*c*) initial nanofibre (*1*), nanofibre with nonpolar faces (*2*), nitrogen-rich nanofibre with polar faces (*3*), and boron-rich nanofibre with nonpolar faces (*4*).

...—B—N—B—N—... inside the tube; similarly to carbyne, they have a coordination number of 2 and the sp^1-type of bonding. In other words, heat treatment of $B_{12}N_{12}$@BN-NT leads to formation of a new structure of the mixed ($sp^1 + sp^2$) type. Peapods retain this structure up to 2000 K. Finally, raising the temperature to 3000 K causes the atomic structure of the peapod shell to break down. The entire system completely loses its initial structure (at 0 K), being transformed to a variety of entanglements and ropes of —B—N—B—N— threads; this is accompanied by partial atomisation of the system.

Thus, thermally induced coalescence of carbon fullerenes in the peapod causes the formation of extended nanocapsules or carbon nanotubes inside the nanotube,[466] whereas coalescence of small fullerenes ($B_{12}N_{12}$) results in the formation of a system of atomic threads —B—N—B—N— (from the initial particles) rather than new cage structures within the nanotube.

b. BN-nanotubes bundles and lattices

Unlike carbon nanotubes, BN-nanotubes are not prone to form compact bundles. A possible reason can be the electronegativity difference between the boron and nitrogen atoms. Indeed, it is very hard to form the most energetically favourable system, which requires a perfectly ordered arrangement of neighbouring nanotubes in such a manner that the nearest atoms be of different nature (B—N).

Nevertheless, estimates[467] point to the possibility of formation of ordered assemblies of BN-nanotubes, because the cohesive energies of nanotube beams at equilibrium intertubular distances ($\sim 0.30-0.31$ nm) are negative, which indicates the possibility of spontaneous formation of BN-nanotube bundles. The bundles retain cylindrical morphology of BN-NTs. Interestingly, the degree of charge transfer ($B \rightarrow N$) in nanotube walls increases upon bundle formation. This indicates strengthening of intertubular interaction as nanotubes approach one another, although the overall charge density distribution in the bundle is essentially anisotropic and depends on the chirality and arrangement pattern of neighbouring nanotubes in the bundle. Apparently, the stabilities of nanotube bundles will depend on the number of B—N pairs in the region of contact between neighbouring nanotubes, which ensure the strongest bonds. Young's modulus of BN-NTs is lower than that of carbon tubes; with respect to conducting properties, the BN-NT bundles are wide-gap semiconductors (forbidden gap width is ~ 4.4 eV).[446]

A particular family includes theoretically designed[387] tubular superstructures representing covalent lattices comprised of fragments of conjugated BN- and carbon nanotubes. These systems are considered as prototypes of electronic nanodevices. As in the case of 'carbon only' nanotubular lattices, all atoms (B, C, N) in these systems have a coordination number of 3 and form sp^2-bonds.

c. Nanowires and other heteroatomic composites containing BN-nanotubes

At present, a large number of theoretically predicted nanocomposites combining BN-nanotubes with nanostructures based on other substances or compounds have been synthesised (Fig. 33). Among them, nanowires (nanoscale conductors sheathed with insulation shell, see above) have attracted the attention of researchers as promising functional elements for various electronic nanodevices. Here, the role of insulation shells is played by BN-nanotubes possessing stable dielectric properties. As mentioned above, the widths of their forbidden gaps remain almost constant (vary between 4 and 5 eV) irrespective of tube diameter and chirality.

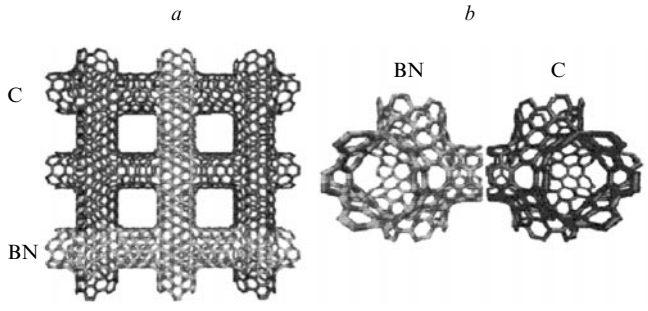


Figure 33. Fragments of 2D- (*a*) and 3D-lattices (*b*) made of carbon and BN nanotubes.[387]

Two types of nanowires have been proposed.[468–480] The first type represents a system of two coaxial nanotubes including a nanotube with metal-like conductivity type, *e.g.*, (C-NT)@(BN-NT)[468,472,473] or (BCN-NT)@(BN-NT)[474] encapsulated within insulation shell (BN-NT). The other type of nanowires includes BN-nanotubes filled with conducting monolithic nanorods (nanofibres), *e.g.*, SiC@(BN-NT),[475] M@(BN-NT),[475] where M is a 3d-metal. The last-named nanocomposites also exhibit attractive magnetic properties.[442,480]

Considerable literature[386,387,468–471,481–486] is devoted to studies of a large set of other (both synthesised and predicted) nanocomposites containing BN-NTs. These are, *e.g.*, BN-nanotubes with different-type impurity atoms (C, Si) on NT walls covered with various adatoms, conjugated with nanotubes of different chemical composition or 'inserted' into various matrices.[386,387] However, analysis of these nanomaterials goes beyond the scope of this review.

VIII. Conclusion

The discovery of carbon fullerenes and nanotubes laid the foundation of present-day step in the development of concepts of carbon nanoforms. Numerous experimental and theoretical studies carried out in the last two decades made it possible to obtain and collect detailed information on the atomic structure and physicochemical properties of carbon nanoforms and to determine fields of their applications.

A new line of investigations in physicochemistry of carbon nanoforms involves search for and synthesis of new nanostructures based on them, namely, quasi-1D, 2D (films) and 3D (crystals) associates of the hollow nanostructures. These efforts are accompanied by studies on the synthesis and properties of new monolithic carbon nanoforms (diamond-like crystallites and fibres) as well as more complex carbon–carbon nanocomposites representing various combinations of the carbon nanoforms mentioned above.

A large class of new carbon nanostructures was predicted theoretically. To date, many systems have been synthesised. They provide a much better insight into the nanosized states of carbon. In addition, they are of considerable practical interest as promising superhard materials, catalysts, materials for gas storage, molecular sieves and nanoelectronics. Clearly, the most interesting avenue of research involves extension of (i) variability ranges of properties and (ii) application fields of carbon nanomaterials. Progress in this area will give an impetus to more thorough investigations of systems in question.

Research in this field is in essence scientific exploration aimed at predicting the atomic structure, stability factors and physicochemical properties and developing methods of synthesis of new nanoforms. It also involves solution of materials science problems concerning the design of novel polyfunctional carbon nanomaterials. Modern quantum chemical methods of computer-assisted materials science also play an important role in elucidation of the structure and properties of these materials.

Concluding, the results obtained in studies of new carbon nanoforms enabled structure determination of some previously found unusual carbon allotropes. These studies also gave an impetus to search for analogous nanoforms of other inorganic compounds. The authors of this review tried to report on some advantages in the last-mentioned investigation line taking new boron nitride nanoforms as examples. Taking account of experience accumulated in studies of fulborene(B_nN_n)-based phases, one can assume that many other compounds with sp^2-type of bonding can form fulborene-like crystal-forming clusters of general formula X_nY_n and therefore one can design a

variety of systems representing new nanoforms of related compounds of the AlN, SiC, *etc*. types. Based on combined lattices of crystal-forming clusters, one can derive a large class of new artificial zeolites, clathrates and polymers.

Small size of these structures can be explained by high degree of their ordering and complexity. Unfortunately, the same reasons preclude large-scale synthesis. Many of the proposed carbon and BN nanoforms are metastable, which also makes their synthesis difficult.

Summing up, in the nearest future one can expect the emergence of novel nanoarchitectures based on metal oxides, metal dichalcogenides and other layered compounds prone to formation of nanotubes and fullerene-like clusters, as well as novel nanomaterials, nano-items and nanodevices based on them. It is these novel nanoarchitectures 'tuned' to detect the predicted size and resonance effects that should be used to observe new phenomena.

References

1. D I Mendeleev *Osnovy Khimii* (Foundations of Chemistry) (Moscow, Leningrad: Goskhimizdat, 1947) Vol. 1
2. V D Fedoseev, N V Novikov, A S Vishnevskii, I G Teremetskaya *Almaz. Spravochnik* (Atlas. Handbook) (Ed. N V Novikov) (Kiev: Naukova Dumka, 1981)
3. A Ubbelohde, F Lewiss *Graphite and Its Crystal Compounds* (Oxford: Clarendon Press, 1960)
4. A V Kurdyumov, A N Pilyankevich *Fazovye Prevrashcheniya v Uglerode i Nitride Bora* (Phase Transformations in Carbon and Nitrite of Boron) (Kiev: Naukova Dumka, 1979)
5. A V Kurdyumov, V G Malogolovets, N V Novikov, A N Pilyankevich, L A Shul'man *Polimorfnye Modifikatsii Ugleroda i Nitrida Bora. Spravochnik* (Polymorphous Modifications of Carbon and Boron Nitride. Handbook) (Moscow: Metallurgiya, 1994)
6. A M Sladkov *Karbin — Tret'ya Allotropnaya Forma Ugleroda* (Carbyne as the Third Allotropic Form of Carbon) (Moscow: Nauka, 2003)
7. G P Vdovykin *Uglerodistoe Veshchestvo Meteoritov* (Carbonic Substance of Meteorite) (Moscow: Nauka, 1967)
8. A S Fialkova *Uglegrafitovye Materialy* (Electrographite Materials) (Moscow: Metallurgiya, 1979)
9. Z I Syunyaev *Neftyanoi Uglerod* (Oil Carbon) (Moscow: Khimiya, 1980)
10. L F Vereshchagin *Sinteticheskie Almazy i Gidroekstruziya* (Synthetic Diamonds and Hydroextrusion) (Moscow: Nauka, 1982)
11. V S Ostrovskii *Iskusstvennyi Grafit* (Artificial Graphite) (Moscow: Metallurgiya, 1986)
12. E Yu Tonkov *Fazovye Prevrashcheniya Soedinenii pri Vysokom Davlenii. Spravochnik* (Phase Transformations at High Pressure) (Moscow: Metallurgiya, 1988)
13. A A Val'ter, G K Eremenko, V N Kvasnitsa, Yu A Polkanov *Udarno-metall-amorfogennye Mineraly Ugleroda* (Percussive Metal Amorphous Minerals of Carbon) (Kiev: Naukova Dumka, 1992)
14. I V Stankevich, M V Nikerov, D A Bochvar *Usp. Khim.* **53** 1101 (1984) [*Russ. Chem. Rev.* **53** 640 (1984)]
15. L I Man, Yu A Malinovskii, S A Semiletov *Kristallografiya* **35** 1029 (1990) [a]
16. V V Pokropivny *Nanostruktur. Materialov.* **1** 39 (2005)
17. L F Vereshchagin, E N Yakovlev, G N Stepanov *Pis'ma Zh. Exp. Teor. Fiz.* **16** 372 (1972) [b]
18. I Konyashin, A Zern, J Mayer *Diamond Relat. Mater.* **10** 99 (2001)
19. I Konyashin, V Khvostov, V Babaev, M Guseva, J Mayer, A Sirenko *Int. J. Refractory Metals Hard Mater.* **24** 17 (2006)
20. G Seifert *Nat. Mater.* **3** 77 (2004)
21. I V Stankevich, A L Chistyakov, E G Gal'pern, N P Gambaryan *Zh. Strukt. Khim.* **36** 976 (1995) [c]
22. V V Pokropivny, A V Pokropivny, V V Skorokhod, A V Kurdyumov *Dokl. Nats. Akad. Nauk Ukr.* **4** 112 (1999)
23. V V Pokropivny, V V Skorokhod, G S Oleinik, A V Kurdyumov, T S Bartnitskaya, A V Pokropivny, A G Sisonyuk, D V Sheichenko *J. Solid State Chem.* **54** 212 (2000)
24. T Oku, T Hirano, M Kuno, T Kusunose, K Niihara, K Suganama *Mater. Sci. Eng. B* **74** 206 (2000)
25. T Oku, M Kuno, H Kitahara, I Narita *Int. J. Inorg. Mater.* **3** 597 (2001)
26. A Kasuya, R Sivamonan, Yu A Barnakov, I M Dmitruk, T Nirasawa, V R Romanyuk, V Kumar, S V Mamykin, K Tohji, B Jeyadevan, K Shinoda, T Kudo, O Terasaki, Z Liu, R V Belosludov, V Sundararsjan, Y Kawazoe *Nat. Mater.* **3** 99 (2004)
27. G Chen, K Tang, Y Qian *Int. J. Nanotechnol.* **1** 366 (2004)
28. T Baruah, M K Pederson, R R Zope, M R Beltrain *Chem. Phys. Lett.* **387** 476 (2004)
29. G S Zakharova, A N Enyashin, V V Ivanovskaya, V L Volkov, A L Ivanovskii *Inzh. Fiz.* (5) 19 (2003)
30. A N Enyashin, A L Ivanovskii *Zh. Fiz. Khim.* **79** 1085 (2005) [d]
31. A A Demkov, W Windl, O F Sankey *Phys. Rev. B* **53** 11288 (1996)
32. M Matsubara, C Mossobrio *J. Chem. Phys.* **122** 084304 (2005)
33. B X Li, P L Cao *Phys. Rev. B* **62** 15788 (2000)
34. V Kumar, Y Kawazoe *Phys. Rev. Lett.* **87** 045503 (2001)
35. R O Jones *J. Chem. Phys.* **110** 5189 (1999)
36. H Kuzmany, J Fink, M Mehring, S Roth *Electronic Properties of the Fullerenes. Solid-State Sciences* (Berlin: Springer, 1993)
37. V I Sokolov, I V Stankevich *Usp. Khim.* **62** 455 (1993) [*Russ. Chem. Rev.* **62** 419 (1993)]
38. *Optical and Electronic Properties of Fullerenes and Fullerene-Based Materials* (Ed. J Shinar) (New York: Marcel Dekker, 1999)
39. *Fullerenes and Related Structures* (Ed. A Hirsch) (Berlin, Heidelberg: Springer, 1999)
40. O Gunnarson *Rev. Mod. Phys.* **69** 575 (1997)
41. B Sundqvist *Adv. Phys.* **48** 1 (1999)
42. T L Makarova *Fiz. Tekhn. Poluprovod.* **35** 257 (2001)
43. *Fullerene Polymers and Fullerene Polymer Composites* (Eds P C Eklund, A M Rao) (Berlin: Springer, 2000)
44. L N Sidorov, M A Yurovskaya, A Ya Borshchevskii, I V Trushkov, I N Ioffe *Fullereny* (Fullerenes) (Moscow: Ekzamen 2005)
45. M Prato *Top. Curr. Chem.* **199** 173 (1999)
46. V N Popov *Mater. Sci. Eng., R* **43** 61 (2004)
47. X Lu, Z Chen *Chem. Rev.* **105** 3643 (2005)
48. *The Science of Fullerenes and Carbon Nanotubes* (Eds M S Dresselhaus, M Dresselhaus, P Eklund) (San Diego, CA: Academic Press, 1996)
49. *The Science and Technology of Carbon Nanotubes* (Eds K Tanaka, T Yamabe, K Fuku) (Oxford: Elsevier, 1999)
50. A L Ivanovskii *Kvantovaya Khimiya v Materialovedenii. Nanotubulyarnye Formy Veshchestva* (Quantum Chemistry in Materials Science. Nanotube Forms of Matter) (Ekaterinburg: Urals Branch of the Russian Academy of Sciences, 1999)
51. P J F Harris *Carbon Nanotubes and Related Structures: New Materials for the Twenty first Century* (Cambridge: University Press, 1999)
52. A V Eletskii *Usp. Fiz. Nauk* **167** 945 (1997) [*Physics-Uspekhi* **40** 899 (1997)]
53. Yu E Lozovik, A M Popov *Usp. Fiz. Nauk* **167** 751 (1997) [*Physics-Uspekhi* **40** 717 (1997)]
54. A L Ivanovskii *Usp. Khim.* **68** 119 (1999) [*Russ. Chem. Rev.* **68** 103 (1999)]
55. E G Rakov *Usp. Khim.* **70** 934 (2001) [*Russ. Chem. Rev.* **70** 827 (2001)]
56. O A Shenderova, V V Zhirnov, D W Brenner *Crit. Rev. Solid State Mater. Sci.* **27** 227 (2002)
57. H Rafli-Tabar *Phys. Rep.* **390** 235 (2004)
58. T Belin, F Epron *Mater. Sci. Eng.* **B119** 105 (2005)
59. A P Ramirez *Bell Labs Techn. J.* **10** 171 (2005)

60. S Ciraci, S Dag, T Yildirim, O Gulseren R T Senger *J. Phys.: Condens. Matter* **16** R901 (2004)
61. T Durkop, B M Kim, M S Fuhrer *J. Phys.: Condens. Matter* **16** R553 (2004)
62. A V Eletskii *Usp. Fiz. Nauk* **174** 1191 (2004) [*Physics-Uspekhi* **47** 1119 (2004)]
63. C N R Rao, A Govindaraj, G Gundiah, S R C Vivekchand *Chem. Eng. Sci.* **59** 4665 (2004)
64. M Burghard *Surf. Sci. Rep.* **58** 1 (2005)
65. A C Dupuis *Prog. Mater. Sci.* **50** 929 (2005)
66. D Tasis, N Tagmatarchis, A Bianco, M Prato *Chem. Rev.* **106** 1105 (2006)
67. K Lau, C Gu, D Hui *Composites, B* **37** 425 (2006)
68. *Nanomaterials Handbook* (Ed. Y Gogotsi) (Boca Raton, FL, London, New York: Taylor and Francis Group, 2006)
69. E H L Falcao, F Wudl *J. Chem. Technol. Biotechnol.* **82** 524 (2007)
70. P N D'yachkov *Uglerodnye Nanomaterialy* (Carbon Nanomaterials) (Moscow: Binom, 2006)
71. M Paradise, T Goswami *Mater. Design* **28** 1477 (2007)
72. R F Gibson, E O Ayorinde, Y F Wen *Compos. Sci. Technol.* **67** 1 (2007)
73. Y Matsuo, E Nakamura *J. Synth. Org. Chem. Jpn.* **65** 44 (2007)
74. B Mahar, C Laslau, R Yip, Y Sun *IEEE Sensors J.* **7** 266 (2007)
75. C H See, A T Harris *Ind. Eng. Chem. Res.* **46** 997 (2007)
76. G Yushin, A Nikitin, Y Gogotsi, in *Nanomaterials Handbook* (Ed. Y Gogotsi) (Boca Raton, FL, London, New York: Taylor and Francis Group, 2006) p. 239
77. V V Pokropivny, R Lohmus, I Hussainova, A Pokropivny, S Vlassov *Introduction to Nanomaterials and Nanotechnology* (Tartu: Tartu University, 2007)
78. H Gleiter *Acta Mater.* **48** 1 (2000)
79. V V Skorokhod, A V Ragulya, I V Uvarova *Nanostrukturnye Materialy* (Nanostructural Materials) (Kiev: Akademperiodika, 2001)
80. V V Pokropivny, V V Skorokhod *Mater. Sci. Eng., C* **27** 990 (2007)
81. V V Pokropivny, V V Skorokhod *Nanostruktur. Materialoved.* (1) 58 (2008)
82. B Wen, J J Zhao, T J Li *Int. Mater. Rev.* **52** 131 (2007)
83. R Kitaura, H Shinohara *Chem. — Asian J.* **1** 646 (2006)
84. E A Belenkov, V V Ivanovskaya, A L Ivanovskii *Nanoalmazy i Rodstvennye Uglerodnye Nanomaterialy. Komp'yuternoe Materialovedenie* (Nanodiamonds and Related Carbon Nanomaterials. Computer Materials Science) (Ekaterinburg: Urals Branch of the Russian Academy of Sciences, 2008)
85. J Robertson *Mater. Sci. Eng., R* **37** 129 (2002)
86. Y Chen, J F Gerald, L T Chadderton, L Chaffron *Appl. Phys. Lett.* **74** 2782 (1999)
87. A V Kurdyumov, V F Britun, N I Borimchuk, V V Yarosh *Martensitnye i Diffuzionnye Prevrashcheniya v Uglerode i Nitride Bora pri Udarnom Szhatii* (Martensite and Diffusive Changes in Carbon and Boron Nitride upon Impact Compression) (Ed. O O Kupriyanova) (Kiev: National Academy of Sciences of Ukraine, 2005)
88. M A Tamor, K S Hass *J. Mater. Res.* **5** 2273 (1999)
89. V V Brazhkin, A G Lyapin, S G Lyapin, S V Popova, R N Voloshin,Yu A Klyuev, A M Naletov, N N Mel'nik *Usp. Fiz. Nauk* **167** 1019 (1997) [*Physics-Uspekhi* **40** 969 (1997)]
90. L N Kostadinov, D D Dobuv *Phys. Status Solidi A* **109** K85 (1998)
91. V I Trefilov, D V Shchur, B P Tarasov, Yu M Shul'ga, A V Chernogorenko, V K Pishchuk, S Yu Zaginaichenko *Fullereny — Osnova Materialov Budushchego* (Fullerenes as a Base for the Future Materials) (Kiev: Adef, 2001)
92. R S Ruoff, A L Ruoff *Nature (London)* **350** 663 (1991)
93. N R Serebryanaya, V D Blank, V A Ivdenko, L A Chernozatonskii *Solid State Commun.* **118** 183 (2001)
94. M Popov, M Kyotani, R J Nemanich, Y Koga *Phys. Rev. B* **65** 033408 (2002)
95. S G Buga, V D Blank, N R Dubitsky, N R Serebryanaya, A Fransson, T Wagberg, B Sundqvist *High Press. Res.* **23** 259 (2003)
96. S G Buga, V D Blank, N R Serebtyanaya *Diamond Relat. Mater.* **14** 896 (2005)
97. V D Blank, S G Buga, G A Dubitskya N R Serebryanaya, V M Prokhorov, B N Mavrin, V N Denisov, L A Chernosatonskii, S Berezina *Z. Naturforsch., B* **61** 1547 (2006)
98. V V Pokropivny, L I Ovsyannikova, S V Kovrigin *Fiz. Tv. Tela* **49** 2224 (2007) [e]
99. V V Pokropivny, V L Bekenev *Fiz. Tekhn. Poluprovod.* **40** 656 (2006) [f]
100. M D Blyander, L Kleinman *Phys. Rev. B* **47** 10967 (1993)
101. H Prinzbach, A Weller, P Landenberger, F Wahl, J Worth, L T Scot, M Gelmont, D Olevano, B V Issendorff *Nature (London)* **407** 60 (2000)
102. M Saito, Y Miyamoto *Phys. Rev. Lett.* **87** 035503 (2001)
103. S Okada, Y Miyamoto, M Saito *Phys. Rev. B* **64** 245405 (2001)
104. G B Adams, O F Sankey, J B Page, M O'Keeffe *Chem. Phys.* **176** 61 (1993)
105. A Devos, M Lannoo *Phys. Rev. B* **58** 8236 (1998)
106. Y Miyamoto, M Saito *Phys. Rev. B* **63** 161401 (2001)
107. Z Chen, T Heine, H Jiao, A Hirsch, W Thiel, P Schleyer *Chem. – Eur. J.* **10** 963 (2004)
108. A W Phelps *Mater. Res. Soc. Symp. Proc.* **162** 213 (1990)
109. F P Bundy, J S Kasper *J. Chem. Phys.* **46** 3437 (1967)
110. V V Fedoseev, B V Deryagin, V P Varnin, S P Vnukov, I G Teremetskaya, N D Polyanskaya *Dokl. Akad. Nauk SSSR* **228** 371 (1976) [g]
111. V V Slodkevich *Dokl. Akad. Nauk SSSR* **253** 697 (1980) [g]
112. A S Smolyar, Yu I Sozin, V A Barkholenko, S N Maloshtan, V A Kuts, V G Gurin, A P Arkhipov, A Yu Gerasimov, N A Razvadovskii, A N Titenko *Sverkhtv. Mater.* (2) 79 (2002)
113. V V Pokropivny, A V Pokropivny *Fiz. Tv. Tela* **46** 380 (2004) [e]
114. R B Aust, H G Drickamer *Science* **140** 817 (1963)
115. R O Jones, G Seifert *Phys. Rev. Lett.* **79** 443 (1997)
116. L A Openov, V F Eleshin *Pis'ma Zh. Eksp. Teor. Fiz.* **80** 572 (1998) [b]
117. D M Sheichenko, A V Pokropivny, V V Pokropivny *Semicond. Phys. Quantum Electron. Optoelectron.* **3** 550 (2000)
118. I V Stankevich, A L Chistyakov, E G Gal'pern, L A Chernozatonskii *Zh. Strukt. Khim.* **36** 976 (1993) [c]
119. V L Bekenev, V V Pokropivny *Fiz. Tv. Tela* **48** 1324 (2005) [e]
120. V V Pokropivny, V L Bekenev *Fullerenes, Nanotubes Carbon Nanostruct.* **13** 1 (2005)
121. D Shamiryan, T Abell, F Iacopi, K Maex *Mater. Today* 34 (2004)
122. T Guo, M D Diener, Y Chai, M J Alford, R E Haufler, S M McClure, T Ohno, J H Weawer, G E Scuseria, R E Smalley *Science* **257** 1661 (1992)
123. H W Kroto, D R M Walton *Chem. Phys. Lett.* **214** 353 (1993)
124. Z Chen, H Jiao, M Buehl *Theor. Chem. Acc.* **106** 352 (2001)
125. Yu N Makurin, A A Sofronov, A I Gusev, A L Ivanovskii *Chem. Phys.* **270** 293 (2001)
126. J Kim, G Galli, J W Wilkins, A Canning *J. Chem. Phys.* **108** 2631 (1998)
127. A N Enyashin, V V Ivanovskaya, Yu N Makurin, A L Ivanovskii *Fiz. Tv. Tela* **46** 1522 (2004) [e]
128. A N Enyashin, A L Ivanovskii *Pis'ma Zh. Eksp. Teor. Fiz.* **86** 609 (2007) [b]
129. A N Enyashin, A L Ivanovskii *Phys. Rev. B* **77** 113402 (2008)
130. G Seifert, A N Enyashin, Th Heine *Phys. Rev. B* **72** 012102 (2005)
131. A N Enyashin, S Gemming, Th Heine, G Seifert, L Zhechkov *Phys. Chem. Chem. Phys.* **8** 3320 (2006)
132. X Blase *Phys. Rev. B* **67** 035211 (2000)
133. M Menon, E Richter, L Chernozatonskii *Phys. Rev. B* **62** 15420 (2000)
134. M C Abramo, C Caccamo *J. Chem. Phys.* **128** 074503 (2008)
135. L M Zeger, Yu M Juan, E Kaxiras, A Antonelli http://www arXiv:cond-mat/950205

136. C A Perotton, J A Jornada *Phys. Rev. B* **65** 224208 (2002)
137. R Phillips, D A Draborg, T Lenosky, G B Adams, J F Sankey *Phys. Rev. B* **46** 1941 (1992)
138. A L Mackay, H Terrones *Nature (London)* **352** 762 (1991)
139. D Vanderbilt, J Tersoff *Phys. Rev. Lett.* **68** 511 (1992)
140. T Lenosky, X Gonze, M Teller, V Elser *Nature (London)* **355** 333 (1992)
141. B I Dunlap *Phys. Rev. B* **4** 1933 (1992)
142. L A Chernozatonskii *Phys. Lett. A* **170** 37 (1992)
143. R Martel, H R Shea, P Avouris *Nature (London)* **398** 299 (1999)
144. S Ihara, S Itoh, J Kitakami *Phys. Rev. B* **47** 12908 (1993)
145. J K Johnson, B N Davidson, M R Pederson, J Q Broughton *Phys. Rev. B* **50** 17575 (1994)
146. V Meunier, Ph Lambin, A A Lucas *Phys. Rev. B* **57** 14886 (1998)
147. L Yang, J Chen, J Dong *Phys. Status Solidi, B* **241** 1269 (2004)
148. C C Tsai, F L Shyu, C W Chiu, C P Chang, R B Chen, M F Lin *Phys. Rev. B* **70** 075411 (2004)
149. R Tamura, M Ikuta, T Hirahara, M Tsukada *Phys. Rev. B* **71** 045418 (2005)
150. F L Shyu, C C Tsai, C H Lee, M F Lin *J. Phys.: Condens. Matter* **18** 8313 (2006)
151. M T Lusk, N Hamm *Phys. Rev. B* **76** 125422 (2007)
152. R B King *Mol. Phys.* **102** 1241 (2004)
153. R B King *J. Phys. Chem.* **100** 15096 (1996)
154. L Song, L Ci, L Sun, C Jin, L Liu, W Ma, D Liu, X Zhao, S Luo, Z Zhang, Y Xiang, J Zhou, W Zhou, Y Ding, Z Wang, S Xie *Adv. Mater.* **18** 1817 (2006)
155. M Monthioux, B W Smith, B Burteaux, A Claye, J E Fischer, D E Luzzi *Carbon* **39** 1251 (2001)
156. J Liu, A G Rinzler, H Dai, J H Hafner, R K Bradley, P J Boul, A Lu, T Iverson, K Shelimov, C B Huffman, F Rodriguez-Macias, Y S Shon, T R Lee, D T Colbert, R E Smalley *Science* **280** 1254 (1998)
157. M Endo, H Muramatsu, T Hayashi, Y A Kim, M Terrones, M S Dresselhaus *Nature (London)* **433** 476 (2005)
158. Y A Kim, O N Torrens, J M Kikkawa, E Abou-Hamad, C Goze-Bac, D E Luzzi *Chem. Mater.* **19** 2982 (2007)
159. R H Baughman, A A Zakhidov, W A de Heer *Science* **297** 787 (2002)
160. Z F Ren, Z P Huang, J W Xu, J H Wang, P Bush, M P Siegal, P N Provencio *Science* **282** 1105 (1998)
161. C H Sun, F Li, C G Liu, G Q Lu, H M Cheng, C H Sun, G Q Lu *Appl. Phys. Lett.* **86** 203106 (2005)
162. G S Zakharova, V V Volkov, V V Ivanovskaya, A L Ivanovskii *Nanotrubki i Rodstvennye Nanostruktury Oksidov Metallov* (Nanotubes and Related Nanostructures of Metal Oxides) (Ekaterinburg: Urals Branch of the Russian Academy of Sciences, 2005)
163. B I Yacobson, C J Brabec, J Bernholc *Phys. Rev. Lett.* **76** 2511 (1996)
164. M J López, A Rubio, J A Alonso, L-C Qin, S Iijima *Phys. Rev. Lett.* **86** 3056 (2001)
165. J Tang, L C Qin, T Sasaki, M Yudasaka, A Matsushita, S Iijima *Phys. Rev. Lett.* **85** 1667 (2000)
166. T Vodenitcharova, K Mylvaganam, L C Zhang *J. Mater. Sci.* **42** 4935 (2007)
167. M H F Sluiter, V Kumar, Y Kawazoe *Phys. Rev. B* **65** 161402 (2002)
168. S Rols, I N Goncharenko, R Almairac, J L Sauvajol, I Mirebeau *Phys. Rev. B* **64** 153401 (2001)
169. E Saether *Compos. Sci. Technol.* **63** 1551 (2003)
170. E Saether, S J V Frankland, R B Pipes *Compos. Sci. Technol.* **63** 1543 (2003)
171. J Z Liu, Q S Zheng, L F Wang, Q Jiang *J. Mech. Phys. Solids* **53** 123 (2005)
172. B I Yakobson, L S Couchman *J. Nanopart. Res.* **8** 105 (2006)
173. T W Cheng, W K Hsu *Appl. Phys. Lett.* **90** 123102 (2007)
174. S J Jeong, K A Park, S H Jeong, H J Jeong, K H An, C W Nah, D Pribat, S H Lee, Y H Lee *Nano Lett.* **7** 2179 (2007)
175. J Zang, O Aldas-Palacios, F Liu *Commun. Comput. Phys.* **2** 451 (2007)
176. B Chen, M Gao, J M Zuo, S Qu, B Liu, Y Huang *Appl. Phys. Lett.* **83** 3570 (2003)
177. C H Sun, F Li, H M Cheng, G Q Lu *Appl. Phys. Lett.* **87** 193101 (2005)
178. L A Girifalco, M Hodak, R S Lee *Phys. Rev. B* **62** 13104 (2000)
179. S Reich, C Thomsen, P Ordejon *Phys. Rev. B* **65** 155411 (2002)
180. Z Liu, L C Qin *Carbon* **43** 2146 (2005)
181. S J Wu, Y H Ho, C P Chang, M F Lin *Physica E* **32** 581 (2006)
182. M Ferrier, F Ladieu, M Ocio, B Sacepe, T Vaugien, V Pichot, P Launois, H Bouchiat *Phys. Rev. B* **73** 094520 (2006)
183. E Perfetto, J Gonzalez *Phys. Rev. B* **74** 201403 (2006)
184. M J López, A Rubio, J A Alonso *IEEE Transact. Nanotechol.* **3** 230 (2004)
185. M C Gordillo, J Marti *Phys. Rev. B* **67** 205425 (2003)
186. M C Gordillo *Phys. Rev. B* **76** 115402 (2007)
187. J Gou, Z Liang, C Zhang, B Wang *Composites B* **36** 524 (2005)
188. A N Enyashin, A L Ivanovskii *Pis'ma Zh. Eksp. Teor. Fiz.* **87** 373 (2008) [b]
189. W B Choi, E Bae, D Kang, S Chae, B Cheong, I Ko, E Lee, W Park *Nanotechnology* **15** S512 (2004)
190. L A Chernozatonskii *Chem. Phys. Lett.* **297** 257 (1998)
191. T Yildirim, O Gülseren, C Kilic, S Ciraci *Phys. Rev. B* **62** 12648 (2000)
192. H S Domingos *J. Phys.: Condens. Matter* **16** 9083 (2004)
193. S Dag, R T Senger, S Ciraci *Phys. Rev. B* **70** 205407 (2004)
194. S G Louie *Top. Appl. Phys.* **80** 113 (2001)
195. G B Adams, O F Sankey, J B Page, M O'Keeffe, D A Drabold *Science* **256** 1792 (1992)
196. Z H Xia, P R Guduru, W A Curtin *Phys. Rev. Lett.* **98** 245501 (2007)
197. T Tanabe *Phys. Scr.* **64** 7 (1996)
198. J Seldin, C W Nezbeda *J. Appl. Phys.* **41** 3389 (1970)
199. S F Braga, D S Galvao *J. Comput. Chem.* **28** 1724 (2007)
200. S F Braga, D S Galvao *Chem. Phys. Lett.* **419** 394 (2006)
201. L Chernozatonskii, E Richter, M Menon *Phys. Rev. B* **65** 241404 (2002)
202. E G Gal'pern, A R Sabirov, I V Stankevich, L A Chernozatonskii, A L Chistyakov *Pis'ma Zh. Eksp. Teor. Fiz.* **73** 556 (2001) [b]
203. A Kuc, G Seifert *Phys. Rev. B* **74** 214104 (2006)
204. J Klett, R Hardy, E Romine, C Walls, T Burchell *Carbon* **38** 953 (2000)
205. J Klett, A D McMillan, N C Gallego, C Walls *J. Mater. Sci.* **39** 3659 (2004)
206. A V Rode, E G Gamaly, A G Christy, J G FitzGerald, S T Hyde, R G Elliman, B Luther-Davies, A I Veinger, J Androulakis, J Giapintzakis *Phys. Rev. B* **70** 054407 (2004)
207. A T Balaban, D J Klein, C A Folden *Chem. Phys. Lett.* **217** 266 (1994)
208. H R Karfunkel, T Dressler *J. Am. Chem. Soc.* **114** 2285 (1992)
209. K Umemoto, S Saito, S Berber, D Tomanek *Phys. Rev. B* **64** 193409 (2001)
210. N Park, J Ihm *Phys. Rev. B* **62** 7614 (2000)
211. J A Van Vechten, D A Keszler *Phys. Rev. B* **36** 4570 (1987)
212. G E Scuseria *Chem. Phys. Lett.* **195** 543 (1992)
213. L A Chernozatonskii *Phys. Lett. A* **172** 173 (1992)
214. D Zhou, S Seraphin *Chem. Phys. Lett.* **238** 286 (1995)
215. J M Romo-Herrera, M Terrones, H Terrones, S Dag, V Meunier *Nano Lett.* **7** 570 (2007)
216. V R Coluci, D S Galvao, A Jorio *Nanotechnology* **17** 617 (2006)
217. V R Coluci, N M Pugno, S ODantas, D S Galvao, A Jorio *Nanotechnology* **18** 335702 (2007)
218. M Wang, X Qiu, X Zhang, Y Yin *Nanotechnology* **18** 295708 (2007)
219. Yu P Kudryavtsev, N A Bystrova *Izv. Akad. Nauk, Ser. Khim.* 2805 (1996) [h]
220. V G Babaev, M B Guseva, A Z Zhuk *Dokl. Akad. Nauk* **343** 176 (1995) [g]
221. V I Kasatochkin, A M Sladkov, Yu P Kudryavtsev, N M Popov, V V Korshak *Dokl. Akad. Nauk SSSR* **177** 358 (1967) [g]
222. A El Goresy, G Donney *Science* **161** 363 (1968)

223. V V Korshak, Yu P Kudryavtsev, A M Sladkov *Vestn. Akad. Nauk SSSR* (1) 70 (1978) [i]
224. J B Donner, E Fousson, M Samirant, T K Wang, M Pontier-Johnson, A Eckhardt *C. R. Acad. Sci. Ser. Chem.* **3** 359 (2000)
225. A El Goresy, L S Dubrovinsky, P Giller *Lunar Planetary Sci.* **34** 1016 (2003)
226. C Piskoti, J Yargert, A Zettl *Nature (London)* **393** 771 (1998)
227. J Tersoff, R S Ruoff *Phys. Rev. Lett.* **73** 676 (1994)
228. E G Gal'pern, A R Sabirov, I V Stankevich, A L Chistyakov, L A Chernozatonskii *Fiz. Tv. Tela* **44** 599 (2002) [e]
229. V V Danilenko *Sintez i Spekanie Almaza Vzryvom* (Synthesis and Caking of Diamond by Explosion) (Moscow: Energoatomizdat, 2003)
230. V Yu Dolmatov *Ul'tradispersnye Almazy Detonatsionnogo Sinteza. Poluchenie, Svoistva, Primeneniya* (Superdispersed Diamonds of Detonation Synthesis. Production, Properties, Applications) (St Petersburg: St Petersburg State Polytechnic University, 2003)
231. V V Danilenko *Fiz. Tv. Tela* **46** 693 (2004) [e]
232. T G Shumilova, in *Nanomineralogiya. Ul'tra- i Mikrodispersnoe Sostoyanie Mineral'nogo Veshchestva* (Nanomineralogy. Super- and Microdispersed State of Mineral Substance) (Eds N P Yushkin, A M Askhabov, V I Rakin) (St Petersburg: Nauka, 2005) p. 80
233. R S Lewis, M Tang, J G Wackler, E Anders, E Steel *Nature (London)* **326** 160 (1987)
234. Z R Dai, J P Bradley, D J Joswiak, D E Brownlee, H G M Hill, M J Genge *Nature (London)* **418** 157 (2002)
235. O A Shenderova, C W Padgett, Z Hu, D W Brenner *J. Vac. Sci. Technol. B* **23** 2456 (2005)
236. A S Barnard *Rev. Adv. Mater. Sci.* **6** 94 (2004)
237. A S Barnard *Synthesis, Properties and Applications of Ultrananocrystalline Diamond (NATO Sci. Ser.)* (Ed. D Gruen) (Amsterdam: Springer, 2005)
238. G C McIntosh, M Yoon, S Berber, D Tománek *Phys. Rev. B* **70** 045401 (2004)
239. A S Barnard, M Sternberg *J. Phys. Chem. B* **110** 19307 (2006)
240. F H Ree, N W Winter, J N Glosli, J A Viecelli *Physica, B+C* **265** 223 (1999)
241. J A Viecelli, F H Ree *J. Appl. Phys.* **88** 683 (2000)
242. J A Viecelli, S Bastea, J N Glosli, R F Ree *J. Chem. Phys.* **115** 2730 (2001)
243. A S Barnard *Diamond Relat. Mater.* **15** 285 (2006)
244. Q Jiang, Z P Chen *Carbon* **44** 79 (2006)
245. A S Barnard, S P Russo, I K Snook *J. Chem. Phys.* **118** 5094 (2003)
246. A S Barnard, S P Russo, I K Snook *Phys. Rev. B* **68** 073406 (2003)
247. R Astala, M Kaukonen, R M Nieminen *Phys. Rev. B* **65** 245423 (2002)
248. N F Goldshleger, A P Moravskii *Usp. Khim.* **66** 353 (1997) [*Russ. Chem. Rev.* **66** 323 (1997)]
249. Yu S Nechaev, O K Alekseeva *Usp. Khim.* **73** 1308 (2004) [*Russ. Chem. Rev.* **73** 1211 (20004)]
250. G Seifert *Solid State Ionics* **168** 265 (2004)
251. O Gulseren, T Yildirim, S Ciraci *Phys. Rev. B* **66** R121401 (2002)
252. O Gulseren, T Yildirim, S Ciraci *Phys. Rev. B* **68** 115419 (2003)
253. S P Russo, A S Barnard, I K Snook *Surf. Rev. Lett.* **10** 233 (2003)
254. A S Barnard, S P Russo, I K Snook *Int. J. Mod. Phys., B* **17** 3865 (2003)
255. V L Kuznetsov, A L Chuvilin, Y V Butenko, I Y Mal'kov, V M Titov *Chem. Phys. Lett.* **209** 72 (1994)
256. V L Kuznetsov, I L Zilberberg, Y V Butenko, A L Chuvilin, B Seagall *J. Appl. Phys.* **86** 863 (1999)
257. S Tomita, T Sakurai, H Ohta, M Fujii, S Hayashi *J. Chem. Phys.* **114** 7477 (2001)
258. F Banhart, P M Ajayan *Nature (London)* **382** 433 (1996)
259. F Banhart *J. Appl. Phys.* **81** 3440 (1997)
260. M Zaiser, F Banhart *Phys. Rev. Lett.* **79** 3680 (1997)
261. Ph Redlich, F Banhart, Y Lyutovich, P M Ajayan *Carbon* **36** 561 (1998)
262. M Zaiser, Y Lyutovich, F Banhart *Phys. Rev. B* **62** 3058 (2000)
263. N W Winter, F H Ree *J. Comput. Mater. Des.* **5** 279 (1998)
264. R F Ree, N W Winter, J N Glosli, A J Viecelli *Physica, B* **265** 223 (1999)
265. F Fugaciu, H Hermann, G Seifert *Phys. Rev. B* **60** 10711 (1999)
266. H Hermann, F Fugaciu, G Seifert *Appl. Phys. Lett.* **79** 63 (2001)
267. A S Barnard, S P Russo, I K Snook *Philos. Mag. Lett.* **83** 39 (2003)
268. R Astala, M Kaukonen, G Jungnickel, Th Frauenheim, R M Nieminen *Phys. Rev. B* **63** 081402 (2001)
269. N M Hwang, J H Hahn, D Y Yoon *J. Cryst. Growth* **162** 55 (1996)
270. Q Jiang, J C Li, G Wilde *J. Phys.: Condens. Matter* **12** 5623 (2000)
271. A S Barnard, M Sternberg *J. Phys. Chem. B* **109** 17107 (2005)
272. A S Barnard, S P Russo, I K Snook *J. Nanosci. Nanotechnol.* **5** 1395 (2005)
273. A S Barnard, M Sternberg *Nanotechnology* **18** 025702 (2007)
274. D A Areshkin, O A Shenderova, S P Sadiga, D W Brenner *Diamond Relat. Mater.* **13** 1826 (2004)
275. L Zeger, E Kaxiras *Phys. Rev. Lett.* **19** 2920 (1993)
276. V Ya Shevchenko, A E Madison *Glass Phys. Chem.* **32** 118 (2006)
277. A N Enyashin, A L Ivanovskii *Fiz. Tv. Tela* **49** 378 (2007) [e]
278. S Dimovski, Y Gogotsi, in *Nanomaterials Handbook* (Ed. Y Gogotsi) (Boca Raton, FL, London, New York: Taylor and Francis Group, 2006)
279. A S Barnard, S P Russo, I K Snook *Nano Lett.* **3** 1323 (2003)
280. A S Barnard, S P Russo, I K Snook *Surf. Sci.* **538** 204 (2003)
281. V V Ivanovskaya, A L Ivanovskii *Teor. Eksp. Khim.* **42** 199 (2006) [j]
282. V V Ivanovskaya, A L Ivanovskii *Neorg. Mater.* **43** 410 (2007) [k]
283. O Shenderova, D Brenner, R S Ruoff *Nano Lett.* **3** 805 (2003)
284. S Erkoc *Int. J. Mod. Phys., C* **11** 1247 (2003)
285. O B Malcioglu, S Erkoc *Int. J. Mod. Phys., C* **14** 441 (2003)
286. V V Ivanovskaya, A L Ivanovskii *Ros. Nanotekhnol.* **2** 12 (2007) [l]
287. Y K Chih, C H Chen, J Hwang, A P Lee, C S Kou *Diamond Relat. Mater.* **13** 1614 (2004)
288. O A Shenderova, D Areshkin, D W Brenner *Mol. Simul.* **29** 259 (2003)
289. M L Terranova, S Orlanducci, A Fiori, E Tamburri, V Sessa, M Rossi, A S Barnard *Chem. Mater.* **17** 3214 (2005)
290. T Suzuki, M Yagi, K Shibuki, M Hasemi *Appl. Phys. Lett.* **65** 540 (1994)
291. L T Sun, J L Gong, Z Y Zhu *Appl. Phys. Lett.* **84** 2901 (2004)
292. P Ruffieux, O Groening, M Bielmann *Phys. Rev. B* **66** 245416 (2002)
293. A S Barnard, M L Terranova, M Rossi *Chem. Mater.* **17** 527 (2005)
294. A T Balaban, C C Rentia, E Ciupitu *Rev. Roum. Chim.* **13** 231 (1968)
295. A F Wells *Three-Dimensional Nets and Polyherda* (New York: Wiley, 1977)
296. V H Crespi, L X Benedict, M L Cohen, S G Louie *Phys. Rev. B* **53** R13303 (1996)
297. M Terrones, H Terrones *Fullerene Sci. Technol.* **4** 517 (1996)
298. A J Stone, D J Wales *Chem. Phys. Lett.* **128** 501 (1986)
299. M Deza, P W Fowler, M Shtogrin, K Vietze *J. Chem. Inf. Comput. Sci.* **40** 1325 (2000)
300. Yu B Kuz'ma *Kristallokhimiya Boridov* (Crystal Chemistry of Borides) (L'vov: Vishcha Shkola, 1983)
301. H Terrones, M Terrones, E Hernandez, N Grobert, J C Charlier, P M Ajayan *Phys. Rev. Lett.* **84** 1716 (2000)
302. R H Baughman, H Eckhard, M Kertesz *J. Chem. Phys.* **87** 6687 (1987)
303. N Narita, S Nagai, S Suzuki, K Nakao *Phys. Rev. B* **58** 11009 (1998)
304. N Narita, S Nagai, S Suzuki, K Nakao *Phys. Rev. B* **62** 11146 (2000)

305. M M Haley, S C Brand, J Pak *Angew. Chem., Int. Ed. Engl.* **36** 836 (1997)
306. Y Hou, S Feng *Solid State Commun.* **122** 307 (2002)
307. S Hino, Y Okada, K Iwasaki, M Kijima, H Shirakawa *Chem. Phys. Lett.* **372** 59 (2002)
308. V Moliner, J Andres, A Arnau, E Silla, I Tunon *Chem. Phys.* **206** 57 (1996)
309. G Schermann, T Grosser, F Hampel, A Hisrch *Chem. – Eur. J.* **3** 1105 (1997)
310. F Cataldo *Polymer Int.* **48** 15 (1999)
311. G Frenking, N Frohlich *Chem. Rev.* **100** 717 (2000)
312. T Gibtner, F Hampel, J P Gisselbrecht, A Hirsch *Chem. – Eur. J.* **8** 408 (2002)
313. A Scemama, P Chaquin, M C Gazeau, Y Benilan *Chem. Phys. Lett.* **361** 520 (2002)
314. M Ohkita, M Kawano, T Suzuki, T Tsuji *Chem. Commun.* 3054 (2002)
315. A J Matzger, M Shim, K Vollhardt *Chem. Commun.* 1871 (1999)
316. N Tyutyulkov, F Dietz, K Mullen, M Baumgarten *Chem. Phys. Lett.* **272** 111 (1997)
317. M Ouyang, J L Huang, C M Lieber *Science* **291** 97 (2001)
318. H Kim, J Lee, S J Kahng, Y W Son, S B Lee, C K Lee, J Ihm, Y Kuk *Phys. Rev. Lett.* **90** 216107 (2003)
319. A L Ivanovskii *Zh. Neorg. Khim.* **50** 1514 (2005) [m]
320. P Lambin, L P Biro *New J. Phys.* **5** 141 1 (2003)
321. P M Ajayan, V Ravikumar, J C Charlier *Phys. Rev. Lett.* **81** 1437 (1998)
322. M B Nardelli, B Yakobson, J Bernholc *Phys. Rev. B* **57** R4277 (1998)
323. L P Biro, G I Mark, A A Koos, J B Nagy, P Lambin *Phys. Rev. B* **66** 165405 (2002)
324. P Lambin, G I Mark, L P Biro *Phys. Rev. B* **67** 205413 (2003)
325. I Laszlo, A Rassat *Int. J. Quantum Chem.* **84** 136 (2001)
326. V R Coluci, S F Braga, S B Legoas, D S Galvao, R H Baughman *Phys. Rev. B* **68** 035430 (2003)
327. V R Coluci, S F Braga, S B Legoas, D S Galvao, R H Baughman *Nanotechnology* **15** S142 (2004)
328. E A Belenkov *Izv. Chelyabinskogo Nauch. Tsentra* (1) 25 (2001)
329. E A Belenkov *Izv. Chelyabinskogo Nauch. Tsentra* (1) 12 (2001)
330. A N Enyashin, A A Sofronov, Yu N Makurin, A L Ivanovskii *J. Mol. Struct. (THEOCHEM)* **684** 29 (2004)
331. J E Kehoe, J H Kiley, J J English *Org. Lett.* **2** 969 (2000)
332. M Sonoda, A Inaba, K Itahashi, Y Tobe *Org. Lett.* **3** 2419 (2001)
333. J E Anthony, S I Khan, Y Rubin *Tetrahedron Lett.* **38** 3499 (1997)
334. M Srinivasan, S Sankararaman, I Dix, P G Jones *Org. Lett.* **2** 3849 (2000)
335. M L Bell, R C Chiechi, C A Johnson, D B Kimball, A J Matzger, W B Wan, T J R Weakley, M M Haley *Tetrahedron* **57** 3507 (2001)
336. M E Gallagher, J E Anthony *Tetrahedron Lett.* **42** 7533 (2001)
337. W Brad Wan, M M Haley *J. Org. Chem.* **66** 3893 (2001)
338. D Rana, G Gangopadhyay *Chem. Phys. Lett.* **334** 314 (2001)
339. Y Tobe, N Nakagawa, J Kishi, M Sonoda, K Naemura, T Wakabayashi, T Shida, Y Achiba *Tetrahedron* **57** 3629 (2001)
340. J Fayos *J. Solid State Chem.* **146** 278 (1999)
341. B M Smith, M Monthioux, D E Luzzi *Nature (London)* **396** 323 (1998)
342. A L Ivanovskii *Zh. Neorg. Khim.* **48** 945 (2003) [m]
343. D A Britz, A N Khlobystov *Chem. Soc. Rev.* **35** 637 (2006)
344. I V Krive, R I Shekhter, M Jonson *Low Temp. Phys.* **32** 887 (2006)
345. R Kitaura, H Shinohara *Jpn. J. Appl. Phys.* **46** 881 (2007)
346. A N Khlobystov, D A Britz, A Ardavan, G Briggs *Phys. Rev. Lett.* **92** 245507 (2003)
347. A Oshiyama, S Okada, S Saito *Physica B: Condens. Matter* **323** 21 (2002)
348. D E Luzzi, B W Smith *Carbon* **38** 1751 (2000)
349. B W Smith, D E Luzzi *Chem. Phys. Lett.* **321** 169 (2000)
350. S Iijima *Physica B: Condens. Matter* **323** 1 (2002)
351. T Pichler, X Liu, M Knupfer, J Fink *New J. Phys.* **5** 156 (2003)
352. H Hirahara, K Suenaga, S Bandow, S Iijima *Chem. Phys. Lett.* **324** 224 (2000)
353. H Kataura, Y Maniwa, T Kodama, K Kikuchi, K Hirahara, K Suenaga, S Iijima, S Suzuki, Y Achiba, W Kratschmer *Synth. Met.* **121** 1195 (2001)
354. M Yudasaka, K Ajima, K Suenaga, T Ichihashi, A Hashimoto, S Iijima *Chem. Phys. Lett.* **380** 42 (2003)
355. S Bandow, M Takizawa, K Hirahara, M Yudasaka, S Iijima *Chem. Phys. Lett.* **337** 48 (2001)
356. T Pichler, H Kuzmany, H Kataura, Y Achiba *Phys. Rev. Lett.* **87** 7401 (2001)
357. K Hirahara, S Bandow, K Suenaga, Y Kato, T Okazaki, H Shinohara, S Iijima *Phys. Rev. B* **64** 115420 (2001)
358. H Kataura, Y Maniwa, M Abe, A Fujiwara, T Kodama, K Kikuchi, H Imahori, Y Misaki, S Suzuki, Y Achiba *Appl. Phys. A* **74** 349 (2002)
359. S Bandow, M Takizawa, H Kato, T Okazaki, H Shinohara, S Iijima *Chem. Phys. Lett.* **347** 23 (2001)
360. A H R Palser *Phys. Chem. Chem. Phys.* **1** 4459 (1999)
361. A A Farajian, M Mikami *J. Phys.: Condens. Matter* **13** 8049 (2001)
362. S Okada, S Saito, A Oshiyama *Phys. Rev. Lett.* **86** 3835 (2001)
363. S Berber, Y-K Kwon, D Tomanek *Phys. Rev. Lett.* **88** 5502 (2002)
364. S Okada, S Saito, A Oshiyama *Phys. Rev. B* **64** 1303 (2001)
365. S Okada, M Otani, A Oshiyama *Phys. Rev. B* **67** 205411 (2003)
366. S Okada, M Otani, A Oshiyama *New J. Phys.* **5** 122 (2003)
367. M Otani, S Okada, A Oshiyama *Phys. Rev. B* **68** 125424 (2003)
368. L A Girifalco, M Hodak *Phys. Rev. B* **65** 5404 (2002)
369. G T Pickett, M Gross, H Okyama *Phys. Rev. Lett.* **85** 3652 (2000)
370. M Hodak, L A Girifalco *Phys. Rev. B* **67** 075419 (2003)
371. W Mickelson, S Aloni, W Han, J Cumings, A Zettl *Science* **300** 467 (2003)
372. A G Nasibulin, P V Pikhitsa, H Jiang, D V Brown, A V Krasheninnikov, A S Anisimov, P Queipo, A Moisala, D Gonzalez, G Lientschnig, A Hassanien, S D Shandakov, G Lolli, D E Resasco, M Choi, D Tomanek, E I Kauppinen *Nat. Nanotechnol.* **2** 156 (2007)
373. N Dragoe, K Nakahara, H Shimotani, L Xiao, S Tanibayashi, T Higuchi, K Kitazawa *Fullerene Sci. Technol.* **8** 545 (2000)
374. A R Sabirov, I V Stankevich, L A Chernozatonskii *Pis'ma Zh. Eksp. Teor. Fiz.* **79** 153 (2004) [b]
375. T Ren, B Sun, Z L Chen, L Qu, H Yuan, X Gao, S Wang, R He, F Zhao, Y Zhao, Z Liu, X Jing *J. Chem. Phys. B* **111** 6344 (2007)
376. E David *J. Mater. Proc. Technol.* **162 – 163** 169 (2005)
377. S Patchkovskii, J S Tse, S Yurchenko, L Zhechkov, Th Heine, G Seifert *Proc. Natl. Acad. Sci. USA* **102** 10439 (2005)
378. C C Chen, C F Chen, I H Lee, C L Lin *Diamond Relat. Mater.* **14** 1897 (2005)
379. A N Enyashin, A L Ivanovskii *Mendeleev Commun.* **17** 199 (2007)
380. J M Du, Z M Liu, Z H Li, B X Han, Z Y Sun, Y Huang *Mater. Lett.* **59** 456 (2005)
381. E A Belenkov, A L Ivanovskii, S N Ul'yanov, F K Shabiev *Zh. Strukt. Khim.* **46** 1001 (2005) [c]
382. R T Paine, C K Narula *Chem. Rev.* **90** 73 (1990)
383. R Tenne *Prog. Inorg. Chem.* **50** 269 (2001)
384. A L Ivanovskii *Usp. Khim.* **71** 203 (2002) [*Russ. Chem. Rev.* **71** 175 (2002)]
385. M Law, J Golberger, P Yang *Annu. Rev. Mater. Res.* **34** 83 (2004)
386. R Ma, D Golberg, Y Bando, T Sasaki *Philos. Trans. R. Soc. London, Ser. A* **362** 2161 (2004)
387. M Terrones, J M Romo-Herrera, E Cruz-Silva, F Lopez-Urias, E Munoz-Sandoval, J J Velazquez-Salazar, H Terrones, Y Bando, D Golberg *Mater. Today* **10** 30 (2007)
388. F L Deepak, C P Vinod, K Mukhopadhyay, A Govindaraj, S N R Rao *Chem. Phys. Lett.* **353** 345 (2002)
389. T Oku, I Narita, A Nishiwaki *Mater. Manufact. Proc.* **19** 1215 (2004)

390. T Oku, I Narita, A Nishiwaki, N Koi *Defect Diffusion Forum* **226–228** 113 (2004)
391. D Golberg, Y Bando, C C Tang, C Y Zhi *Adv. Mater.* **19** 2413 (2007)
392. V V Pokropivny *Poroshk. Metallurg.* (9–10) 50 (2001) [n]
393. V V Pokropivny *Poroshk. Metallurg.* (11–12) 51 (2001) [n]
394. V V Pokropivny *Poroshk. Metallurg.* (3–4) 13 (2002) [n]
395. V V Pokropivny *Poroshk. Metallurg.* (5–6) 45 (2002) [n]
396. O Stephan, Y Bando, A Loiseau, F Williame, N Shramchenko, T Tamiya, T Sato *Appl. Phys. A* **67** 107 (1998)
397. R R Zope, B I Dunlap *Chem. Phys. Lett.* **386** 403 (2004)
398. D Golberg, A Rode, Y Bando, T Mitome, E Gamaly, B Luther-Davies *Diamond Relat. Mater.* **12** 1269 (2003)
399. R Ma, Y Bando, T Sato *Chem. Phys. Lett.* **337** 61 (2001)
400. T Oku, I Narita, A Nishiwaki *J. Eur. Ceram. Soc.* **26** 443 (2006)
401. D Golberg, Y Bando, M Eremets, K Takemura, K Kurashima, K Tamiya, H Yusa *Chem. Phys. Lett.* **279** 191 (1997)
402. V V Pokropivny, A V Pokropivny *Pis'ma Zh. Tekhn. Fiz.* **29** (12) 21 (2003) [o]
403. Y Saito, M Maida *J. Phys. Chem. A* **103** 1291 (1999)
404. T Bartnitskaya, G S Oleinik, A V Pokropivny, V V Pokropivny *Pis'ma Zh. Eksp. Teor. Fiz.* **69** (2) 163 (1999) [b]
405. H C Choi, S Y Bae, W S Jang, J Park *J. Phys. Chem. B* **109** 7007 (2005)
406. R Ma, Y Bando, T Sato, L Bourgeois *Diamond Relat. Mater.* **11** 1397 (2002)
407. C Y Zhi, J D Guo, X D Bai, E G Wang *J. Appl. Phys.* **91** 5325 (2002)
408. A Nishiwaki, T Oku *Diamond Relat. Mater.* **14** 1183 (2005)
409. A Nishiwaki, T Oku *J. Eur. Ceram. Soc.* **26** 435 (2006)
410. T Oku, K Hiraga, T Matsuda, T Hirai, M Hirabayashi *Diamond Relat. Mater.* **12** 1918 (2003)
411. I Narita, T Oku *Diamond Related Mater.* **12** 1146 (2003)
412. P W Fowler, D E Manolopoulos *An Atlas of Fullerenes* (Oxford: Clarendon Press, 1995)
413. T Oku, A Nishiwaki, I Narita, M Gonda *Chem. Phys. Lett.* **380** 620 (2003)
414. M Terauchi, M Tanaka, H Matsuda, M Takeda, K Kimura *J. Electron. Microsc.* **46** 75 (1997)
415. T Hirano, T Oku, K Suganuma *Diamond Relat. Mater.* **9** 625 (2000)
416. S S Batsanov, G E Blokhina, A A Deribas *Zh. Strukt. Khim.* **6** 227 (1965) [c]
417. A V Kurdyumov, A N Pilyankevich, in *Bor. Poluchenie, Struktura i Svoistva* (Boron. Synthesis, Structure and Properties) (Moscow: Nauka, 1974) p. 49
418. T Akashi, H-R Pack, A B Sawaoka *J. Mater. Sci.* **21** 4060 (1986)
419. A Sokoowska, A Olszyna *Diamond Relat. Mater.* **1** 334 (1992)
420. J B Wang, X L Zhong, C Y Zhang, B Q Huang, G W Yang *J. Mater. Res.* **18** 2774 (2003)
421. A Olszyna, M Muftah, A Sokolowska *Diamond Relat. Mater.* **4** 386 (1995)
422. A Olszyna, J Konwerska-Hrabowska, M Lisicki *Diamond Relat. Mater.* **6** 617 (1997)
423. A Rusek, M Sokolowski, A Sokolowska *J. Mater. Sci.* **16** 2021 (1981)
424. V V Pokropivny, A S Smolyar, A V Pokropivny *Fiz. Tv. Tela* **49** 562 (2007) [c]
425. A V Pokropivny *Diamond Relat. Mater.* **15** 1492 (2006)
426. *Fizicheskie Svoistva Almaza. Spravochnik* (Physical Properties of Diamond. Handbook) (Ed. N V Novikov) (Kiev: Naukova Dumka, 1987)
427. J Wang, V K Kayastha, Y K Yap, Z Fan, J G Lu, Z Pan, I N Ivanov, A A Puretsky, D B Geohegan *Nano Lett.* **5** 2528 (2005)
428. Y Shimizu, Y Moriyoshi, H Tanaka *Appl. Phys. Lett.* **75** 929 (1999)
429. H Chen, Y Chen, J Yu, S Williams *Chem. Phys. Lett.* **425** 315 (2006)
430. C T Kresge, M E Leonowicz, W J Roth, J C Vartuli, J S Beck *Nature (London)* **359** 710 (1992)
431. J M Kim, S K Kim, R Ryoo *Chem. Commun.* 259 (1998)
432. N Li, X Li, W Geng, L Zhao, G Zhu, R Wang, S Qiu *Mater. Lett.* **59** 925 (2005)
433. P W Fowler, K M Rogers, G Seifert, M Terrones, H Terrones *Chem. Phys. Lett.* **299** 359 (1999)
434. A N Enyashin, V V Ivanovskaya, Yu N Makurin, A L Ivanovskii *Dokl. Akad. Nauk* **395** 64 (2004) [g]
435. A N Enyashin, Yu N Makurin, A L Ivanovskii *Carbon* **42** 2081 (2004)
436. V V Ivanovskaya, A N Enyashin, A L Ivanovskii *Zh. Fiz. Khim.* **80** 451 (2006) [d]
437. S V Lisenkov, G A Vinogradov, T Yu Astakhova, N G Lebedev *Pis'ma Zh. Eksp. Teor. Fiz.* **81** 431 (2005) [b]
438. S V Lisenkov, G A Vinogradov, T Yu Astakhova, N G Lebedev *Fiz. Tv. Tela* **48** 179 (2006) [c]
439. G S Zakharova, V L Volkov, V V Ivanovskaya, A L Ivanovskii *Usp. Khim.* **74** 651 (2005) [*Russ. Chem. Rev.* **74** 587 (2005)]
440. V V Ivanovskaya, Yu N Makurin, A L Ivanovskii, in *Nanostructures — Novel Architectures* (New York: Nova Sci. Publ., 2005) p. 9
441. V V Ivanovskaya, A N Enyashin, Yu N Makurin, A L Ivanovskii *Nanotekhnika* **5** (1) 126 (2006)
442. A L Ivanovskii *Usp. Fiz. Nauk* **177** 1083 (2007) [*Physics Uspekhi* **50** 1031 (2007)]
443. A L Ivanovskii *Ros. Nanotekhnol.* **2** 83 (2007) [l]
444. A N Enyashin, Yu N Makurin, A L Ivanovskii *Teor. Eksp. Khim.* **40** 70 (2004) [j]
445. A L Ivanovskii *Al'ternativ. Energet. Ekol.* **7** (15) 28 (2004)
446. H Zhang, J D FitzGerald, L T Chadderton, J Yu, Y Chen *Phys. Rev. B* **74** 045407 (2006)
447. Y J Chen, B Chi, D C Mahon, Y Chen *Nanotechnology* **17** 2942 (2006)
448. F K Huo, Z Hu, F Chen, J J Fu, Y Chen, B H Liu, J Ding, Z L Dong, T White *Appl. Phys. Lett.* **80** 3611 (2002)
449. Y J Chen, H Z Zhang, Y Chen *Nanotechnology* **17** 786 (2006)
450. J Zhan, X Hao, S Wen, M Jiang *Physica E* **25** 409 (2005)
451. V V Ivanovskaya, A Zobelli, G Zaifert, A L Ivanovskii *Pis'ma Zh. Eksp. Teor. Fiz.* **85** 761 (2007) [b]
452. T Sekiguchi, Q Liu, T Tanaka, J Hu, Y Zhu, Y Bando *Eur. Phys. Appl. Phys.* **27** 107 (2004)
453. K Albe *Phys. Rev. B* **55** 6203 (1997)
454. V V Ivanovskaya, A N Enyashin, A A Sofronov, Yu N Makurin, A L Ivanovskii *Zh. Obshch. Khim.* **74** 778 (2004) [p]
455. A Trave, F J Ribeiro, S G Louie, M L Cohen *Phys. Rev. B* **70** 205418 (2004)
456. W H Moon, M S Son, J H Lee, H J Hwang *Phys. Status Solidi B* **241** 1783 (2004)
457. J W Kang, H J Hwang *J. Phys.: Condens. Matter* **16** 3901 (2004)
458. A N Enyashin, G Zeifert, A L Ivanovskii *Neorg. Mater.* **41** 687 (2005) [k]
459. W Song, M Ni, J Lu, Z Gao, S Nagase, D Yu, H Ye, X Zhang *J. Mol. Struct. (THEOCHEM)* **730** 119 (2005)
460. V V Ivanovskaya, A A Sofronov, A L Ivanovskii *Teor. Eksp. Khim.* **37** 331 (2001) [j]
461. A A Sofronov, V V Ivanovskaya, Yu N Makurin, A L Ivanovskii *Chem. Phys. Lett.* **351** 35 (2002)
462. V V Ivanovskaya, A A Sofronov, A L Ivanovskii *Phys. Lett. A* **297** 436 (2002)
463. V V Ivanovskaya, A A Sofronov, Yu N Makurin, A L Ivanovskii *J. Mol. Struct. (THEOCHEM)* **594** 31 (2002)
464. W Y Choi, J W Kang, H J Hwang *Physica E* **23** 135 (2004)
465. A N Enyashin, A L Ivanovskii *Fiz. Tv. Tela* **50** 374 (2008) [c]
466. S Bandow, T Hiraoka, T Yumura, K Hirahara, H Shinohara, S Iijima *Chem. Phys. Lett.* **384** 320 (2004)
467. F Zheng, G Zhou, S Hao, W Duan *J. Chem. Phys.* **123** 124716 (2005)
468. A N Enyashin, G Zeifert, A L Ivanovskii *Pis'ma Zh. Eksp. Teor. Fiz.* **80** 709 (2004) [b]
469. Z Zhou, J Zhao, Z Chen, P von R Schleyer *J. Phys. Chem. B* **110** 25678 (2006)
470. L A Thesing, P Piquini, T Kar *Nanotechnology* **17** 1637 (2006)

471. N P Bansal, J B Hurst, S R Choi *J. Am. Ceram. Soc.* **89** 388 (2006)
472. A N Enyashin, A L Ivanovskii *Nanotechnology* **16** 1304 (2005)
473. Z Zhang, W Guo, G Tai *Appl. Phys. Lett.* **90** 133103 (2007)
474. D Golberg, P S Dorozhkin, Y Bando, Z-C Dong, N Grobert, M Reyes-Reyes, H Terrones, M Terrones *Appl. Phys. Lett.* **82** 1275 (2003)
475. K Saulig-Wenger, M Bechelany, D Cornu, T Epicier, F Chassagneux, G Ferro, Y Monteil, P Miele *J. Phys. IV, France* **124** 99 (2005)
476. F F Xu, Y Bando, D Golberg, M Hasegawa, M Mitome *Acta Mater.* **52** 601 (2004)
477. N Koi, T Oku, M Nishijima *Solid State Commun.* **136** 342 (2005)
478. G W Peng, A C H Huan, Y P Feng *Appl. Phys. Lett.* **88** 193117 (2006)
479. D Golberg F F Xu, Y Bando *Appl. Phys. A* **76** 479 (2003)
480. H J Xiang, J Yang, J G Hou, Q Zhu *New J. Phys.* **7** 39 (2005)
481. C Zhi, Y Bando, C Tang, D Golberg *Phys. Rev. B* **74** 153413 (2006)
482. C Zhi, Y Bando, C Tang, R Xie, T Sekiguchi, D Golberg *J. Am. Chem. Soc.* **127** 15996 (2005)
483. C Zhi, Y Bando, C Tang, S Honda, K Sato, H Kuwahara, D Golberg *Angew. Chem., Int. Ed.* **44** 7932 (2005)
484. J Rossato, R J Baierle, W Orellana *Phys. Rev. B* **75** 235401 (2007)
485. F Piazzaa, J E Nocua, A Hidalgo, J De Jesus, R Velazquez, B L Weiss, G Morell *Diamond Relat. Mater.* **14** 965 (2005)
486. H Pan, Y P Feng, J Y Lin *Phys. Rev. B* **73** 035420 (2006)

[a] — *Crystallogr. Rep. (Engl. Transl.)*
[b] — *J. Exp. Theor. Phys. Lett. (Engl. Transl.)*
[c] — *J. Struct. Chem. (Engl. Transl.)*
[d] — *Russ. J. Phys. Chem. (Engl. Transl.)*
[e] — *Phys. Solid. State (Engl. Transl.)*
[f] — *Semiconductors (Engl. Transl.)*
[g] — *Dokl. Phys. Chem. (Engl. Transl.)*
[h] — *Russ. Chem. Bull., Int. Ed. (Engl. Transl.)*
[i] — *Herald Russ. Acad. Sci. (Engl. Transl.)*
[j] — *Theor. Exp. Chem. (Engl. Transl.)*
[k] — *Inorg. Mater. (Engl. Transl.)*
[l] — *Nanotechnol. Russ. (Engl. Transl.)*
[m] — *Russ. J. Inorg. Chem. (Engl. Transl.)*
[n] — *Powder Metall. Met. Ceram. (Engl. Transl.)*
[o] — *J. Techn. Phys. Lett. (Engl. Transl.)*
[p] — *Russ. J. Gen. Chem. (Engl. Transl.)*